



## Review

# Chiral recognition by enantioselective liquid chromatography: Mechanisms and modern chiral stationary phases

Michael Lämmerhofer\*

Christian Doppler Laboratory for Molecular Recognition Materials, Department of Analytical Chemistry and Food Chemistry, University of Vienna, Waehringer Strasse 38, A-1090 Vienna, Austria

## ARTICLE INFO

## Article history:

Available online 22 October 2009

## Keywords:

Chiral separation  
Drug discovery  
Pharmaceutical analysis  
Chiral stationary phase  
Chiral recognition  
Thermodynamics  
Additivity principle  
Site-selective thermodynamics  
Extrathermodynamic approaches  
Intermolecular interactions  
IR  
NMR  
X-ray diffraction  
Computational methods  
Polysaccharides  
Macrocyclic antibiotic  
Pirkle type CSP  
Chiral selector

## ABSTRACT

An overview of the state-of-the-art in LC enantiomer separation is presented. This tutorial review is mainly focused on mechanisms of chiral recognition and enantiomer distinction of popular chiral selectors and corresponding chiral stationary phases including discussions of thermodynamics, additivity principle of binding increments, site-selective thermodynamics, extrathermodynamic approaches, methods employed for the investigation of dominating intermolecular interactions and complex structures such as spectroscopic methods (IR, NMR), X-ray diffraction and computational methods. Modern chiral stationary phases are discussed with particular focus on those that are commercially available and broadly used. It is attempted to provide the reader with vivid images of molecular recognition mechanisms of selected chiral selector–selectand pairs on basis of solid-state X-ray crystal structures and simulated computer models, respectively. Such snapshot images illustrated in this communication unfortunately cannot account for the molecular dynamics of the real world, but are supposed to be helpful for the understanding. The exploding number of papers about applications of various chiral stationary phases in numerous fields of enantiomer separations is not covered systematically.

© 2009 Elsevier B.V. All rights reserved.

## Contents

1. Introduction.....	815
2. Basic principles of chiral recognition—from a historic perspective to a dynamic view.....	816
3. Thermodynamics.....	819

**Abbreviations:** Ac-Phe, *N*-acetyl-phenylalanine; AGP,  $\alpha_1$ -acid glycoprotein; ADMPC, amylose tris(3,5-dimethylphenylcarbamate); ANN, artificial neural networks; ANOVA, analysis of variance; ATR, attenuated total reflectance; AX, anion-exchanger; CBH, cellobiohydrolase; CE, crown-ether (in context of chiral selector); CD, circular dichroism (in context of spectroscopy); CD, cyclodextrin (in context of chiral selector); CDMPC, cellulose tris(3,5-dimethylphenylcarbamate); CIS, complexation-induced chemical shift ( $\Delta\delta$ ); CLEC, chiral ligand exchange chromatography; CMPA, chiral mobile phase additive; CoMFA, comparative molecular field analysis; CoMSIA, comparative molecular similarity index analysis; CS, chiral selector; CSP, chiral stationary phase; DEA, diethylamine; DNB, 3,5-dinitrobenzoyl; DNP, 2,4-dinitrophenyl; EEC, enthalpy–entropy compensation; ELSD, evaporative light scattering detection; FMOC, fluorenylmethoxycarbonyl; Glob-MolInE, global molecular interaction evaluation; HOMO, highest occupied molecular orbital; HILIC, hydrophilic interaction chromatography; HR/MAS, high-resolution magic angle spinning; HSA, human serum albumin; IRE, internal reflection element; Leu, leucine; LFER, linear free energy relationship; LSER, linear solvation energy relationship; LUMO, lowest unoccupied molecular orbital; MCTA, microcrystalline cellulose triacetate; MD, molecular dynamic; MLR, multiple linear regression; MM, molecular mechanics; *N*-Me-Leu, *N*-methyl leucine; NOE, nuclear Overhauser effect; NOESY, nuclear Overhauser effect spectroscopy; NP, normal-phase; OVM, ovomucoid; PLS, partial least squares in latent variables; PO, polar organic (mode); QD, quinidine; QM, quantum mechanical; QN, quinine; QSERR, quantitative structure–enantioselective retention relationship; QSPR, quantitative structure–property relationship; QSRR, quantitative structure–retention relationship; ROE, rotating frame nuclear Overhauser effect; ROESY, rotating frame nuclear Overhauser effect spectroscopy; SA, selectand; SCX, strong cation exchanger; SFC, super-/subcritical fluid chromatography; SMB, simulated moving bed; TAG, teicoplanin aglycone; TFA, trifluoroacetic acid; trNOE, transferred nuclear Overhauser effect; VCD, vibrational circular dichroism; WAX, weak anion-exchanger (WAX); Wf, warfarin; XRD, X-ray diffraction; ZWIX, zwitterionic ion-exchanger.

\* Tel.: +43 1 4277 52323; fax: +43 1 4277 9523.

E-mail address: [Michael.Laemmerhofer@univie.ac.at](mailto:Michael.Laemmerhofer@univie.ac.at).

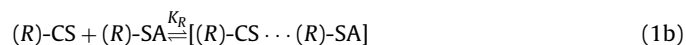
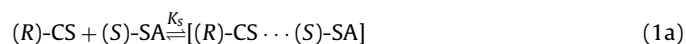
3.1.	Thermodynamics of CS–SA association .....	819
3.2.	Additivity of incremental contributions .....	819
3.3.	Thermodynamics of direct liquid chromatographic enantiomer separation .....	819
3.4.	Site-selective thermodynamics .....	822
4.	Extrathermodynamic approaches to study chiral recognition .....	824
5.	Kinetics, peak dispersion and tailing .....	826
6.	Tools and methods for the investigation of retention and chiral recognition mechanisms .....	827
6.1.	Chromatographic studies and retention models .....	827
6.2.	Vibrational spectroscopy .....	828
6.3.	NMR spectroscopy .....	830
6.4.	Single-crystal X-ray diffraction analysis .....	832
6.5.	Computational methods .....	833
6.5.1.	Chemoinformatics .....	833
6.5.2.	Molecular modeling .....	833
7.	Chiral stationary phases and their properties .....	833
7.1.	Polysaccharide CSPs .....	834
7.2.	CSPs based on synthetic polymers .....	836
7.3.	Protein CSPs .....	838
7.4.	Cyclodextrin CSPs .....	839
7.5.	Macrocyclic antibiotics CSPs .....	841
7.6.	Chiral crown-ether CSPs .....	844
7.7.	Donor–acceptor phases (brush-type or Pirkle-type CSPs) .....	847
7.8.	Chiral ion-exchangers .....	848
7.9.	Chiral ligand-exchange CSPs .....	851
8.	Concluding remarks .....	851
	Nomenclature .....	852
	Acknowledgements .....	852
	References .....	852

## 1. Introduction

Chiral recognition and enantiomer distinction are fundamental phenomena in nature and chemical systems. It has impact in various chemical fields that are dealing with bioactive compounds, in particular drug discovery, development of agrochemicals, research on food additives, fragrances, chiral pollutants, etc. [1,2]. In general, however, most significant developments in chirotechnologies were spurred by demands of drug discovery in pharmaceutical industries [3]. Since a majority of newly developed drug candidates are chiral and the individual enantiomers of such chiral species usually exhibit distinct pharmacological profiles (either in view of pharmacodynamics, pharmacokinetics or both), it is now common to perform biological and toxicological tests of new drug entities with racemate and individual enantiomers as well. To cope with stereoselectivity issues in such research enantioselective liquid chromatography emerged as one of the major workhorses. In fact, liquid chromatographic enantiomer separation methods have thus been established as important tools in drug discovery, for both analytical purposes (like enantiomer composition determination, quality control of enantiomeric drugs or stereoselective pharmacokinetic analysis) and as preparative technique [4,5] which gives rapid access to individual enantiomers for biological testing.

The fundamental basis for distinction of enantiomers, be it in a biological or chromatographic system, is transformation of enantiomers to diastereomers or creation of a diastereomeric relationship between ligated enantiomers (selectand, SA) and a receptor (chiral selector, CS). Along this line, various methodologies are, in principle, amenable for liquid chromatographic enantiomer separation: (1) One approach involves the formation of diastereomers through precolumn derivatization of the selectand with a single enantiomer of a chiral derivatizing agent followed by chromatographic separation on achiral stationary phases with achiral eluents (*indirect approach*) [6]. Stringent demands on enantiomeric purity of the derivatizing agent, demand of a suitable functionality for straightforward and smooth derivatization, phenomena like kinetic resolution and racemization make this indirect method

less attractive. (2) A second approach makes use of a chiral auxiliary which is added to the mobile phase in enantiomeric form and separation relies on the reversible formation of transient diastereomeric molecule associates in the mobile phase yielding eventually inequivalent adsorption and retention for individual enantiomers of selectands on an achiral stationary phase. This *chiral mobile phase additive (CMPA) mode* has virtually no practical utility in HPLC nowadays due to chiral selector consumption and detection interferences caused by the additive. (3) The third mode, direct liquid chromatographic enantiomer separation with chiral stationary phase (CSP) (*CSP mode*) is nowadays the method of choice. It makes use of chiral adsorbents, in most cases spherical porous silica supports functionalized with a chiral selector that is covalently linked or physically adsorbed. It relies on the reversible formation of transient diastereomeric molecule associates on the surface of the adsorbent according to the equilibrium reactions outlined in the following equations:



The energetic differences between the two diastereomeric complexes (right hand side species in Eqs. (1a) and (1b)) as indicated by distinct association constants  $K_R$  and  $K_S$  are the fundamental physical basis for stereoselective retention in that chromatographic system.

Over the last two decades or so, a lot of CSPs have been developed for HPLC by various research groups with pioneering works stemming amongst others from Davankov, Pirkle, Okamoto, Blaschke, Allenmark, Hermansson, Armstrong, Gasparrini, and Lindner [7,8]. Powerful chiral separation media and enantioselective columns, respectively, emerged from this evolution which can be classified as follows:

- Macromolecular selectors:
  - Biopolymer-derived (proteins, polysaccharide derivatives);

- Synthetic polymers (polytartaramides, poly(meth)acrylamides).
- Macrocylic selectors:
  - Cyclodextrins;
  - Macrocylic antibiotics;
  - Chiral crown ethers.
- Low-molecular mass selectors:
  - Donor–acceptor (Pirkle-type) selectors;
  - Chiral ion-exchange type selectors;
  - Ligand exchange selectors (chelating agents).

In many instances, for a long time it remained somehow veiled how these CSPs distinguish between enantiomers and in fact there still exists a widespread deficiency in the understanding of the underlying molecular basis of such chiral chromatographic ligands. Nevertheless, a number of studies appeared in recent literature which addressed specific molecular recognition phenomena of chiral stationary phases and corresponding selector moieties, respectively, with modern methods of chromatographic, spectroscopic, computational chemistry and so forth. The present article is attempted as tutorial review providing an updated overview about most important modern CSPs and their chiral recognition and separation mechanisms [9]. Due to the overwhelming number of literature on this topic the cited papers need to be restricted to selected representative and/or educational examples.

## 2. Basic principles of chiral recognition—from a historic perspective to a dynamic view

Early attempts to rationalize chiral distinction at the molecular level have led to the proposal of rigid geometric models which from biochemical/pharmacological viewpoint have been reviewed by Bentley [10]. In 1933, Easson and Stedman postulated a structural model to explain stereoselective binding of chiral molecules to a protein receptor and its implication on physiological activities of enantiomers [11]. In its original form this model states that a minimum of three configuration-dependent attractive contact points between a chiral receptor, the three binding sites of which were assumed to be on a planar surface, and a chiral substrate is required for chiral distinction (“three-point attachment model”) (Fig. 1). When three groups (a, b, c) of the tetrahedral carbon atom bind to a receptor surface at specific sites A, B, and C (Fig. 1) it is impossible that the enantiomer undergoes an equivalent binding via the same three-contact points. It was later adapted by Ogsten for enzyme reactions (1948) [12]. However, a fourth condition, not explicitly stated by Easson and Stedman, is often neglected, namely that the substrate can approach the receptor only from the surface, but not from the interior. This fourth requirement, yet, was clearly emphasized later by Wilcox et al. [13]. By the early 1980s, several researchers had emphasized that diastereoisomerism was the fundamental prerequisite and that a three-contact point interaction is not needed for chiral recognition. In this context, Salem et al. shifted the discussion to differential interaction energies calculated between two chiral tetrahedral molecules for homo- and heterochiral situations expressing his belief that six-center forces occurring simultaneously between triplets of atoms (one triplet in each molecule) were responsible for chiral recognition [14]. The Salem model was criticized by Topiol and Sabio who extended it to an eight-center (four-contact point) interaction model as requirement for enantiodifferentiation (Fig. 2) [15]. While the six-center interactions ABC with A'B'C' in Fig. 2 are identical for RS' and RR' complexes, the three-point rule excludes the RR' structure due to the steric collision involving D'. This RR' structure is excluded on the basis of differences for calculations with an eight-center term which can thus explain chirality effects. The interactions at the four-contact points could be either attractive or repulsive. In absence of con-

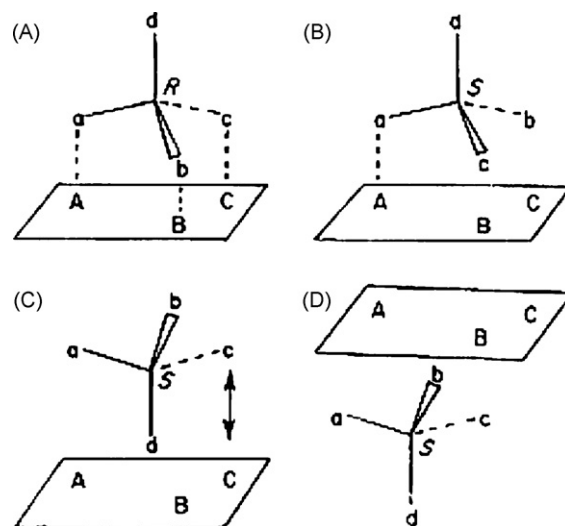


**Fig. 1.** The Easson–Stedman model as proposed originally. For the purpose of making *RS* configurational assignments, it is assumed that the priority sequence is  $a > b > c > d$ . The binding sites for a, b, and c are represented as A, B, and C. In the Easson–Stedman model (A), the *R*-enantiomer can bind at all three sites and would be assumed to be the physiologically active material. However, the *S*-enantiomer is limited to a single contact point (B). An alternative possibility (C) for the *S*-enantiomer is ruled out because of steric hindrance by the d group. The distances, a–A, b–B, and c–C (indicated by the double arrow) are too large to permit binding. Further, the approach of the *S*-enantiomer from the interior (D) is not allowed. Reprinted with permission from Ref. [10].

straints such as imposing a specific orientation, a four-contact point model was finally concluded to be the minimal requirement for chiral recognition, and this was also claimed by Bentley [10,16]. In a later paper, Topiol provided a more general criterion for molecular recognition [17]. This criterion was the inequality of the distance matrices of diastereomeric complexes of chiral compounds with a

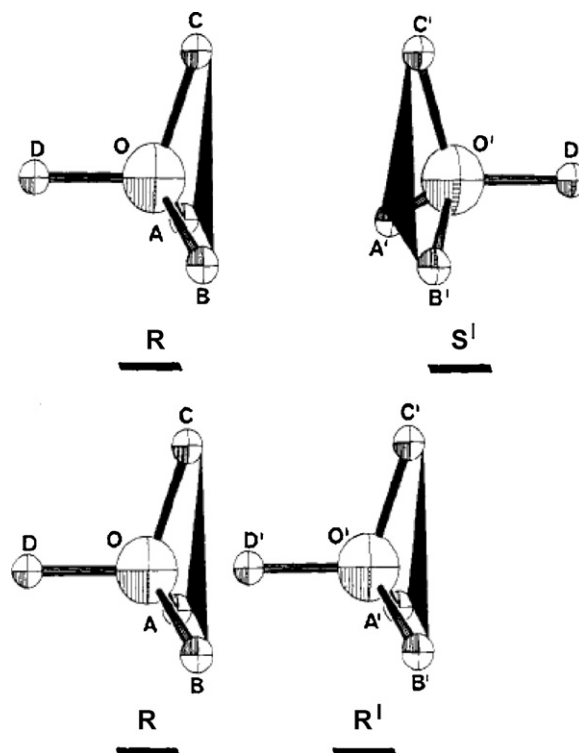


**Fig. 2.** Topiol model of chiral recognition. Reprinted with permission from Ref. [15].

selector. As example, the RR and RS complexes of CHFCIBr were analyzed with regards to their distance terms. Of 100 collected distance terms, there were 8 unequal elements. Such a distance matrix analysis approach was suggested to relieve the demand for the arbitrary assignment of contact points, but seems to be less illustrative. Further extensions and details on these and similar models about chiral recognition can be found elsewhere [10,18,19].

Many of the above considerations have found their way to explain mechanisms of chromatographic enantiomer distinction [9]. Basically, the “three-point interaction model” is still the most prominent model invoked to explain chiral recognition. Already in 1952 Dalglish adapted the “3-point attachment model” for chromatographic enantiomer separation by TLC [20]. Pirkle and Pochapsky restated this “three-point rule” in a slightly modified version [7] and a newer interpretation can be found in a paper by Davankov [21].

Like in the biochemical field, this simplistic model has been under debate since then also in the chromatographic community [19,21,22] and nowadays it is common agreement that not all three interactions need to be attractive, but both attractive and repulsive interactions are equivalent forces in generating stereoselectivity. For example, two interactions can be repulsive if the third one is strong enough to promote the formation of at least one of the two diastereomeric complexes [21]. Moreover, one has to bear in mind that many typical interactions are rather multipoint than single-point interactions in their nature and thus minimize the need for additional supportive interactions. While, for example, hydrogen bonding and end-to-end dipole interactions are considered as single-point interactions and therefore count only for one interaction point each, dipole–dipole stacking and  $\pi$ – $\pi$ -interactions are multipoint interactions in nature and may be worth for at least two interaction points each [7]. Molecules intrinsically containing chiral centers incorporated into rigid elements such as a cyclic ring require less interactions; they meet the geometrical requirements for chiral recognition more easily than do conformationally labile structures [21]. Two of the four bonds of the asymmetric centers that are incorporated into a rigid ring system are fixed which enforces a molecular rigidity and thus the stereoisomers can be easier distinguished. It is now common perception that a single interaction with a rigid plane or its surface can count for at least two contacts. Last but not least it was emphasized that the environment (solvent molecules and adsorbent surfaces) may assist in chiral recognition [21].

In spite of its criticism, the “three-point interaction model” is still frequently employed to explain chiral recognition to students because of its favorable illustrative character. We use it here as a starting point for the following discussion. Its adaption and modification for chiral distinction by CSPs is graphically illustrated in Fig. 3. The CSP is composed of a chiral selector and a support (usually porous silica) that are connected by a spacer. The selectand enantiomers are approaching the selector that accommodates the active chiral distinction site, driven by some physical forces or incidentally colliding with it, and due to specific spatial constraints one of the enantiomers binds more strongly (*ideal fit*) than the other (*non-ideal fit*) leading eventually to distinct binding constants  $K_S$  and  $K_R$  for the underlying CS–SA equilibrium reactions (Eqs. (1a) and (1b)) (note that in the given example  $K_S > K_R$ ). Effective binding can be achieved if there is

- *steric fit* (i.e. size and shape complementarity) of the binding guest (SA) with regards to binding site of CS which is often prearranged as binding pocket or cleft.
- *electrostatic fit (functional fit)* (i.e. a favorable geometric and spatial orientation of complementary functional groups that are amenable for electrostatic type interactions such as ionic interaction, H-bond-mediated ionic interaction, hydrogen bonding,

dipole–dipole interactions, face-to-face or face-to-edge  $\pi$ – $\pi$ -interactions, cation– $\pi$ - and anion– $\pi$  interactions; see Fig. 4).

- *hydrophobic fit* (i.e. if hydrophobic regions of both binding partners can spatially match each other as to release, in aqueous media, their entropically unfavorable, structurally ordered water shell on the molecular surface, and eventually allow for close intermolecular contacts of the lipophilic moieties thus leading to mutual saturation of their hydrophobic surfaces. Such hydrophobic interactions in aqueous media are regarded as merely entropic in nature).
- *dynamic fit and induced fit* (as to maximize binding interactions by dynamic and conformational adaptation in the course of complex formation) [19,23–25].
- mutual saturation of extended molecular surfaces by each other (i.e. of host and guest).

Overall, in the majority of cases complex stability is driven by the strength of non-covalent interactions (Fig. 4) (see also later). Thereby, the components of the mobile phase need to be considered as important factors, as they define the properties of interaction environment in which chromatographic chiral recognition takes place. Solvents can interfere in a highly specific manner with specific CS–SA interactions and thus modulate both strength and quality of the molecular recognition processes. Solvents of high polarity effectively attenuate the strength of electrostatic interactions. In contrast, hydrophobic interactions are of substantial relevance in aqueous or hydro-organic eluents only. In this context, it is noted that in a binding pocket the local dielectric may constant differ dramatically from that of the bulk medium. For example, for proteins in aqueous solutions the local dielectric constants (relative permittivity in relation to permittivity in vacuum) within binding pockets may reach values in the range of 1–20, very low values as compared to 80 in the surrounding bulk water medium [28]. Evidently, hydrophobic environments may clearly strengthen the efficiency of electrostatic interactions while polar environments will most likely weaken them. Hydrogen bonds that are shielded by hydrophobic moieties may be particularly suitable to stabilize CS–SA complexes.

Ionic interactions are fairly strong, even in polar protic solvents, but they may be readily weakened by ionic shielding through addition of salts or buffer ions. Due to their long-range nature they may be effective for establishing the first contact between the CS and SA species. As long as they are not mediated via a H-bond, they are owing to their non-directional long-range character most likely occurring non-stereoselectively. In sharp contrast, H-bond interactions,  $\pi$ – $\pi$ -interactions and dipole stacking are short-range directional forces that become activated only if the binding geometries are matched within more or less narrow constraints. For example, H-bond distances are typically in the range of 2.8–3.2 Å between involved heteroatoms and to a large extent determine the strength of a H-bond. H-bond angles are different for distinct H-bond types as exemplified below for N–H...O=C H-bonding and are less of relevance for their strength (Fig. 5). On the other hand, typical distances between planar surfaces involved in face-to-face  $\pi$ – $\pi$ -interactions are also in the range of about 3–3.5 Å. Due to their directed nature, H-bonds,  $\pi$ – $\pi$ -interactions and dipole stacking are often responsible for chiral recognition as they may more likely evolve stereoselectively due to narrow constraints and thus induce or trigger stereoselectivity.

Intuitively, one may expect that effective enantioselectivity may arise upon strong binding between CS and SA (i.e. for host–guest complexes with high binding constants or low dissociation constants). While this is not necessarily the case, it is indeed often observed within a homologous series that enantioselectivity increases with binding strength. For instance, an  $\alpha$  with  $k_2$  was observed for DNB-amino acids on quinine carbamate based CSPs



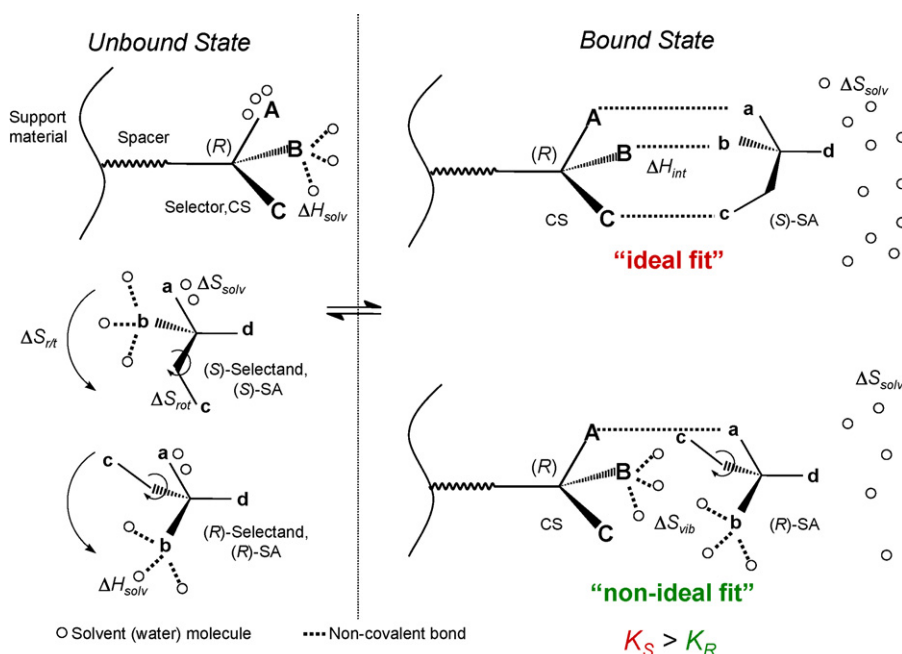


**Fig. 3.** “Three-point interaction model” and thermodynamic contributions to Gibbs free energy of CS–SA complexation according to Eq. (6), as adapted from Refs. [10,11,20] and Ref. [26] to explain chiral recognition by a CSP (here with arbitrary *R*-configuration of the chiral selector). In the unbound state the SA enantiomers can freely move which is associated with a favorable translational and rotational entropy contribution ( $\Delta S_{rt}$ ) that will be lost in the bound state (complex destabilizing binding increment). Moreover, the SA is flexible with a considerable degree of freedom for internal rotations ( $\Delta S_{rot}$ ) which may be lost upon binding (like illustrated in the figure for the *S*-SA enantiomer) (complex destabilizing) or may still exist (at least partly) (as illustrated for *R*-SA). Whatsoever, even in the complexed state there may be some dynamic movement of the SA in the binding site ( $\Delta S_{vib}$ ) which may be energetically favorable as compared to a situation where this is possible only to a minor degree (e.g. *S*-SA). Binding sites of CS and SA (e.g. B and b) may be solvated in free state (e.g. amide groups via H-bonds) ( $\Delta H_{solv}$ ). In order to form a non-covalent bond between the interaction sites B and b, the solvation shell must be stripped off, a process for which a part of the energy gain originating from the intermolecular CS–SA interaction ( $\Delta H_{int}$ ) will be consumed again. Solvent molecules that are loosely associated in an ordered manner (unfavorable from an entropic point of view) such as water molecules on a hydrophobic surface (as schematically indicated at A and a groups of CS and SA, respectively) will be set free upon interaction of these moieties releasing the solvent molecules into a non-ordered state ( $\Delta S_{solv}$ ) which is associated with an increase in entropy (complex stabilizing effect, e.g. of hydrophobic interactions). Overall, the energy balance over all binding contributions will decide about the resultant Gibbs free energy of CS–SA association and the (relative) binding strength of the individual enantiomers.

(note,  $\log \alpha$  vs.  $\log k$  plots may sometimes be helpful in identifying peculiarities in terms of chiral recognition mechanisms within a series of structural analogs) [29]. This *theorem* has been known for long time in pharmacology as *Pfeiffer's rule* [30] which states that the stereoselectivity of drugs will increase with their potency. The validity has been debated and it is accepted today that this principle is of limited applicability only. While multiple interactions facilitate the stereodistinction process (as above stated by the three-point

interaction rule), it is also important that the distinct interactions are well balanced. Binding interactions have sometimes been differentiated into “leading interactions” (dominating interactions), which are strongest and drive the association of the analyte and the CS and which bring the solute in close proximity to the CS, as well as “secondary interactions” (supporting interactions) [31,32]. The leading interaction is usually the strongest type of non-covalent force and will determine the retention of a pair of enantiomers on a CSP, while the secondary interaction (of short-range type) will determine the enantiorecognition. Since the leading interaction usually occurs non-stereoselectively, it needs to be balanced so that the secondary stereoselectively occurring interactions gain on influence.

Interaction forces	Lipophilicity	Relative strength [kJ·mol <sup>-1</sup> ]
<b>Electrostatic interactions (Complementarity)</b>		40
Ionic interactions (salt bridge) via H-bond		20
without H-bond		4 to 17
Ion-dipole interactions		4 to 17
H-bonds		4 to 17
Van der Waals forces		4 to 17
Orientation forces (permanent dipole -permanent dipole)		2 to 4
Induction forces (permanent dipole -induced dipole)		4 to 17
Dispersion forces (induced dipole -instantaneous dipole)		4
Aryl-aryl charge transfer ( $\pi$ - $\pi$ -interactions) face-to-face		
face-to-edge		
<b>Hydrophobic interactions (Similarity)</b>	Hydrophobicity	4

**Fig. 4.** Non-covalent interactions and intermolecular recognition forces, respectively, as well as their relative strengths *in vacuo*. Electrostatic interactions are governed by complementarity of involved functional groups in host and guest molecules and hydrophobic interactions (entropic contribution) on similarity principles of interactive sites. Their strength will be significantly altered by respective experimental conditions. Compiled from Ref. [27].

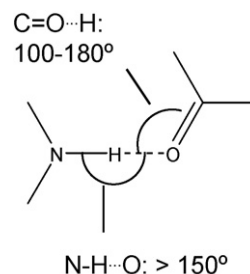


**Fig. 5.** Preferred geometries of directional H-bonds. The atoms N, H, and O are lying more or less on the same axis and the distances between N and O are typically between 2.8 and 3.2 Å. The angle N–H...O is almost always larger than 150°. On contrary, the angle C=O...H may vary to a larger extent and is typically found in the range between 100° and 180°. Adapted from Ref. [26].

Moreover, steric factors such as steric repulsion may play a major role in chiral recognition and hence it is not surprising that steric barriers such as bulky residues often enhance enantioselectivity levels. They may prohibit the access of the “unfavorable” enantiomer towards the active binding site thus leading to sometimes exceptional enantioselectivities. It is remarked that many of the powerful CSPs have some sort of rigid bulky elements incorporated for this purpose.

### 3. Thermodynamics

#### 3.1. Thermodynamics of CS–SA association

Equilibrium processes such as the CS–SA complexation depicted in Fig. 3 can be explained by energy balances of free and complexed states (see Eq. (1)) and are often studied based on thermodynamic considerations.

The equilibrium binding constant  $K_i$  (Eq. (1)) which measures the binding strength between CS and SA is related to the standard Gibbs free energy change  $\Delta G_i^\circ$  upon CS–SA complexation according to the following equation:

$$\Delta G_i^\circ = -RT \ln K_i \quad (2)$$

wherein  $R$  is the universal gas constant ( $8.3144 \text{ J mol}^{-1} \text{ K}^{-1}$ ),  $T$  the absolute temperature (in K), and subscript  $i$  denotes the corresponding species, i.e. here  $S$ - or  $R$ -enantiomer. It is evident that if a large energy difference is set free upon CS–SA association due to favorable energetical state of the bound versus the free SA this will inherently lead to strong binding with large association constant or low dissociation constant (which is the reciprocal of the former).

The Gibbs free energy of an equilibrium process is composed of enthalpic and entropic contributions ( $\Delta H_i$  and  $\Delta S_i$ ). The benefit from strong binding driven by intermolecular interactions as measured by the enthalpy change  $\Delta H_i$  of the process of complexation is usually paid off by an increase of order or decrease of disorder (entropic cost  $\Delta S_i$ ). This is cast into simple mathematics by the following well-known *Gibbs–Helmholtz equation*:

$$\Delta G_i^\circ = \Delta H_i^\circ - T \Delta S_i^\circ \quad (3)$$

Its combination with Eq. (2) gives the *van't Hoff equation* (Eq. (4)) which paves the way for straightforward determination of the macroscopic thermodynamic quantities of equilibrium processes such as the CS–SA complexation from slopes and intercepts of plots of  $\ln K_i$  versus  $1/T$  (van't Hoff plots) by thermodynamic analysis.

$$\ln K_i = -\frac{1}{T} \frac{\Delta H_i^\circ}{R} + \frac{\Delta S_i^\circ}{R} \quad (4)$$

The difference for two enantiomers in their Gibbs free energy changes upon complexation gives a measure for the enantioselectivity  $\alpha$  of a chiral selector for the given SA–enantiomer pair and the corresponding Eq. (5) can be derived from Eq. (2) (with  $K_S > K_R$ ; i.e.  $S$ -enantiomer stronger interacting with CS) as

$$\Delta \Delta G_{R,S}^\circ = \Delta G_S^\circ - \Delta G_R^\circ = -R \cdot T \ln \frac{K_S}{K_R} = -R \cdot T \ln \alpha \quad (5)$$

By its combination with the Gibbs–Helmholtz eq. the van't Hoff plot with  $\ln \alpha$  versus  $1/T$  allows to derive the corresponding enthalpic and entropic contributions ( $\Delta \Delta H^\circ$  and  $\Delta \Delta R^\circ$ ) to enantiomer distinction (enantioselectivity).

#### 3.2. Additivity of incremental contributions

One should be aware that the Gibbs free energy of CS–SA binding is a macroscopic entity which is the result of a number of additive contributions (see also below). In absence of cooperative effects it may, for a better understanding or calculation purposes (such as

in force fields), be partitioned into a number of additive energy components (see also Fig. 3) [33–35] as given by the following equation:

$$\Delta G_{binding}^{CS-SA} = \Delta G_{solv} + \Delta G_{int} + \Delta G_{conf} + \Delta G_{motion} \quad (6)$$

wherein the individual terms account for the change in free energies upon CS–SA binding due to (1) solvation effects ( $\Delta G_{solv}$ ), (2) CS–SA interactions (non-covalent bonds) ( $\Delta G_{int}$ ), (3) conformational changes in CS and SA upon binding ( $\Delta G_{conf}$ ), and (4) motional restrictions and residual motions in the complex ( $\Delta G_{motion}$ ). In this context, it needs to be emphasized that the interaction term ( $\Delta G_{int}$ ) itself represents a macroscopic thermodynamic quantity which is obtained as a weighted average (by a Boltzmann distribution) of all possible microscopic diastereomeric complexes [36]. A microstate in this context is any unique orientation of the SA towards the chiral selector in a diastereomeric complex. The latter term ( $\Delta G_{motion}$ ) is made up by free energy quantities due to loss of internal rotations in CS and SA ( $\Delta G_{rot}$ ), due to loss of rotational and translational degrees of freedom ( $\Delta G_{r/t}$ ), and due to new vibrational modes in the associated state ( $\Delta G_{vib}$ )

$$\Delta G_{motion} = \Delta G_{rot} + \Delta G_{r/t} + \Delta G_{vib} \quad (7)$$

Likewise, also the chiral recognition process can be partitioned into such increments ( $\Delta \Delta G_j$ ). In the common perception, chiral distinction arises from a different number or significantly different strength of non-covalent binding interactions in the diastereomeric CS–SA complexes yielding  $\Delta \Delta G_{int} \neq 0$ . However, also energy differences from other components might contribute to chiral distinction in a positive or negative way such as for example solvational effects. Solvated functional groups must strip off the solvation shell before they can interact with complementary functional groups of the binding partner. The energy cost for desolvation is identical for two enantiomers, while the resolution process after formation of the diastereomeric complexes may be energetically distinct for the two enantiomers providing a weak component  $\Delta \Delta G_{solv} \neq 0$  to the overall process of chiral recognition. The free energy component  $\Delta G_{motion}$  is mostly entropic in nature. As long as there is no on/off scenario with regards to the two enantiomers (i.e. one enantiomer is bound, the other not), the loss of translational and rotational degrees of freedom is supposed to be largely identical for two enantiomers, i.e.  $\Delta \Delta G_{r/t} = 0$ . On the other hand, both  $\Delta G_{rot}$  and  $\Delta G_{vib}$  are conceivable to be distinct in diastereomeric complexes. For example, if a rotatable group is exposed to the exterior in one of the diastereomeric complexes it may retain a large portion of rotational degree of freedom. If such a rotation is sterically hindered and thus frozen in the other diastereomeric complex, a significant free energy difference  $\Delta \Delta G_{rot} \neq 0$  may arise. Likewise, the  $\Delta G_{vib}$  component may be distinct for two complexed SA–enantiomers. Upon complexation, new vibrational modes are introduced and a looser complex may have a larger vibrational entropy contribution than a tighter one. Hence, such components might also produce a contribution to chiral distinction from a purely energetic point of view.

Overall, the net effect in binding energies is a result of the energy balance over all individual contributions.

#### 3.3. Thermodynamics of direct liquid chromatographic enantiomer separation

Thermodynamic quantities of chromatographic equilibrium processes such as the direct enantiomer separation with CSPs can be deduced by measurement of the chromatographic parameters over a certain temperature range from van't Hoff plots by substituting in Eq. (2)  $k_i/\phi$  for  $K_i$  according to the following equation:

$$k_i = \phi \cdot K_{D,i} \quad (8)$$

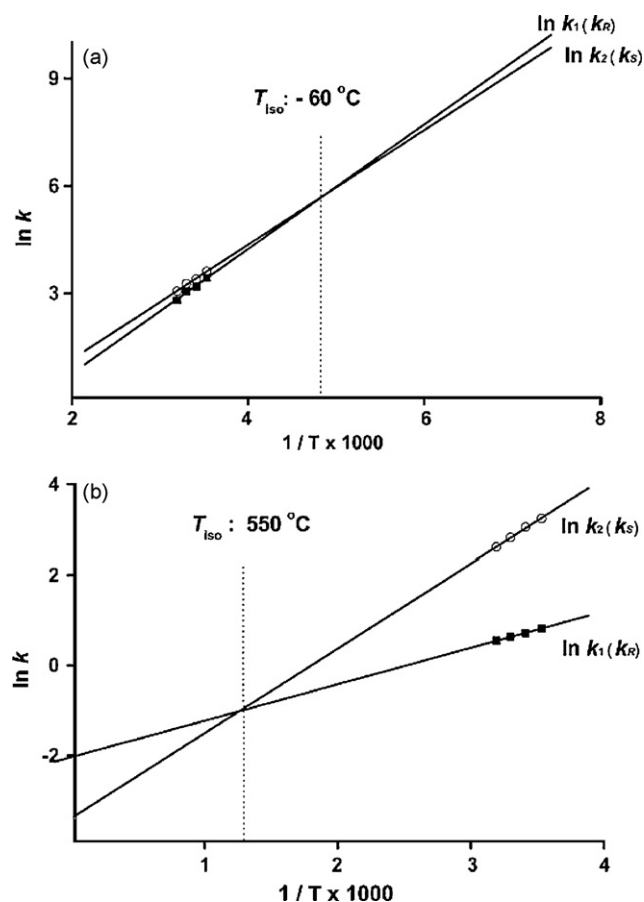


**Fig. 6.** Plots of relationships between  $\ln k$  vs.  $1/T$  (van't Hoff plots) for two distinct scenarios, as measured for 2-(*N*-isopropylamino)-1-phenylethanol (a) and 2-(*N*-isopropylamino)-2-phenylethanol (b) on a chiral crown ether based CSP. The two lines in (a) and (b) represent the trend lines for the two enantiomers. Each line has a characteristic slope corresponding to  $\Delta H^\circ/R$  and a characteristic  $y$ -intercept corresponding to  $\Delta S^\ddagger$  ( $\Delta S^\ddagger = \Delta S^\circ + \ln \phi$ ). Reprinted with permission from Ref. [39].

wherein  $\phi$  represents the volume phase ratio of stationary and mobile phase ( $V_s/V_m$ ) which is equal to  $\phi = (1 - \varepsilon)/\varepsilon$  wherein  $\varepsilon$  is the total porosity of the column, and  $K_{D,i}$  is the equilibrium distribution coefficient.

While the slope of  $\ln k$  versus  $1/T$  plots provides information on the enthalpy change upon adsorption of the overall process  $\Delta H$  (heat of adsorption), it must be borne in mind that the intercept represents an apparent entropy change  $\Delta S^\ddagger$  ( $\Delta S^\ddagger = \Delta S^\circ + \ln \phi$ ) [37]. The intersection of the lines is commonly referred to as the isoelectronic temperature ( $T_{iso}$ ), where enthalpy and entropy compensate each other and the two enantiomers coelute. Note the reversal of elution order when this  $T_{iso}$  is traversed (see Fig. 6). In an analogous way, the corresponding thermodynamic quantities for enantiomer separation  $\Delta \Delta H^\circ$  and  $\Delta \Delta S^\circ$  can be deduced from slope and intercept of van't Hoff plots of the chromatographic separation factor  $\ln \alpha$  versus  $1/T$  (note, the phase ratio is cancelled out in this case). In general, four distinct scenarios are conceivable: enthalpic control with or without entropic compensation effect (*vide infra*), and entropic control with or without compensation effect (the latter being seldom observed [38]).

It is important to realize that the thermodynamic quantities thus derived are macroscopic entities for the adsorption process of the SA-enantiomers on the CSP surface which do not account for the surface heterogeneity of CSPs and the associated distinct adsorption behavior of enantiomers at different sites [40]. Rather these

individual contributions are simply lumped together (*vide infra*). Nevertheless, such van't Hoff analysis may still yield useful global information about the adsorption process.

As far as liquid chromatographic enantiomer separation is concerned, in most instances van't Hoff plots reveal linear relationships ( $\Delta H^\circ$  invariant with  $T$ ) with a strong preference for exothermic adsorption processes as can be inferred from a negative sign of the derived  $\Delta H^\circ$  values (as exemplified in Fig. 6). This is in line with our perception that the retention of enantiomers in HPLC on most CSPs is dominated by adsorption processes that are driven by (mostly electrostatic type) non-covalent interactions. In the majority of cases, there is also an opposing (destabilizing) entropic effect. This "entropic cost" is known as "enthalpy-entropy compensation" or simply "compensation effect". It may be readily explained by the increase of order (or loss of degree of freedom) and thus loss of entropy in complexed (adsorbed) state. A favorable entropy contribution, in contrast, has been frequently explained by excessive solvent molecule release upon CS-SA binding associated with an increase in entropy. Similar considerations as for adsorption hold for the corresponding thermodynamic quantities for enantiomer separation.

Thermodynamic parameters are depending on type of solute, CSP and mobile phase and have been determined for virtually all important CSPs with more or less extended sets of analytes including, e.g. polysaccharide [41–44], protein [45], tartaric acid [46], macrocyclic antibiotics [47–49], cyclodextrin [50–52], crown ether [39], donor-acceptor (Pirkle-type) [53], ligand exchange [54] and cinchona carbamate type CSPs [33,55–57]. It is evident that most useful findings can be derived by comparison of thermodynamic data of CS-SA pairs (e.g. of structural analogs) with identical or distinct conditions. Careful inspection of the thermodynamic quantities for a wide variety of different CSP-analyte-mobile phase systems has shown that in most cases heats of adsorption are negative (exothermic reaction), a situation that usually becomes evident in a decrease in retention with increasing temperature. Moreover, retention and chiral recognition on CSPs is usually *enthalpically controlled*, i.e.  $|\Delta H^\circ| > |T\Delta S^\circ|$  and  $|\Delta \Delta H^\circ| > |T\Delta \Delta S^\circ|$ . However, the opposite behavior of *entropically controlled* adsorption [40] and more often separation, viz. enantioselectivity being improved on increasing temperature, has also been observed in various cases [49,58–63]. An experimental example in which both of these cases were obtained for two structural analogs, namely 2-(*N*-isopropylamino)-1-phenylethanol and 2-(*N*-isopropylamino)-2-phenylethanol, on a single chiral crown ether based CSP is given in Fig. 6a and b [39]. Based on van't Hoff equations,  $T_{iso}$  was calculated by extrapolation for 2-(*N*-isopropylamino)-1-phenylethanol and 2-(*N*-isopropylamino)-2-phenylethanol to be  $-60^\circ\text{C}$  and  $550^\circ\text{C}$ , respectively. In the former case, the HPLC running temperatures were above  $T_{iso}$  (Fig. 6a) so that the separation of the enantiomers increased as column temperature was raised (*entropically controlled separation*), while in the latter case they were below  $T_{iso}$  (Fig. 6b) so that the enantiomer separation could be improved with a temperature decrease (*enthalpically controlled situation*). As can be seen from above example,  $T_{iso}$  is usually not within the investigated experimental temperature range and temperature is therefore not an instrumental variable to reverse the elution order. However, Pirkle found a reversal of elution order on a brush-type CSP at about  $0^\circ\text{C}$  which has been interpreted as a change in the dominating mechanism (in terms of enthalpy-entropy control) due to binding site-related (de)solvation phenomena [64]. Recently, Yao et al. reported on the temperature-induced inversion of elution order in the chromatographic enantiomer separation of 1,1'-bi-2-naphthol on an immobilized polysaccharide CSP [63].  $T_{iso}$  was calculated to be  $31.4^\circ\text{C}$  with hexane/2-propanol (92:8, v/v) and dropped to  $-8.2^\circ\text{C}$  with hexane/2-propanol/THF (93:2:5, v/v/v).

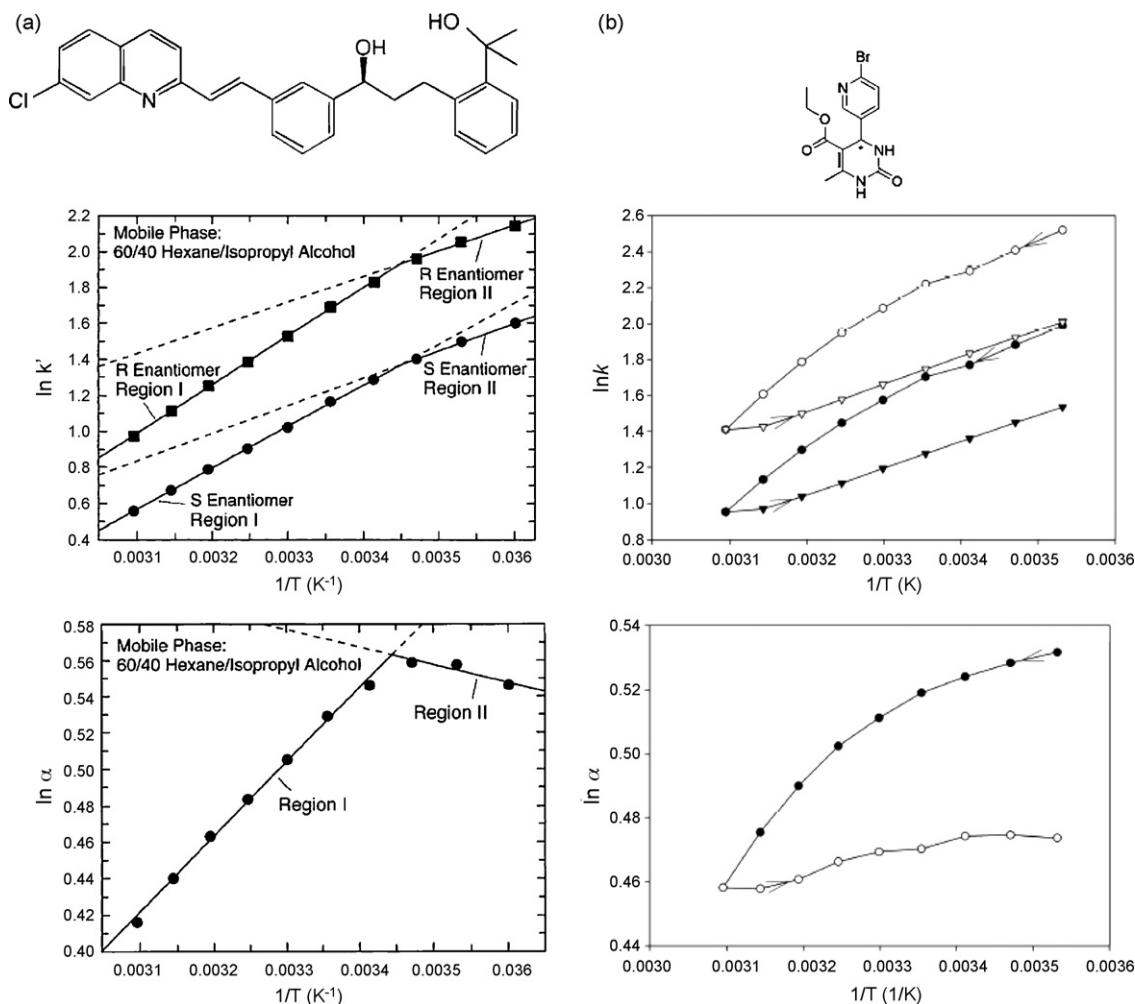


**Fig. 7.** Non-linear van't Hoff plots (a) due to conformational changes of the polysaccharide selector [71], and (b) hysteresis behavior due to slow temperature-dependent equilibration [70]. Experimental conditions: (a) CSP, Chiralcel OJ; eluent, 40% (v/v) 2-propanol in *n*-hexane; (b) CSP, Chiralpak AD; eluent, 15% (v/v) ethanol in *n*-hexane. Reprinted with permission from Refs. [71,70].

Contrary to these situations where enthalpy is invariant with temperature, also non-linear van't Hoff plots have been reported and are certainly of particular interest from a mechanistic point of view (Fig. 7). If the CSP is subject to a significant structural change at a specific temperature (e.g. change in the conformational state), van't Hoff plots may be non-linear indicating an alteration in the adsorption mechanism (Fig. 7a). This has been observed with protein type CSPs in HPLC [65,66], and polysaccharide CSPs in HPLC [67] as well as SFC [37,61,68]. Pirkle found non-linear van't Hoff plots for conformationally rigid spirolactams on a brush-type CSP [69]. Since the shape of the plots depended on the 2-propanol content in the eluent, it was argued that solvation effects of the selector were responsible for this uncommon behavior.

Recently, unusual temperature-induced behaviors have been identified for HPLC enantiomer separation of chiral dihydropyrimidinones on polysaccharide CSPs in which van't Hoff plots acquired by gradually heating the column from 10 to 50 °C and then stepwise cooling from 50 to 10 °C were not superimposable, e.g. on an ethanol-solvated Chiralpak AD-H column. The generated van't Hoff plots showed a significant hysteresis form (Fig. 7b) [70]. The thermally induced path-dependent behaviors were caused by slow equilibration which was evidenced by the disappearance of the hysteresis in the second heating to cooling cycle and in a cooling to heating cycle.

In spite of some serious criticisms [72–76], remarkable popularity for the investigation of mechanisms in enantioselective chromatography enjoys also enthalpy–entropy compensation (EEC) [77] that can mathematically be expressed by the following equation:

$$\Delta H^\circ = \beta_{\text{EEC}} \cdot \Delta S^\circ + \Delta G_\beta^\circ \quad (9)$$

wherein  $\Delta G_\beta^\circ$  is the Gibbs free energy at compensation temperature  $\beta_{\text{EEC}}$ . EECs can be deduced from thermodynamic studies that yield linear van't Hoff plots, yet is actually an extrathermodynamic approach (*vide infra*). Plotting  $\Delta H^\circ$  versus  $\Delta S^\circ$  (or alternatively  $\Delta \Delta H^\circ$  vs.  $\Delta \Delta S^\circ$ ) of a series of thermodynamic data obtained from a congeneric set with minor structural or conditional variation yields a compensation plot, typically a straight line whose slope has the dimension of temperature. Similar compensation temperatures are taken as indication for a mechanistic similarity. Contrarily, distinct compensation temperatures (outliers in compensation plots) may help to identify objects that follow a fundamentally different mechanism. Carr and coworkers criticized such interpretations as being not rigorously allowed [76]. If compensation temperatures for two processes are identical all what can be concluded is that the relative contributions of enthalpy and entropy to the overall free energy are the same in the two processes. Since they could be by chance identical even if two processes occur via different mechanisms, identical



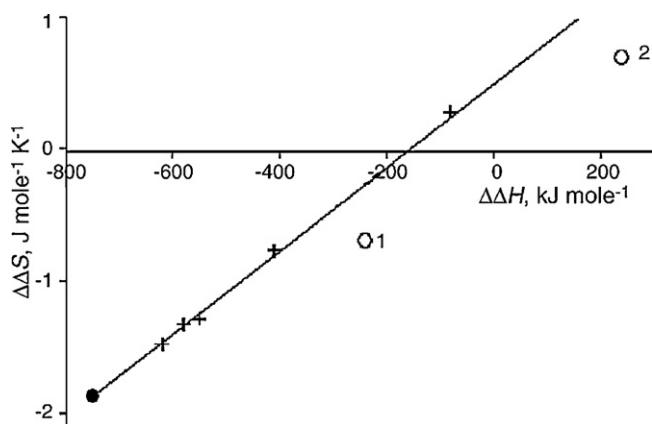


**Fig. 8.** Illustration of the compensation effect. Markers: (+) 3-chloro-1-phenylpropanol; (●) 1-phenylpropanol; (○) 2-phenylpropanol. 2-Phenylpropanol is plotted twice, once with derived thermodynamic values (positive values for both  $\Delta\Delta H$  and  $\Delta\Delta S$ ) (point ○1) and once with coordinates ( $-\Delta\Delta H$ ;  $-\Delta\Delta S$ ) to take into account the inversion of elution order (point ○2). Note that neither one is on the compensation effect line.

Reprinted with permission from Ref. [56].

compensation temperatures are no strong evidence for mechanistic identity. On contrary, if two processes exhibit different compensation temperatures, it can be concluded that the two processes follow distinct mechanisms.

In numerous studies such an EEC as revealed by linear correlations of  $\Delta H^\circ$  versus  $\Delta S^\circ$  plots and  $\Delta\Delta H^\circ$  versus  $\Delta\Delta S^\circ$  plots, respectively, were reported [47,48,53,56,78–84] while also lack of linear correlation and thus absence of EEC was observed [52,62,79,84]. Employing such an approach Péter et al. could classify solutes that were investigated on a ristocetin column into two groups based on different EEC behavior, i.e. different compensation temperatures [47]. Similarly, Berthod et al. studied EEC on 4 different macrocyclic antibiotics CSPs (teicoplanin, teicoplanin aglycone, vancomycin and ristocetin based CSPs) for a large set of structurally distinct solutes in three different elution modes [48]. EEC was found for retention and enantioselectivity for RP and polar organic mode for all four CSPs, while no EEC resulted for NP modes. For statistical uncertainty reasons, no safe conclusion was made except that outliers such as oxazepam in polar organic mode and 5-methyl-5-phenylhydantoin followed a different mechanism. Kazusaki et al. studied the thermodynamics of enantiomer separations on cellulose and amylose tris(3,5-dimethylphenylcarbamate) in the reversed-phase mode [78]. Enthalpy–entropy compensation concerning enantioseparations indicated that enthalpic gain/loss was substantially cancelled out by the entropic loss/gain on both columns. This led to constant  $\Delta\Delta G^\circ$  for enantioseparations, with lower  $\Delta\Delta G^\circ$  values and thus worse separation factors than would result without this compensation effect. Asnin and Guiochon reported on the enantiomer separation mechanism of phenylpropanol enantiomers on a quinidine carbamate CSP in dependence of eluent composition under normal-phase conditions composed of *n*-hexane and different ethylacetate percentages (with and without triethylamine pre-treatment and water additive, respectively) [56]. It was found that  $\Delta\Delta H$  correlated with  $\Delta\Delta S$  in a series of distinct conditions for 3-chloro-1-phenylpropanol (see Fig. 8). Also the structurally related 1-phenylpropanol was lying on the same compensation effect line leading to the conclusion that it follows a similar separation mechanism. In contrast, 2-phenylpropanol which eluted with reversed enantiomer order did not belong to the same compensation effect line suggesting a different mechanism of chiral recognition.

In general, thermodynamics investigations have been performed in great numbers. Besides the above mentioned phase ratio

problem, a weak point is also the uncertainty in the determination of the (apparent) entropic contribution to adsorption and separation, respectively. One has to be aware that their numerical values are estimated by extrapolation very far from the experimental data (see Fig. 6b) which is associated with considerable uncertainty in  $\Delta S^\ddagger$  and  $\Delta\Delta S^\circ$ , respectively. A small error in the slope determination may be accompanied with a much larger error in the intercept determination. In this context it has to be criticized that very seldom experimental errors and confidence intervals of the estimated coefficients  $\Delta\Delta H^\circ$  and  $\Delta\Delta S^\circ$  are given so that absolutely no information on the uncertainty is usually available for the reader. Moreover, the information content from thermodynamic studies and derived quantities is, due to their macroscopic nature, actually limited unless differences in series of experiments can be made out. Along this line, outliers from normal behavior deliver the most interesting information, i.e. entropically controlled systems, systems where there is no compensation effect, or deviation from linearity in van't Hoff plots and so forth. Last but not least, the above outlined methodology does not account for heterogeneous adsorption mechanisms.

### 3.4. Site-selective thermodynamics

Chiral stationary phases are heterogeneous surfaces usually harboring more than one type of adsorption site, viz. besides enantioselective ones (type II sites) usually a considerable number of non-enantioselective ones (type I sites) as well [40,85–98]. The latter may originate from binding to the supporting matrix, to linker groups, spacer units, residues stemming from silanol end-capping and last but not least from non-enantioselective binding sites of the selector itself as well. Interactions at type I sites are commonly termed nonspecific interactions and are well known to be detrimental binding contributions (*vide infra*). The binding affinity at these nonspecific sites (type I site) is usually much lower than that at the enantioselective sites (type II site). However, their density may exceed by orders of magnitude that of the enantioselective ones. Therefore, the contribution of such nonspecific interactions to the overall retention is usually not negligible. The resultant heterogeneous adsorption mechanism on chiral adsorbents can usually be reasonably well described by the following *bi-Langmuir model* [86,90,92,93,98]:

$$q = \frac{a_I C}{1 + b_I C} + \frac{a_{II} C}{1 + b_{II} C} \quad (10)$$

wherein  $q$  represents the adsorbed amount of respective enantiomers at equilibrium,  $a$  the distribution coefficient or initial slope of the adsorption isotherm ( $a = q_s b$  with  $q_s$  and  $b$  being the saturation capacities (number of accessible binding sites) and the equilibrium binding constants at the respective sites),  $C$  is the equilibrium concentration of a given enantiomer in the mobile phase, and subscripts I and II denote site I (non-enantioselective) and site II (enantioselective). This model has been used successfully to describe the adsorption behavior on protein CSPs [40,86,87,89,90,94], tartardiamide CSP [92], polysaccharide CSP [95], teicoplanin CSP [99,100] and quinidine carbamate CSP [91,93,96]. Besides, competitive bi-Langmuir models were applied as well [93]. A more complex situation existed for the adsorption of naproxen on a chiral anion-exchanger and a *tri-Langmuir model* fitted well to the experimental adsorption isotherms [97]. In some studies, it was accounted for additive effects which may strongly influence the adsorption behavior [96,100]. Also more uncommon adsorption isotherms were sometimes found such as a multilayer adsorption (with no competitive but a cooperative effect) for Tröger's base on a polysaccharide CSP [101,102].

For systems for which the bi-Langmuir model is valid retention factors  $k$  under linear chromatography conditions with infinite

sample dilution are composed of two terms according to the following equation [88]:

$$k = \phi(q_{s,I}b_I + q_{s,II}b_{II}) = \phi(a_I + a_{II}) = k_I + k_{II} \quad (11)$$

Since adsorption at type I site occurs non-enantioselectively, the coefficients  $q_{s,I}$  and  $b_I$  are identical for *R*- and *S*-enantiomers. In contrast, the corresponding figures at type II sites should be different for enantiomers. An apparent separation factor  $\alpha_{app}$  may thus be defined by the following equation [88]:

$$\alpha_{app} = \frac{a_I + a_{II,S}}{a_I + a_{II,R}} \quad \text{if } k_S > k_R \quad (12)$$

It is obvious that any adsorption contribution at the non-enantioselective type I sites will reduce the observed separation factor as compared to the true enantioselectivity  $\alpha_{true}$  ( $=a_{II,S}/a_{II,R}$ ). Hence, it becomes obvious that an optimization of enantiomer separation can be afforded by either maximizing the selectivity at the enantioselective type II sites or minimizing non-enantioselective retention contributions at the type I sites [88].

According to Eq. (11), analytical injections give only the sum of the distribution constants at the distinct adsorption sites. If the goal is to separate the different contributions, one must determine adsorption isotherms. Methods employed for the measurement of adsorption isotherms include frontal analysis, perturbation peak, elution by characteristic points, adsorption–desorption, and inverse methods, and have been reviewed recently along with adsorption isotherm models, common pitfalls, and applications by Samuelsson et al. [98].

If adsorption isotherms and individual contributions are determined in dependence on experimental variables such as pH [86,90], organic modifier content [94,95,97], additive concentration [96] or temperature [40,91,93,94], a more differentiated picture on the retention and chiral recognition mechanism can be obtained, which shows how binding constants and saturation capacities of distinct adsorption sites vary with these factors and how they affect the separation.

From this discussion it becomes clearly evident that the shortcoming of the above approach to derive thermodynamic parameters by linear chromatography which assumes a homogeneous adsorption mechanism and neglects the surface heterogeneity of the CSP does not differentiate between contributions from its distinct adsorption sites. They are simply lumped together. If adsorption isotherms are acquired at variable temperatures over a reasonably wide range, the corresponding thermodynamic parameters can be deconvoluted for each site by construction of van't Hoff plots for each site (Eq. (13)) (site-selective thermodynamics measurements) [40,91,93,94]. Thus, the adsorption equilibrium constants of the individual sites  $b_i$  are related to the enthalpy ( $\Delta H_i$ ) and entropy ( $\Delta S_i$ ) changes upon adsorption onto site  $i$  ( $i$  = site I, site II) according to the following equation [93]:

$$b_i = \exp\left(\frac{-\Delta H_i}{RT}\right) \exp\left(\frac{\Delta S_i}{R}\right) \quad (13)$$

By use of this methodology, thermodynamic quantities were determined site-selectively for propranolol on cellobiohydrolase I (CBH I) CSP [40], propranolol on amyloglucosidase CSP [94] and for 2,2,2-trifluoro-1-(9-anthryl)-ethanol [91] and 3-chloro-1-phenylpropanol [93] on *O*-9-*tert*-butylcarbamoylquinidine-modified silica. Results that were afforded for propranolol on CBH I are summarized as an illustrative example in Tables 1 and 2. It can be seen that the estimated coefficients for site I are identical within experimental error for *R*- and *S*-enantiomers while there is a significant difference in site II coefficients for the two enantiomers. Saturation capacities increase with temperature at each site and both of the enantiomers (except for *S*-enantiomer at site II). This behavior might be explained by a

**Table 1**

Bi-Langmuir adsorption isotherm parameters for propranolol on cellobiohydrolase I. Eluent: acetic acid buffer at pH 5.47 and ionic strength of 0.02.

Site	Isomer	<i>T</i> (K)	<i>a</i>	RSD <sup>a</sup> (%)	<i>b</i> (mM <sup>-1</sup> )	RSD (%)	<i>q<sub>s</sub></i> (mM)
I	<i>R</i>	278.1	7.78	(3.4)	0.382	(7.0)	20.4
		288.1	7.19	(3.5)	0.330	(7.4)	21.8
		298.1	6.62	(3.1)	0.287	(6.7)	23.1
		308.1	5.59	(4.2)	0.210	(10.5)	26.6
		318.1	5.73	(3.2)	0.220	(7.9)	26.0
I	<i>S</i>	278.1	7.23	(2.3)	0.347	(5.5)	20.8
		288.1	6.95	(1.7)	0.320	(4.6)	21.7
		298.1	6.95	(1.7)	0.323	(4.8)	21.5
		308.1	6.57	(1.5)	0.297	(4.3)	22.1
		318.1	6.14	(1.4)	0.266	(4.7)	23.1
II	<i>R</i>	278.1	8.79	(3.8)	13.652	(14.1)	0.64
		288.1	8.08	(3.0)	10.295	(12.7)	0.78
		298.1	7.14	(2.3)	8.215	(10.2)	0.87
		308.1	6.68	(2.6)	5.979	(10.5)	1.12
		318.1	5.58	(2.4)	6.385	(10.1)	0.87
II	<i>S</i>	278.1	18.05	(2.0)	18.137	(5.9)	1.0
		288.1	19.89	(1.7)	22.286	(4.6)	0.89
		298.1	22.30	(2.1)	29.790	(4.9)	0.75
		308.1	24.30	(1.8)	33.970	(4.0)	0.72
		318.1	25.80	(2.1)	40.254	(4.2)	0.64

Reprinted with permission in slightly modified form from Ref. [40].

<sup>a</sup> RSD = relative standard deviation.

thinner solvation shell of binding sites at elevated temperatures and thus better access of solutes to the interaction sites. They are by a factor of about 30 higher for non-enantioselective site I than enantioselective site II. The binding constants  $b$  decrease with increasing temperature indicating enthalpic control, except for the *S*-enantiomer at the enantioselective site II which features a remarkable increase. Adsorption enthalpies were derived from slopes of van't Hoff plots of  $\ln a$  versus  $1/T$  for each enantiomer and adsorption site individually, and were found to be  $-1.10$  kcal/mol for both enantiomers at non-enantioselective sites and  $-1.92$  and  $+1.61$  kcal/mol at enantioselective sites for *R*- and *S*-enantiomer, respectively. It is obvious that the retention mechanism changes from an enthalpically controlled, exothermic adsorption for the first eluted *R*-enantiomer to an entropically controlled, endother-

**Table 2**

Thermodynamic parameters for propranolol enantiomers on cellobiohydrolase I derived for individual binding sites.

Site	Isomer	<i>T</i> (K)	$\Delta G^\circ$ (kcal/mol)	$\Delta H^\circ$ (kcal/mol)	$\Delta S^\circ$ (cal/mol K)
I	<i>R</i>	278.1	-1.13	-1.10	+0.14
		288.1	-1.13	-1.10	+0.12
		298.1	-1.12	-1.10	+0.08
		308.1	-1.05	-1.10	-0.13
		318.1	-1.10	-1.10	+0.03
	<i>S</i>	278.1	-1.09	-1.10	-0.01
		288.1	-1.11	-1.10	+0.05
		298.1	-1.15	-1.10	+0.18
		308.1	-1.15	-1.10	+0.19
		318.1	-1.15	-1.10	+0.16
II	<i>R</i>	278.1	-1.20	-1.92	-2.60
		288.1	-1.20	-1.92	-2.52
		298.1	-1.16	-1.92	-2.55
		308.1	-1.16	-1.92	-2.47
		318.1	-1.09	-1.92	-2.63
II	<i>S</i>	278.1	-1.60	+1.61	+11.55
		288.1	-1.71	+1.61	+11.54
		298.1	-1.84	+1.61	+11.58
		308.1	-1.95	+1.61	+11.57
		318.1	-2.05	+1.61	+11.53

Reprinted with permission in slightly modified form from Ref. [40].

mic retention mechanism for the second eluted S-enantiomer at the chiral sites.

Overall, such investigations of adsorption isotherms have been established as an important and valuable methodology to derive detailed informations on retention and chiral separation mechanisms of CSPs.

#### 4. Extrathermodynamic approaches to study chiral recognition

As outlined above, thermodynamic studies are often performed in order to study retention and chiral recognition mechanisms. Such studies may yield valuable information on enthalpic and entropic contributions to retention and separation, especially if they have been derived site-selectively. Yet, these thermodynamic quantities are macroscopic entities, which do not provide detailed microscopic information on individual structural group contributions or types of interactions involved in the CS–SA binding event and being responsible for chiral recognition. For that purpose, spectroscopic methods (e.g. NMR, FT-IR), X-ray diffraction of co-crystallized CS–SA complexes as well as molecular modeling have been proposed, amongst others (*vide infra*). Extrathermodynamic approaches are another means to provide valuable insight on how CSPs are retaining chiral solutes and how they are differentiating between enantiomers [103].

Extrathermodynamic relationships are empirical correlations of thermodynamic quantities that can be employed to examine the role of molecular structural parameters in chemical equilibria and rate processes, such as in chromatography [77,104,105]. Classical representatives of extrathermodynamic approaches are (i) enthalpy–entropy compensation (EEC) (*vide supra*), (ii) linear free energy relationships (LFER), and (iii) linear solvation energy relationship (LSER) (which is actually a subset of LFER). EEC has been dealt with in some detail above, and at this point it is just emphasized that they are empirical correlations without strict fundamental physical deterministic model character. The same, of course, applies to both of the latter (LFER and LSER) that are based on the assumption that the free energy of a process ( $\Delta G_i^\circ$ ) is additively composed of free energy increments ( $\Delta G_j^\circ$ ) contributed by structural elements of the chemical entities involved in a given chemical process. The fundamental equation of LFERs can be written as follows [77]:

$$\Delta G_i^\circ = \sum_1^z \Delta G_j^\circ \quad (14)$$

This concept of additivity of group contributions was first described for chromatography by Martin [106]. It states that each group  $j$  of a molecule contributes a certain constant incremental free energy change  $\Delta G_j^\circ$  and all individual group contributions sum up to the free energy change for a given solute  $\Delta G_i^\circ$ .

In view of enantioseparation, it can also be applied in an analogous manner to the differential free energy of binding for R- and S-enantiomers.

$$\Delta \Delta G_i^\circ = \sum \Delta \Delta G_j^\circ \quad (15)$$

This concept has been rigorously applied in 1992 by Berthod et al. for LC enantiomer separation in normal-phase mode of 121 and 74 racemic compounds on (R)- and (S)-1-(1-naphthylethyl)carbamoylated- $\beta$ -cyclodextrin CSPs, respectively [107]. The free energy group contributions to chiral separation were simply computed from  $\Delta \Delta G$  values (as determined chromatographically according to Eq. (5)) of a chiral compound exhibiting a certain structural feature in relation to a reference compound in which this element was absent. The concept was similarly applied

recently by Nadalini et al. for a series of dihydropyrimidines on polysaccharide-based CSP [108].

A great number of studies dealt with classical forms of LFER, especially with the so called Hansch approach, more often found in the literature as QSPR (quantitative structure–property relationship), QSRR (quantitative structure–retention relationship), QSERR (quantitative structure–enantioselective retention relationship), and similar acronyms [109]. The basic concept is to correlate dependent variables (responses; y-variables) such as chromatographic retention (expressed by e.g.  $\log k$ ;  $\log K$ ;  $\Delta G$ ) and enantioselectivity data ( $\log \alpha$ ;  $\Delta \Delta G$ ) of a more or less homologous series of structural analogs that adhere to the same binding mechanism on a certain CSP with some kind of structural descriptors (independent or predictor variables;  $x_1, x_2, \dots, x_n$ ) employing usually linear models such as

$$y = a_0 + a_1x_1 + a_2x_2 + \dots + a_nx_n \quad (16)$$

wherein  $a_0, a_1, \dots, a_n$  are the coefficients of the individual predictor variables. Commonly employed molecular descriptors are physicochemical properties ( $\log P, \log D, pK_a$ ), substituent and fragmental constants ( $\pi, f, \sigma, E_s$ ), topological descriptors (molecular connectivity indices  $\chi$ ), calculated descriptors (HOMO, LUMO, partial atomic charge, dipole moment), interaction fields (3D set of computed interaction energy values with probe at grid points), etc., which reasonably well describe the structural variability in the set of congeners [27,110–113]. Also quadratic terms may be incorporated, e.g.  $(\log P)^2$  (yet still yielding a linear model according to linear algebra). The goal is to find statistically significant relationships between dependent and independent variables (i.e. structural descriptors) that allow computing the response in dependence on the factors in the model. The resultant empirical mathematical models allow to derive some information on influential factors as well as to predict the response of compounds fitting to the same lead yet not included in the data set that was used to derive the model. In other words, in the present context they provide a means to figure out the structural factors which have the strongest influence on retention of the chiral solute on a given CSP as well as on their enantioseparation.

Various QSPR methodologies of the LFER type have been proposed in the context of enantioselective liquid chromatography employing normally multiple linear regression (MLR) analysis technique to derive estimates for the individual predictor variable (independent variables) [103,114–126]. The validity of the models has to be proven by analysis of variance (ANOVA) and cross-validation procedures, respectively [105]. MLR is limited to long and lean data sets, i.e. data sets with many objects and few factors. The factors themselves must not be significantly correlated, i.e. they must be independent, and according to strict definition should be free of error. A prerequisite that MLR is applicable is also that residuals are randomly distributed (i.e. assumption of a normal distribution). To overcome these hurdles also other statistical techniques have been employed to establish QSPR models with statistical significance including partial least squares in latent variables (PLS) [127], artificial neural networks (ANN) [126,128], or swarm intelligence and support vector machines [129]. An advantage of these techniques is that they may model data in a non-linear fashion, but may be less straightforward and less illustrative in their interpretation [130]. A special form of QSPR approaches are 3D-QSPR CoMFA (comparative molecular field analysis) [120–122,126,128,131,132] and CoMSIA (comparative molecular similarity index analysis) methods [132], respectively, which both were tested for their capability to model retention and enantioselectivity in enantioselective HPLC. The basic idea of the CoMFA technique is to bring geometry optimized, aligned molecules of the data set into a three-dimensional grid where at each grid point the Coulomb (for electrostatic field) and Lennard

Jones potential (for steric field) is calculated between a probe and the molecules of the data set. The entirety of the interaction energy values of each type (called molecular field) is employed as molecular descriptors and can be correlated by PLS with the dependent variables, i.e. retention or enantioselectivity [120,131]. The results of the correlation are graphically displayed by isocontour plots for each field which illustrate regions around the molecules where a change in the electrostatic or steric field is correlated with a change in the response. The technique is not very robust and hence COMSIA represents an advancement [132]. Instead of molecular fields distance-dependent similarity indices between a probe and the molecules are calculated at each grid point yielding property-specific similarity fields which are more rugged and easier to interpret. In yet another approach, Natalini et al. used a classification model (partition tree) and molecular surface area descriptors (Jurs descriptors) as well as Shadow descriptors (which encode the geometric arrangement of the molecules), both computed by a molecular modeling program, to identify the “separation-likeness” of amino acids in chiral ligand exchange chromatography [133]. Other techniques used in QSAR are also applicable.

QSPR models can be derived on data sets which have been assembled from a set of structurally distinct solutes that were analyzed on a given CSP. For example, Altomare et al. investigated the interaction mechanism of 21 chiral substituted aryl alkyl sulfoxides on a  $\pi$ -acidic donor-acceptor phase, viz. *N,N'*-bis(3,5-dinitrobenzoyl)-*trans*-1,2-diaminocyclohexane based CSP, in normal-phase mode [120]. Correlations between retention factors and various molecular descriptors could be afforded, like amongst others

$$\log k_S = -0.67(\pm 0.14)\sigma - 0.40(\pm 0.12)\pi + 1.50(\pm 0.06)$$

$$n = 11, r^2 = 0.951, s = 0.070$$

and

$$\log k_R = -0.74(\pm 0.14)\sigma - 0.38(\pm 0.12)\pi + 1.60(\pm 0.06)$$

$$n = 11, r^2 = 0.956, s = 0.070$$

thereby,  $\sigma$  and  $\pi$  are Hammett's electronic substituent constant and Hansch's lipophilicity parameter, respectively, of the aryl substituent,  $n$  denotes the number of objects included in the model (i.e. no. of compounds),  $r$  is the correlation coefficient,  $s$  the standard deviation of the residuals. 95% confidence intervals are given in parentheses for the estimated coefficients which confirm their statistical significance in the model. The models show that retention factors increase for both enantiomers, albeit with some minor enantioselectivity, with a decrease in the electron-withdrawing effect of the aromatic substituent. It actually proves the importance of  $\pi$ - $\pi$ -interactions on such type of CSPs. They further decrease with increase in lipophilicity which can be expected for a normal-phase separation system. About 95% of the variance in the dependent variable could be explained by the model.

Vice versa, also structural effects of CSP variation have been modeled with a single solute, for example as described by Schefzick et al. employing 3D-QSPR CoMFA approach for a set of differently derivatized quinine carbamate CSPs and *N*-(3,5-dinitrobenzoyl)-leucine (DNB-Leu) as analyte [131]. Steric factors of the CSPs close to the carbamate group could be identified as major determinants for the enantioselectivity of the selectors of the investigated set.

Last but not least, recently both structural variation on selector (series of quinine carbamate derivatives) and solute (series of DNB-amino acids) were combined in a mixed QSPR model to describe mutual steric effects of structural changes in the selectors' carbamate residue and selectands' amino acid residue on enantioselectivity [103]. Taft's steric parameter ( $E_S$ ) served as steric

descriptor for the distinct alkyl-substituents employed and subscripts CS and SA indicate substituent positions in the selector and analyte. The following QSPR model was obtained:

$$\log \alpha = -1.63(\pm 0.33) - 1.83(\pm 0.32)E_{S,SA} - 0.40(\pm 0.08)E_{S,SA}^2$$

$$- 0.59(\pm 0.09)E_{S,CS} - 0.08(\pm 0.01)E_{S,CS}^2$$

$$- 0.06(\pm 0.02)E_{S,SA}E_{S,CS}$$

$$n = 52, r = 0.9720, s = 0.059, F = 157.15, p\text{-value} < 0.0001$$

(19)

wherein  $F$  is the calculated value for Fisher's test (ANOVA) and the  $p$ -value denotes the statistical significance level. This model suggests that steric interactions play a major role: with increase of the steric bulk (encoded by the steric descriptor Taft's parameter  $E_S$ ) in both the amino acid side chain and the carbamate residue enantioselectivity factors first increase, traverse an optimum and then decrease upon a certain bulkiness (note the more bulky the substituent, the larger negative  $E_S$  will be). Since there is also a statistically significant interrelation term (last term in Eq. (19)) it was concluded that the SA and CS residues interact with each other. This steric interaction was confirmed by X-ray crystal structures of co-crystallized CS-SA complexes.

A frequently employed extrathermodynamic approach in liquid chromatography used to understand types and relative strengths of chemical interactions makes use of linear solvation energy relationships (LSER), and has been reviewed comprehensively and in very much detail recently [134]. LSER has been used to describe solvation phenomena (that can be characterized by the individual steps of cavity formation, solute insertion and activation of solute-solvent interactions), but has proven to be a useful tool also for other processes such as the phase transfer process in chromatography. It states that solvent-dependent solute properties (SP) of free energy related processes are made up of several contributions, in general of a cavity term (V-term accounting for the unfavorable, i.e. endergonic process of cavity formation; see below) and of several terms accounting for the favorable intermolecular interactions (exergonic).

LSER equations are found in the literature in numerous forms as they have been adapted to the specific application that has been investigated. In a general form, the solvation equation can be written as follows [135]:

$$SP = \text{const.} + M(\delta_s^2 - \delta_m^2) \frac{V_a}{100} + S(\pi_s^* - \pi_m^*)\pi_a^* + A(\beta_s - \beta_m)\alpha_a$$

$$+ B(\alpha_s - \alpha_m)\beta_a$$

(20)

wherein SP is a linear free energy related solute property (such as  $\log k$ ,  $\log \alpha$ ,  $\Delta G$ ,  $\Delta \Delta G$ ), subscripts  $a$ ,  $m$  and  $s$  stand for analyte, mobile phase and stationary phase property, and  $V$ ,  $\pi^*$ ,  $\alpha$ ,  $\beta$  are the analytes' molar volume, polarizability/polarity, hydrogen bond acidity and basicity, respectively, or corresponding properties of mobile and stationary phase (in parentheses).  $\delta$  represents the Hildebrand solubility parameter and is proportional to the cohesive energy of the phases (if the solvent molecules strongly adhere to each other the energy required to put them apart and form a cavity will be large which is unfavorable for solvation of the analyte in this phase). Each analyte property parameter gets a coefficient (term in parentheses and denoted with a capital letter;  $M$ ,  $S$ ,  $A$ ,  $B$ ) that is determined by MLR and expresses the relative importance of this interaction to the investigated SP. It actually reflects the difference of the two phases in their ability to interact with the solute through a given property. Note that the coefficients representing relative strengths of interactions are complementary to the corresponding solute parameter (e.g. the coefficient for solute H-bond acidity reflects differences in the H-bond basicity of stationary and



mobile phase). For example, a solute with strong H-bond acidity will feature a large SP, e.g.  $\log k$ , by H-bonding if the stationary phase HB-basicity  $\beta_s$  is large and the mobile phase HB-basicity  $\beta_m$  is small. If H-acceptor groups are absent in the stationary phase, yet are available in mobile phase solvent molecules, this H-bond interaction term will negatively contribute to the SP (due to negative sign of the corresponding coefficient) which means that the interaction with the stationary phase will be weakened due to good solubility in the mobile phase. Similar considerations are valid for solute H-bond basicity and solute polarizability  $\pi^*$ . A detailed description of the evolution of solvation equations, the parameters (including H-bond acidity scales) and an in-depth interpretation in terms of their interactions can be found elsewhere [134]. Moreover also a collection of solute input parameters (structural descriptors) for a representative test set that can be used to derive LSER equations can be found there.

If a series of solutes is analyzed on a given stationary phase with the same mobile phase the above equation can be simplified and assumes a form similar to that given in Eq. (21). The coefficients reflect the difference in the degree of interactions in the two phases. The magnitude of the coefficients gives information on the relative strength of the corresponding interaction term and its sign indicates whether the respective term increases (positive sign) or decreases (negative sign) the given SP. For the comparison of the relative influence of the individual interaction terms, normalized regression coefficients should be computed [136].

The most widely accepted representation of the LSER model is nowadays the Abraham equation [134] as given in the following equation:

$$SP = \text{const.} + eE + sS + aA + bB + vV \quad (21)$$

The solute-dependent input parameters, termed  $E$ ,  $S$ ,  $A$ ,  $B$ , and  $V$  in this equation, are respectively related to measures of the solute's excess polarizability (in relation to a comparably sized  $n$ -alkane reference compound), dipolarity, hydrogen bond acidity (H-donor propensity), hydrogen bond basicity (H-acceptor propensity), and molecular volume.

The concept has been adopted for investigating retention and enantioselectivity, respectively, on various stationary phases by a number of researchers. Nesterenko used a reduced form of LSER equation to take a closer look into the effect of the nature and composition of the eluent for the enantiomer separation of 2,2,2-trifluoro-1-(9-anthryl)ethanol on a quinine bonded CSP [137].

Tesarova and coworkers [136,138], Berthod et al. [139,140], and Mitchell et al. [141] examined which type of interactions are of dominance for retention and separation, respectively, on macrocyclic antibiotic CSPs. In the investigation of Mitchell et al. also immobilized polysaccharide CSPs were compared in view of derived solvation parameters. Just recently, West et al. utilized LSER to compare different CSPs in SFC including various polysaccharide based CSPs from different suppliers allowing to elucidate their characteristics in terms of retention and selectivity [142]. Thereby, an extended form of the LSER equation was employed to account for contributions in chiral separations, viz. shape recognition, that are not very well covered by the original solvation equation.

A more comprehensive list of studies of LFER, LSER and other QSPR approaches can be found in a recent review article by Rio [130] in which these methodologies are described in greater detail as part of the broader topic of chemoinformatic techniques employed for exploration of enantioselective molecular recognition (*vide infra*).

## 5. Kinetics, peak dispersion and tailing

Above discussions focused on thermodynamic properties of CSPs. However, to some extent also the kinetic characteristics may be informative mechanistically in terms of binding interactions via

their rate constants of adsorption–desorption because the CS–SA equilibrium binding constant is defined by the ratio of association and dissociation rate constants [143].

Information on rate constants is convoluted in chromatographic efficiencies of enantiomer separation with plate number  $N$  or plate height  $H$  as descriptive measure. Chromatographic efficiencies of CSPs are often fairly low if compared to other types of LC, even under linear chromatography conditions, with plate numbers seldom exceeding 40,000 theoretical plates per meter for 5  $\mu\text{m}$  particles. Moreover, the eluted bands frequently tail, more so than in other types of LC, especially RP-HPLC. Since it may be assumed that axial dispersion phenomena (Eddy and molecular diffusion) are in the same order in well packed enantioselective columns as in achiral columns, the lower plate counts may be intrinsic to this type of chromatography and may be ascribed to slow adsorption–desorption kinetics at the chiral sites. It is commonly accepted that in particular the desorption process at such sites is slow because of the formation of relatively long-lived CS–SA complexes that are subject of strong stabilization by simultaneous multiple interactions. Assuming a homogeneous kinetics with a single type of adsorption sites, i.e. solely chiral adsorption sites, the relationship between plate number  $N$  and rate constant  $k_r$  of the adsorption–desorption process at these sites can be described by the following equation [144]:

$$\frac{1}{N} = \frac{2k}{(1+k)^2} \frac{u}{k_r L} \quad (22)$$

wherein  $k$  denotes the retention factor of the solute and  $L$  the column length. If the adsorption–desorption kinetics  $k_r$  at the chiral sites is fast, a highly efficient separation can be achieved in which the axial dispersion contribution and diffusion-limited mobile phase mass transfer become the dominant factor for band spreading.

Furthermore, Guiochon and coworkers have demonstrated that under linear conditions peak tailing of enantioselective columns may originate from the heterogeneous mass transfer kinetics according to a multisite adsorption model with different individual kinetic coefficients  $k_{r,I}$  and  $k_{r,II}$ . This was explained by modeling band profiles using the transport-dispersive model which was modified to account for heterogeneous mass transfer kinetics [144]. Fig. 9 illustrates simulated band profiles obtained by using this model and different values for the rate constant at the chiral sites  $k_{r,II}$  (between 1.0 and 100  $\text{min}^{-1}$ ). The chiral sites, which have a higher adsorption energy, have a slow desorption rate and thus a longer residence time than the non-enantioselective sites  $k_{r,I}$  (which were held constant at  $k_{r,I} = 10,000 \text{ min}^{-1}$ ). When  $k_{r,II}$  was set to 1  $\text{min}^{-1}$ , the chiral sites are mostly not accessible due to a very slow adsorption–desorption kinetics and the compound elutes thus with a retention factor of  $\phi \cdot a_I$  (peak 1). When the rate constant for the enantioselective sites becomes fast enough, the compound elutes, in accordance with Eq. (11), with its expected retention factor  $\phi \cdot (a_I + a_{II})$  (peaks 5–7). In the latter case, the peak asymmetry gets smaller the larger the rate constant of the chiral site  $k_{r,II}$  (for corresponding asymmetry factors see caption of Fig. 9). It was also noticed that axial dispersion dampens the effect and hence the peak tailing of the kinetic origin is usually more pronounced in a (well-packed) highly efficient column [144]. In a subsequent work the additional influence of sample overload was investigated by the same research group [145].

Hage recently reviewed the chromatographic methods that can be employed to deconvolute adsorption–desorption kinetics from other kinetic contributions in an LC column, with specific focus on biointeraction chromatography (esp. drug–protein binding) [143]. Some of the reported methods have been adopted to derive rate constants of CS–SA association and dissociation stereoselectively. For example, in one study plate height measurements

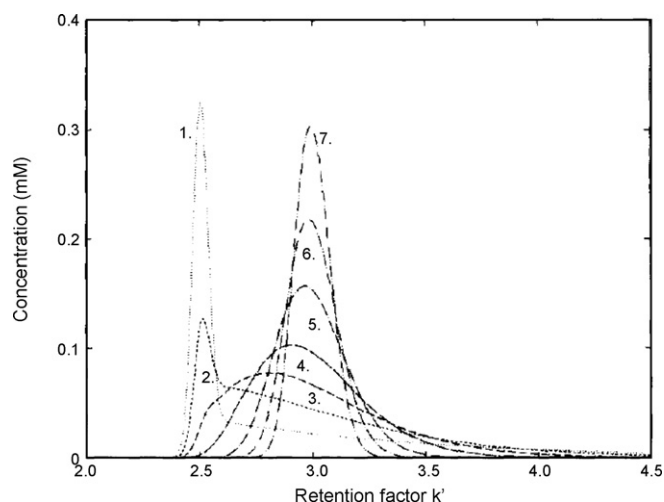


**Fig. 9.** Simulated band profiles for the adsorption behavior of a compound considering a heterogeneous thermodynamics and a heterogeneous mass transfer kinetics with very fast kinetics on the general type of sites (non-enantioselective ones) and slow kinetics on the enantioselective sites. The individual equilibrium constants were set to  $a_I = 10$  and  $a_{II} = 2$  (see Eq. (22)) and the rate constant at the non-enantioselective sites was held constant at  $k_{r,I} = 10,000 \text{ min}^{-1}$ . The rate constant at the slow enantioselective sites  $k_{r,II}$  was varied between 1.0 and  $100 \text{ min}^{-1}$ . Peak notation ( $k_{r,II}, \text{min}^{-1}$ ): (1) 1; (2) 2.5; (3) 5; (4) 10; (5) 25; (6) 50; (7) 100. Peak asymmetry factor: (4) 1.81; (5) 1.39; (6) 1.25; (7) 1.19. Reprinted with permission from Ref. [144].

were used to investigate the kinetics of (*R*)- and (*S*)-warfarin binding to an immobilized HSA (human serum albumin) stationary phase [146]. After subtraction of other peak dispersion contributions, rate constants were determined from the plate height contribution due to stagnant mobile phase mass transfer resistance according to Eq. (22). Dissociation rate constants for (*R*)- and (*S*)-warfarin on this column increased from  $0.06$  to  $1.9 \text{ s}^{-1}$  and from  $0.06$  to  $0.36 \text{ s}^{-1}$  between  $4$  and  $45^\circ\text{C}$ . The corresponding association rate constants increased from  $2.4 \times 10^4$  to  $3.2 \times 10^5 \text{ M}^{-1} \text{ s}^{-1}$  for (*R*)-warfarin and from  $4.4 \times 10^4$  to  $7.2 \times 10^4 \text{ M}^{-1} \text{ s}^{-1}$  for (*S*)-warfarin over the same temperature range. A different technique was utilized in another study. Assuming a homogenous adsorption mechanism dissociation rate constants for (*R*)- and (*S*)-warfarin from columns containing immobilized HSA were measured at several temperatures, giving values of  $0.56 \text{ s}^{-1}$  ( $\pm 0.01$ ) and  $0.66 \text{ s}^{-1}$  ( $\pm 0.01$ ) at pH 7.4 and  $37^\circ\text{C}$  employing a non-competitive peak decay analysis method [147]. Overall, such kinetic data may complement corresponding thermodynamic data, yet are so far mainly reported for CSPs in the context of protein–drug interactions.

## 6. Tools and methods for the investigation of retention and chiral recognition mechanisms

Chiral recognition mechanisms of CSPs and their soluble analogs, the chiral selectors, respectively, were explored employing various different techniques and binding partners (SAs). By use of distinct orthogonal techniques complementary information may be collected which in their entirety may then provide a more comprehensive picture about intermolecular interaction events and how CSPs differentiate between enantiomers. In principle, methodologies can be classified into those that provide information on the binding strengths (measurement of binding constants and binding energetics) and those that provide information on the type of intermolecular interactions and the structure of the CS–SO complexes (adsorbates).

The measurement of binding constants between CS and SA shall only be briefly mentioned at this point. It has been performed

mainly with low-molecular mass selectors (donor–acceptor phases [148], chiral ion-exchangers [149]), cyclodextrins and derivatives [38,150], macrocyclic antibiotics [151], protein selectors (HSA, AGP) [152] and low-molecular analogs of synthetic polymeric selectors, e.g. *N,N'*-diallyl-tartardiamide bis-(4-*tert*-butylbenzoate) [153]. Techniques that have been used for this purpose to study CS–SA associations included NMR [153] (for technical review see Ref. [154]), UV spectroscopy (due to charge-transfer band of a donor–acceptor system) [148], affinity CE [149], isothermal titration calorimetry [155], ESI-MS [156], amongst others.

The following discussion is mainly focusing on methods that are supposed to derive information on intermolecular interactions and structures of CS–SA complexes.

### 6.1. Chromatographic studies and retention models

The options to derive information on involved intermolecular interaction forces between chiral selectors and the guest SA–enantiomers by chromatography are twofold: (i) via variation of environmental conditions, (ii) via structural variations of SA and/or CS.

Chiral recognition is commonly regarded as a bimolecular process of CS–SA interaction, yet the mobile phase is assumed to play a modulating role for the strength of these interactions enabling to derive information on the involved types of non-covalent bonds. The eluent determines the degree of solvation of interactive sites of selector and selectand, and thus whether these interaction sites are actually available for intermolecular contacts. Solvents and eluents are of course also major determinants of conformational preferences and of ionization states of ionizable selectors and solutes. All these factors influence the degree to which binding partners are capable for intermolecular association. Therefore, the mobile phase decides on whether the intrinsic enantioselectivity potential of a CSP can be utilized or not. Thus, mobile phase variables are instrumental tools for investigating which interactions are involved. There are uncountable studies in the literature in which chromatographic responses ( $k$ ,  $\alpha$ ) have been analyzed in dependence on experimental variables such as (apolar or polar) organic modifier content, pH, ionic strength, and temperature. The observed trends of retention and enantioselectivity allowed to pinpoint primarily involved dominating interaction forces. For example, hydrophobic interactions are weakened in RP-like hydro-organic media with increase in organic modifier and a linear solvent strength (LSS) retention model often applies [157,158].

$$\log k = \log k_0 - S\varphi \quad (23)$$

wherein  $k_0$  represents the (hypothetical) retention factor at 0% organic modifier content (usually obtained by linear extrapolation to the  $y$ -intercept),  $S$  is a solute-dependent parameter related to its solvent-accessible surface. The larger the hydrophobic contact area, the larger the parameter  $S$  and the steeper the curves. According to this LSS model  $\log k$  or  $\ln k$  drops linearly with the percentage of organic modifier  $\varphi$  in the mobile phase which may be taken as indication for existence of hydrophobic interactions if other conditions are kept constant, e.g. ionic strength and pH [157].

Hydrophilic interactions are strengthened in NP-like alkane-based eluents with decrease of polar modifier [57,159]. Several models have been proposed to describe retention in such NP-media on polar surfaces. Among them, the Snyder model [160] supposed an independent monolayer adsorption. Accordingly, upon adsorption of the analyte the number of replaced modifier molecules will be directly proportional to the surface area of the solutes and inversely proportional to that of the polar modifier. A simplified modification represents the Soczewiński model [161]. It states a direct proportional relationship, due to stoichiometric displacement, between  $\log k$  and the molar fraction of the polar modifier

$X_B$  in the eluent

$$\log k = c - n \log X_B \quad (24)$$

In this Eq. (24), the constant  $c$  represents the  $\log k$  obtained with pure weak solvent (diluent) A which is usually an alkane. Linear plots in accordance with the Soczewiński equation were for example obtained for the NP separations of imidazo-quinazoline-dione derivatives on quinine carbamate-based chiral stationary phase [159].

Other authors used retention theory based on a stoichiometric solvent displacement model derived from work of Lanin and Nikitin [162] (Eq. (25)) in order to describe the dependency of retention factors  $k$  as a function of the mobile phase composition (Eq. (25)) [56].

$$\frac{1}{k} = \frac{1}{\phi K_S} + \frac{K_m - 1}{\phi K_S} X_m \quad (25)$$

wherein  $\phi$  is the phase ratio (note, according to IUPAC the phase ratio is defined as the ratio of the volume of the mobile phase  $V_0$  to that of the stationary phase  $V_S$  in a column,  $\beta = V_0/V_S$ , i.e. as reciprocal of  $\phi$  ( $\beta = 1/\phi$ )),  $K_S$  is the equilibrium constant for the stoichiometric exchange of solvent molecule (diluent) on the active site of the sorbent by solute (sorbate) and  $K_m$  the equilibrium constant for the corresponding competitive adsorption reaction of the modifier molecules on the stationary phase surface.  $X_m$  is the mole fraction of the polar modifier in the eluent. According to this stoichiometric displacement model the polar modifier plays the role of a competitor for adsorption with respect to the solute and plots of  $1/k$  versus the mole fraction of polar modifier  $X_m$  should yield straight lines. The alkane like  $n$ -hexane, by contrast, is supposed to act like a diluent or inactive carrier of the polar modifier. Linear trend lines according to this model were indeed observed, for example, for the separation of 3-chloro-1-phenylpropanol on a quinine carbamate CSP in NP mode [56].

Ionic interactions are balanced by increasing ionic strength due to ionic shielding of charged sites of adsorbent and SA. They are further weakened with reduced degree of dissociation of CSP and SA which depend on pH of mobile phase and pKa of involved groups [29]. Characteristic for systems dominated by electrostatic interactions are, according to the stoichiometric displacement model and the Gouy-Chapman model that is based on double-layer theory [163], linear plots of  $\log k$  versus the log of the counterion concentration  $[C_i]$

$$\log k = \log K_Z + Z \log [C_i] \quad (26)$$

The slope  $Z$  (with  $Z$  being proportional to  $m/n$ ; wherein  $m$  is the effective charge number of the solute ion and  $n$  the effective charge number of the counterion in the mobile phase) provides information on how many charges are involved in the ion-exchange process, yet is an empirical coefficient rather than a deterministic one.

For a typical ion-exchange process, i.e. oppositely charged adsorbent and selectand,  $\log k$  decreases linearly with  $\log [C_i]$  and the slope  $Z$  thus adopts negative values. In the above equation the constant  $K_Z$ , which can be calculated from the intercept, represents a system-specific constant that is related to the ion-exchange equilibrium constant  $K$  (in  $\text{L mol}^{-1}$ ), the surface area  $S$  (in  $\text{m}^2 \text{g}^{-1}$ ), the charge density on the surface, i.e. for the number of ion-exchange sites  $q_x$  available for adsorption (in  $\text{mol m}^{-2}$ ) and the mobile phase volume  $V_0$  (in L) in the column as described by the following equation:

$$K_Z = \frac{KS(q_x)^2}{V_0} \quad (27)$$

If solute and adsorbent possess identical charge,  $\log k$  increases with increasing  $\log [C_i]$ . The repulsive electrostatic interactions are

dampened at elevated ionic strength and a positive sign of the coefficient  $Z$  will be derived. If ionic interactions do not play a significant role, the effect of salt (buffer) concentration  $C_i$  in the eluent on retention factors will be negligible. The dependency of Eq. (26) can therefore be utilized as diagnostic tool to probe for existence of ionic interactions.

Similarly, investigations of retention factors in dependence on solvent compositions may provide information on which type of interactions are prevailing. The low polarity of NP-type eluents helps to stabilize polar intermolecular CS-SA interactions, such as hydrogen bonding, dipole-dipole- and  $\pi$ - $\pi$ -stacking interactions, while hydrophobic interactions are effectively disrupted in these media. If polar interactions become too strong in NP-eluent, the polar organic (PO) mode may be an alternative which utilizes nonaqueous mobile phases that are made up of polar organic solvents such as methanol or acetonitrile or a mixture of both to which small amounts of organic acids (acetic acid, formic acid) and base (triethylamine, diethylamine, ammonia) are added as buffer constituents or competing agents. Hydrophilic interactions are the driving force for retention in such media (likewise to NP) leading to stronger retention upon exchange of methanol by acetonitrile or, if ionic interactions are involved, upon reduction of additives. A significant number of papers about enantiomer separations in aqueous-organic media, reported as RP-type, were actually HILIC-type separations (polar stationary phase with usually acetonitrile-rich hydro-organic eluents). Typical for this elution mode are modifier dependencies in which solutes depict stronger retention with increase of organic solvent, in particular acetonitrile [164]. Last but not least the SFC mode resembles the NP-mode in that hydrophilic interactions are strengthened upon decrease of polar modifier in super-/subcritical  $\text{CO}_2$  [165].

The information content that can be derived from temperature studies has been discussed broadly above. Interpretations of such studies with regards to binding and chiral recognition mechanisms using linear chromatography conditions, however, always faces the dilemma that it is usually impossible to unequivocally assign effects to specific CS-SA interactions or nonspecific interactions so that it remains essentially a phenomenological discussion. Literature sees a neglect of this issue and has led to an uncountable number of speculative statements. The same holds for effects of other experimental variables like modifier content, etc. which limits the usefulness of chromatographic studies for investigations of separation mechanisms.

The more effective approach is to analyze a series of structurally related compounds that allows to derive structure-retention and structure-enantioselectivity relationships in qualitative or, more powerful, quantitative manner (*vide supra*) from changes of chromatographic responses upon structural variations. Some examples of qualitative structure-retention relationships can be found in Refs. [166–168] and QSRR studies have already been cited above.

In all of these chromatographic studies, one should be aware that elution orders are an important parameter to determine if interpretations on chiral recognition mechanisms are made.

## 6.2. Vibrational spectroscopy

Fourier transform infrared (FT-IR) spectroscopic studies on CS-SA complexation provides information on the involvement of functional groups in intermolecular and intramolecular interactions. Most characteristic IR frequencies that can be investigated for that purposes include C=O stretching vibrations of carboxylic, carbamate, amide groups (amide I band) as well as of C=C stretch and nitro absorptions which are frequently found in chiral selectors and selectands and constitute major intermolecular binding sites. Besides, the N-H deformation mode (amide II band) may constitute supportive information. Their involvement in intermolecular



interactions such as hydrogen bonding,  $\pi$ - $\pi$ -interactions, or ionic interactions may lead to significant shifts in frequencies as compared to the free state. For example, upon H-bonding a band wavenumber shifts to a lower value for a stretching vibration and to a higher value for a bending vibration [169]. For instance, when a carbonyl group forms a hydrogen bond the C=O stretching vibration is supposed to shift to lower frequency because the force constant gets weakened (due to partial single bond character) [170]. If the C=O stretch is shifted to higher frequencies upon CS-SA association, it may indicate that a hydrogen is broken or replaced by a weaker one. This is observed if a strong H-bond due to solvated functional groups of a binding partner in free state or due to self-association in free uncomplexed state is replaced by a weaker intermolecular H-bond in the CS-SA complex [170]. N-H deformation modes (amide II band) are supposed to shift to higher frequencies upon hydrogen bonding (oscillator frozen in plane strengthening the force constant) [170]. Shifts of C=C stretching vibrations and of (symmetric and asymmetric) nitro stretching vibrations may indicate  $\pi$ - $\pi$ -interactions [170]. One problem, if investigations are performed in solution or suspended state, represents, as indicated, to detach intermolecular CS-SA interactions from solvation effects or from autoassociation phenomena of the individual binding partners.

Attenuated total reflectance (ATR) FT-IR spectroscopy has been used for the study of binding modes of chiral selectors either in solution [170], in solution in the flow-through mode online hyphenated to CE [171], in solid-state [25], in suspended state [169], or directly with the CSP [172,173]. The basic principle of the ATR technique is outlined elsewhere [174]. Lesnik et al. investigated FT-IR spectra of 1:1 complexes of *O*-allylcarbamoyl-10,11-dihydroquinidine with (*S*- and (*R*-) enantiomers of *N*-3,5-dinitrobenzoyl (DNB) and *N*-2,4-dinitrophenyl (DNP) protected leucine (Leu) and *N*-methyl leucine (*N*-Me-Leu), respectively, as well as of the pure binding partners. For the study of the various intermolecular interaction effects, IR spectra were monitored in acetonitrile and acetonitrile/water solutions using attenuated total reflectance with a cylindrical internal reflection cell. Stereoselective hydrogen bonding could be proven unequivocally in the (*R*)-DNB-Leu/quinidine associate (the stronger complex) from the SA's N-H to the CS's C=O, but not in the respective complex with *N*-Me-Leu in which the H-donor group is not available [170]. In the corresponding DNP-complexes such H-bond formation is not possible, yet C=C and nitro band shifts suggested involvement of  $\pi$ - $\pi$ -interactions in both DNP-Leu and *N*-Me-Leu [170]. Less conclusive were the studies in solid-state of complexes with a similar selector, yet a different SA, namely 2-methoxy-2-(1-naphthyl)propionic acid that lacked both intermolecular CS-SA H-bond formation and  $\pi$ - $\pi$ -interaction [25]. Kasat et al. examined the ATR-IR spectra of a polysaccharide selector, cellulose tris(3,5-dimethylphenylcarbamate), in solid and solvent(hexane)-swollen state as well as in complex with several achiral and chiral guest solutes (aminoalcohols and alcohols) [169,175]. For the measurements the polymeric selector was spin-coated onto Si-ATR plates. Upon adsorption, IR spectra of the polymer amide groups changed significantly which indicated H-bond interactions.

A more elegant technology for probing chiral recognition by IR spectroscopy has been proposed by Buergi and coworkers [172,173,176]. ATR IR spectroscopy has been combined with modulation excitation spectroscopy and phase-sensitive detection, and the principles of this methodology have been explained in detail in Refs. [173,174]. The technique aims at suppressing signals arising from non-enantioselective interactions, which may overlap with and hide signals of interest that evolve enantioselectively. For such measurements, the CSP is fixed on the internal surface of an internal reflection element which was mounted in a flow-through cell (Fig. 10). SA enantiomers are flowed over the CSP film through the flow cell. The experimental setup as shown in Fig. 10 allows

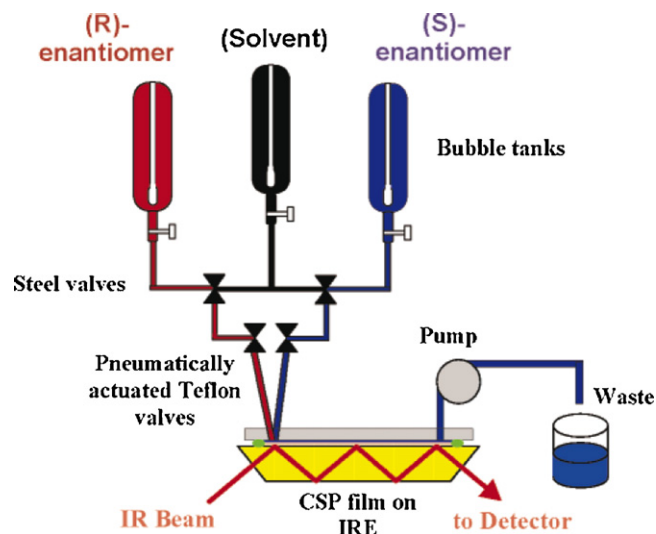


**Fig. 10.** Experimental setup of absolute configuration modulation attenuated total reflection IR spectroscopy. Three bubble tanks containing the neat solvent (acetic acid in acetonitrile), dissolved DNB-(*R*)-Leu, and dissolved DNB-(*S*)-Leu are connected via two steel valves to the flow-through cell in a way that two of these solutions can be alternately flown over the sample ("modulated") by switching the two computer controlled pneumatically actuated Teflon valves. During the "modulation", ATR-IR spectra are measured. IRE, internal reflection element. Reprinted with permission from Ref. [173].

to periodically alter the concentrations of the SA solutions flushed through the detection cell (*concentration modulation*) as well as the configuration of the SA solution (either *R*- or *S*-enantiomer) (*absolute configuration modulation*): hence three distinct experiments, namely modulation of *R*-enantiomer against solvent, modulation of *S*-enantiomer against solvent, and modulation of *R*-enantiomer against *S*-enantiomer were possible. In particular the last one is of significant interest because it directly provides information on stereoselective interactions. During the modulation experiments time-resolved IR spectra are monitored, and by subsequent phase-sensitive data analysis phase-resolved, i.e. demodulated spectra can be obtained. The acquired demodulated spectra are difference spectra between the two distinct states of the system, i.e. the signals that do not change periodically with the stimulation are cancelled out. Noise is efficiently filtered out so that the phase-sensitive data analysis generates high quality spectra with a good signal-to-noise ratio, at least much better than conventional difference spectra. For the case of absolute configuration modulation, only signals were detected that resulted from different interactions of the two opposite enantiomers. This greatly facilitated the interpretation of the spectra.

The method has been employed to study the adsorption of ethyl lactate at the surface of a CSP with amylose tris[(*S*)- $\alpha$ -methylbenzylcarbamate] coated onto silica [172]. The *D*-enantiomer was found to interact stronger with the CSP and spectral shifts revealed a stronger N-H...O=C hydrogen bond between the CSP's amide and the SA's ester group. The spectra also indicated that one of the araliphatic side chains of the amylose derivative is predominantly involved in the interaction with ethyl lactate. More than one interaction mode seemed to be involved and the spectra have lent support to the assumption that interaction with ethyl lactate induces a conformational change of the amide group of the polymeric selector. In another study, this technique was used for investigations of the chiral recognition mechanism of *tert*-butylcarbamoylquinine CSP and DNB-Leu as SA (Fig. 11) [173]. From frequency shifts of amide III (SA), amide II (SA) and amide I (CS) bands a stereoselective H-bond formation could be clearly confirmed, supporting the above stated chiral recognition mechanism obtained by ATR IR with the selector in solution [170].



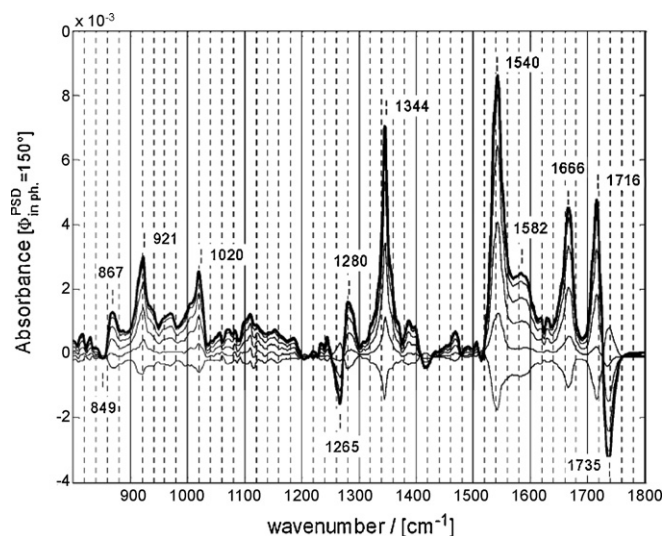


**Fig. 11.** Demodulated spectra of DNB-(R)-Leu vs. DNB-(S)-Leu on tert-butylcarbamoylquinine CSP. Both enantiomers were modulated against each other. All appearing signals are a consequence of the changing absolute configuration of the selectand. Reprinted with permission from Ref. [173].

One of the advantages of the modulation ATR IR technology is also that investigations can be made in media that are identical to chromatographic conditions which render results remarkably reliable and realistic for the real chromatographic situation.

Recently, with vibrational circular dichroism (VCD) another vibrational spectroscopy technique became available which turns out particularly powerful for the investigation of chiral recognition mechanisms. VCD is a form of vibrational optical activity. It is a chiroptical spectroscopy technique that can probe the stereochemical structure of chiral molecules through their vibrational transitions [174]. It actually represents simply an extension of traditional CD arising from transitions in the UV–vis regions of the spectrum to the IR region. A VCD effect may be defined as the difference in the IR absorbance  $A$  between left (L) and right (R) circularly polarized light according to the following equation:

$$\Delta A = A_L - A_R \quad (28)$$

Grinberg and coworkers used VCD for the investigation of structural peculiarities in cellulose and amylose tris(3,5-dimethylphenylcarbamates) and in particular for the explanation of a solute-dependent and polar solvent percentage-dependent reversal of elution order on amylose based CSP but not cellulose based CSP that was explained by solvent-induced conformational changes in the polymer backbone [32]. While IR spectra monitored in the solid film state of the polymeric selector materials were identical for cellulose and amylose tris(3,5-dimethylphenylcarbamate), their “chirality-sensitive” VCD spectra differed significantly for amides I, II, III bands as well as phenyl and C–O–C stretching vibrations (details will be discussed later). Julinek et al. used VCD along with ECD (electronic circular dichroism) to investigate stereoselectively occurring vibrational patterns in *tert*-butylcarbamoylated quinine and quinidine, respectively, (CS) complexed with DNB-Leu (SA) [177]. VCD bands assigned to vibrations of amide (SA), carbamate (CS), quinoline (CS) and carboxylate (SA) evolved partly stereoselectively.

### 6.3. NMR spectroscopy

NMR spectroscopy proved to be a powerful and versatile tool for investigating selector–selectand complex structures and there

are numerous studies in the literature that made use of NMR to study chiral recognition mechanisms of chiral selectors employed in LC. Many of the structural investigations of CS–SA complexes were based or supported by NMR methodologies. The advantage of doing so is that such investigations are done in solution. Although not necessarily rigorously identical, they mimic more closely the environment in liquid chromatography than solid-state (X-ray diffraction) or *in vacuo* experiments such as computations studies. Thus, such studies on bimolecular systems of chiral selectors in complex with selectands may advance the understanding of chiral recognition of LC enantiomer separation.

A survey of the literature shows that NMR was employed as tool for investigating chiral recognition mechanisms with selectors of donor–acceptor phases (Pirkle-type phases) [148,178–187], chiral ion-exchangers (i.e. cinchona alkaloid derived [24,25,33,188,189] and terguride-derived CSPs [190]), cyclodextrin-based CSPs [191–194], chiral crown ether based CSPs [195–201] and polysaccharide CSPs [202–206]. Also protein NMR was shown to be a viable route to information on chiral recognition of ovomucoid protein selector [23,207]. Useful information about CS–SA complexation can be extracted from the various NMR parameters such as chemical shifts, coupling constants, NOE and ROE, and relaxation rates. They may be used to derive various sets of information including the following: (i) Binding stoichiometries and association constants may be unveiled by continuous CS–SA titration experiments [24,191]. (ii) Conformational preferences of the binding partners in free solution and in complex may be obtained from dihedral coupling constants and intramolecular NOEs [24,188]. (iii) Self-association phenomena of selector and selectands may be deduced from shifts of particular NMR signals upon continuous dilution of CS and SA solutions, respectively [148,182,208]. (iv) Deeper insights into intermolecular interactions and 3D-arrangement of the host–guest complex may be gained from significant complexation-induced chemical upfield or downfield shifts and intermolecular NOEs [24,188].

CS–SA complexes measured by NMR have usually lifetimes that are short compared to the NMR time scale and as a result the exchange rate between complexed and free states is fast. Consequently, observed spectral parameters ( $P_{obs}$ ) are usually obtained mole fraction ( $x$ ) weighted averages of the corresponding property of free and complexed species

$$P_{obs} = x_f P_f + x_c P_c \quad (29)$$

wherein subscripts  $f$  and  $c$  refer to free and complexed states.

The main property monitored by NMR are chemical shifts ( $\delta$ ) of nuclei. CS–SA complexation may lead to changes in chemical shifts owing to alterations in local magnetic environments and these complexation-induced chemical shifts (CIS) may evolve stereoselectively in two diastereomeric CS–SA complexes. In this case,  $P$  in Eq. (29) may be substituted by  $\delta$  and CIS ( $\Delta\delta$ ) is simply defined as the difference of  $\delta_{obs}$  and  $\delta_f$ . Of particular interest are signals that yield non-equivalence of CIS in diastereomeric CS–SA associates ( $\Delta\Delta\delta$ ) pointing towards stereoselectively occurring interactions.

Observation of CIS upon CS–SA complexation has been instrumental in validating various kinds of intermolecular interactions. Along this line, significant shifts of amide N–H signals (in non-protic solvents such as chloroform) are indicative for hydrogen bonding [179,181,182], CIS of aromatic protons propose  $\pi$ – $\pi$ -interactions and occur upfield or downfield depending on whether they have a deshielding or shielding effect [24,179,181,182,188,190], and shifts in neighbor protons of ionizable groups such as tertiary amines or carboxylic groups may indicate ionic interactions [24,25,33,188,190]. CIS may be particularly strong and downfield if the involved nuclei are positioned in the deshielding region of ring current [24,179]. There are numerous reports in which CIS has been exploited to derive information on intermolecular inter-

actions (see, e.g. Ref. [24,25,33,148,179,181,182,188,190,196,198]). CIS as large as 1.5 ppm shifted downfield has been found, for example, for the amide NH in the homochiral (S;S)-complex of Whelk-O1 selector with strong stereochemical preference over the heterochiral (S;R)-complex ( $\Delta\delta = 0.24$  ppm) [179]. Noticeable upfield shifts of aromatic protons of each involved species occur frequently due to face-to-face  $\pi$ - $\pi$ -interaction since each aromatic system is shielded by the other one in the complex [24,148,179,181]. To elucidate stereoselectivity of CIS-derived intermolecular interactions, differential CIS ( $\Delta\delta$ ) of corresponding diastereomeric associates should be computed which allows to rule out non-stereoselective effects that frequently occur especially for primary driving interactions, e.g. amide hydrogen bonding in Pirkle systems [179] or ionic interactions in ion-exchange systems [24,190].

Employing a continuous titration experiment of CS with SA information on binding stoichiometry and association constants, respectively, can be derived [24,153,191,194,196]. Binding stoichiometry is usually determined by the continuous variation method in which CS is titrated with SA and CIS of a characteristic diagnostic proton is monitored as function of the molar CS-SA ratio. The data are plotted as product of mol fraction of chiral sector ( $X_{CS}$ ) and its CIS ( $\Delta\delta$ ) versus mole fraction of selectand ( $x_{SA}$ ) (Job's plot) [24,191,194,196,203]. Maxima of Job plots at  $x_{SA}$  of 0.5 and 0.66 indicate 1:1 and 2:1 stoichiometry between SA and CS, respectively. As preferred binding stoichiometry 1:1 complexation was observed in most cases [24,191,196]. From such data set also association constants may be inferred (e.g. by treating the data according to Scott's technique [154]) as described for example in Refs. [153,192,203].

Another way for exploring chiral recognition mechanisms between chiral selectors and selectands takes advantage of the dependence of dipolar interactions on interproton distances [194]. Such dipolar coupled nuclei feature a nuclear Overhauser effect (NOE) which manifests itself as the intensity change of one NMR signal as a result of the perturbation of another signal. It decays rapidly as the distance between involved nuclei increases (proportional with  $r^{-6}$ ) making them an ideal tool to monitor intramolecular and intermolecular proximity, and thus of conformational preferences and complex geometry, respectively. Only interproton distances smaller than 0.5 nm can be reliably measured by NOE [194]. With the advent of modern NMR techniques such investigations have been frequently performed by acquiring 2D-NOESY and 2D-ROESY spectra, respectively, of diastereomeric CS-SA complexes in relation to their free forms [24,148,179,181,182,188,192,193]. It is noted that the intensity of NOEs depends on correlation time  $\tau_c$  and Larmor frequency  $\omega$ ; small ligands have usually a minor positive or weakly negative NOE due to effective correlation times of a fraction of a nanosecond placing them near the transition from positive to negative NOE which results usually in a weak, if any, NOE. In contrast, NOEs in rotating frame are always positive becoming the method of choice for medium sized molecules and complexes, respectively [194]. Along this line intramolecular NOEs have been exploited to pinpoint conformational states of CS and SAs in free and complexed form [24,148,179,181,188].

Intermolecular NOEs, in contrast, provide information about relative orientations of chiral selector and selectand in a complex. In a number of studies, reproducible intermolecular NOEs have been reported [24,179,181,188]. Such intra- and intermolecular NOEs have been pointed out to support rationally designed chiral recognition models as well as to confirm that solid-state complex structures derived from X-ray diffraction or computational models also exist in solution and thus in chromatographic environment as well.

Like other spectral parameters NOEs are averaged over all species in solution and one has to be aware that, owing to  $r^{-6}$  distance dependency, a small fraction of a species with short inter-

proton distance may give rise to a substantial NOE [194], which must not be erroneously pretended as a strongly populated complex conformation. Accordingly, it is not straightforward to obtain populations of different conformers from NOESY or ROESY experiments quantitatively, e.g. by measuring volumes of cross-peak signals due to the uncertainties in knowledge of interatomic distances and thermal averages for all of the conformers; moreover different time constants can be crucial to this analysis [209]. Quantification of conformer populations, by contrast, may be possible in a straightforward manner from dihedral coupling constants [24,188,209]. The experimentally measured vicinal coupling constant of a torsion  ${}^3J_{\text{HxHy}}$  actually represents the average over the populations  $P_{(i)}$  of the different conformers in solution according to [209]

$${}^3J_{\text{HxHy}}(\text{obs}) = \sum P_{(i)} {}^3J_{\text{HxHy}(i)} \quad (30)$$

Based on calculations of torsional angles of different conformers and application of the (modified) Karplus equation (e.g. Altona equation), the coupling constants for the individual conformers may be determined which then allows to derive their relative populations  $P_{(i)}$  in solution from experimentally observed coupling constants  ${}^3J_{\text{HxHy}}(\text{obs})$  by simple calculations [209]. This procedure for example has been very popular for semi-rigid cinchona alkaloid derived selector systems in which the overall conformation was mainly determined by the central torsion H8-C8-C9-H9 (*vide infra*) [24,25,33,188]. Changes of dihedral coupling constants upon complex formation indicate a change of conformations relative to the free form and may provide also valuable information on the dynamic behavior of a system in the course of selector-selectand binding and chiral recognition, respectively [24,25,33,181,188].

Other spectral properties have been less frequently utilized for the investigation of chiral recognition mechanisms of LC-relevant chiral selectors. Only in a few studies different selective relaxation rates  $R^S$  and relaxation times  $T_1$ , respectively, or distinct diffusion coefficients  $D$  by diffusion experiments employing pulsed field gradient technique [154] have been reported for enantiomers upon their interaction with chiral selectors (see for example Refs. [23,148,210,211]). Such investigations are based on the dependency of these NMR parameters according to Eq. (29).

All these NMR studies were performed in solution with various chiral selectors assuming that the situation in solution is directly applicable to LC. With the advent of high-resolution solid-state and suspended state NMR spectroscopy, also examination of chiral recognition directly with a chromatographic system became possible. This has been shown for example by Albert and coworkers [189]. High-resolution magic angle spinning (HR/MAS) 2D transfer-NOESY spectroscopy was utilized to elucidate chiral recognition between amino acid derivatives and a quinine carbamate CSP, which was suspended in the mobile phase. This NMR technology makes use of the observation of a transferred nuclear Overhauser effect (trNOE). Thereby, the weak positive intramolecular NOE of low-molecular mass ligands becomes a strong negative NOE, if the ligand is binding to a macromolecular species such as a CSP. The strong negative NOE can be detected in the ligand after its dissociation from the CSP, indicating its interaction with the CSP. Consequently, this NMR technique allows for straightforward and rapid differentiation between effective binders (negative cross-peaks) and weak binders (positive cross-peaks). HR/MAS 2D trNOESY spectroscopy experiments were performed with a quinine carbamate CSP suspended in a 0.1 mol/L solution of either enantiomer of DNB-Leu or *N*-acetyl-phenylalanine (Ac-Phe) in deuterated methanol [189]. The intensities for the negative cross-peaks were always higher for the stronger binding *S*-enantiomers (factor of 7.4 for DNB-Leu and 2.4 for Ac-Phe). Thus, relative binding affinities and relative magnitudes of enantioselectivities were

correctly predicted by trNOESY experiments. It could serve as fast screening technique for chiral recognition of new CSPs in a microscale format.

#### 6.4. Single-crystal X-ray diffraction analysis

X-ray diffraction experiments provide a three-dimensional map of electron densities and therefore a complete three-dimensional “picture” of the substance in question. Thus, X-ray diffraction analysis of single crystals of CS–SA complexes that were grown from (equimolar) solutions of CS and SA in a favorable crystallization solvent allows to solve their solid-state structure, with a certain resolution and with some uncertainty of atomic positions. It thus directly provides comprehensive information of structural features such as complete sets of atomic distances, angles, dihedral angles, spatial distances as well as to some extent intra- and intermolecular interactions. It is thus a unique experimental technique to provide vivid 3D-images of CS–SA binding states. Such solid-state structures of liquid chromatographic chiral selector in complex with selectand enantiomer have been reported for low-molecular selectors of donor–acceptor (Pirkle) type [212–215] and ion-exchange type (i.e. terguride [216,217] and cinchona alkaloid derived [24,25,33,166,218]), for macrocyclic selectors (cyclodextrins [192] and crown ether [219]), and last but not least for proteins (HSA [220] and cellobiohydrolase [221]) (see Table 3). One has to be aware, though, that solid-state structures may be different compared to solution or chromatographic situation. The medium used for crystallization may affect the resultant 3D structure. Moreover, crystal structures are prone to distortions. While the X-ray structure represents quasi a snapshot of one favorable binding arrangement, the situation in solution may be more complex with a distribution of differently populated CS–SA binding conformations. Nevertheless, X-ray structures should represent energetically favorable arrangements, in which torsional angles are very often, if not at their global, at least at a local optimum. Hence they turned out to be very valuable for gaining insight into CS–SA binding modes especially when combined with other techniques such as NMR. Along this line, Pirkle et al. found basic agreement between the solid-state structures from X-ray diffraction and interaction mod-

els derived from NMR in solution [212,213,215] and the same applied to several of the cinchona alkaloid-derived CS–SA systems [24,25,33]. In the latter systems, it was clearly shown by NMR that besides the predominant binding orientation that was displayed in the solid-state structure a number of other minor populated complex conformations existed in solution [24,25,33,188]. Chankvetadze et al. found basic agreement between the solid-state structure of (+)-pheniramin/ $\beta$ -cyclodextrin with NMR measurements, yet complete disagreement for the solid-state structure of (+)-pheniramin with another chiral selector, namely trimethyl- $\beta$ -cyclodextrin [192].

Last but not least it should be mentioned that it is sometimes cumbersome to get useful co-crystals of CS and SA for X-ray diffraction analysis. Especially the weak complex very often shows a poor crystallization tendency or yields poor quality crystals fully packed with solvents which are destroyed upon irradiation with X-rays. The salt character of the above mentioned ion-exchange selectors provide them with an advantage for this technology. In view of this, it is not surprising that mostly only one structure of the two diastereomeric complexes has been obtained. Of particular interest are, however, those were both of the diastereomeric complex structures are available [214,215,219]. Recently, Bicker et al. could succeed in getting all four isomeric X-ray crystal structures of permethrinic acid, a compound with two stereogenic centers, with a O-9-(2,6-diisopropylphenylcarbamoyl)quinine [33].

The issue of solid-state/solution state structure discrepancy is different for proteins. Protein crystals contain large holes which are filled with solvent molecules. Hence the protein remains more or less in the natural environment. This is why protein structures determined by X-ray crystallography are the same as in solution. Two examples were found in the literature which may be related to liquid chromatography. In one HSA was complexed with either S- or R-enantiomer of warfarin. It is particularly remarkable that both of the diastereomeric complex structures could be resolved. In these complexes, the two enantiomers of warfarin adopt very similar conformations and binding geometry in the binding pocket of the protein. Moreover, they make many of the same specific contacts with amino acid side chains at the binding site, thus accounting for the relatively low stereoselectivity of the HSA-warfarin interaction [220]. In the other one, (S)-propranolol, the stronger binding

**Table 3**  
CS–SA complex single-crystal X-ray diffraction studies for the investigation of chiral recognition in solid-state.

CS	SA	Ref.
<i>Low-molecular selectors</i>		
(S)-N-DNB-Leu <i>n</i> -propylamide	(S)-Methyl (2-naphthyl)alaninate	[212]
(S)-N-Pivaloylproline-3,5-dimethylanilide	(S)-N-(3,5-Dinitrobenzoyl)leucine dimethylamide	[213]
(R)- and (S)-N-1-(1-naphthyl)ethylacetamide	(+)-N-(1-Phenylethyl)-3,5-dinitrobenzamide	[214]
Whelk O1 selector	(R)- and (S)-pivalamide of <i>p</i> -bromo- $\alpha$ -phenylethylamine	[215]
1-Allylterguride	(S)-Naproxen	[216]
(+)-Allylterguride	(S)-Dansyl-tryptophan	[217]
(+)-Allylterguride	(S)-Dansyl-serine	[222]
O-9- $\beta$ -Chloro-tert-butylcarbamoylquinine	(S)-N-3,5-Dinitrobenzoyl-leucine	[218]
O-9- $\beta$ -Chloro-tert-butylcarbamoylquinine	(S)-N-3,5-Dinitrobenzoyl-leucine	[166]
O-9- $\beta$ -Chloro-tert-butylcarbamoylquinidine	(R)-N-3,5-Dinitrobenzoyl-leucine	[166]
O-9- $\beta$ -Chloro-tert-butylcarbamoylquinine	N-3,5-Dinitrobenzoyl-(S)-alanine-(S)-alanine	[166]
O-9-tert-Butylcarbamoyl-6'-neoptoxy-cinchonidine	(S)-N-3,5-Dinitrobenzoyl-leucine	[24]
O-9- $\beta$ -Chloro-tert-butylcarbamoylquinine	(S)-2-Methoxy-2-(1-naphthyl)propionic acid	[25]
O-9-(2,6-Diisopropylphenylcarbamoyl)quinine	(1R;3R)-, (1S;3S)-, (1S;3R)-, and (1R; 3S)-3-(2,2-Dichlorovinyl)-2,2-dimethylcyclopropanecarboxylic (permethrinic acid)	[33]
<i>Macrocyclic selectors</i>		
$\beta$ -Cyclodextrin	(+)-Brompheniramine	[192]
Trimethyl- $\beta$ -cyclodextrin	(+)-Brompheniramine	[192]
(+)-18-Crown-6-tetracarboxylic acid	(R)-1-(1-Naphthyl)ethylamine	[195]
(+)-18-Crown-6-tetracarboxylic acid	D- and L-serine	[219]
(+)-18-Crown-6-tetracarboxylic acid	D- and L-glutamic acid	[219]
<i>Proteins</i>		
Cellobiohydrolase	(S)-Propranolol	[221]
HSA	(R)- and (S)-warfarin	[220]



enantiomer, was complexed with cellobiohydrolase I in the active binding site via a network of ionic and hydrogen bonding interactions (vide infra) [221].

## 6.5. Computational methods

### 6.5.1. Chemoinformatics

In the 1990s researchers around C. Roussel started to collect liquid chromatographic enantiomer separation data and began to build a database called *Chirbase* which has now about 160,000 entries of chiral separations by HPLC, SFC, and SMB that have been achieved on about 1650 commercial and non-commercial CSPs (<http://chirbase.u-3mrs.fr/>) [223]. The database contains about 60,000 chiral compounds. It has been established to aid users in the development of chiral separations. It is obvious that a data collection of this size is extremely rich in information on chiral recognition mechanisms which however needs to be somehow extracted [224]. For data mining from this and similar data collections various chemoinformatic tools could and have been adopted [225] as has been reviewed in detail recently by Del Rio [130]. Chemoinformatics and data mining, respectively, uses mathematically statistically based methods for pattern recognition and some classical problems chemoinformatics in chiral separation is dealing with are deriving chirality descriptors, quantification of chirality, classical and modern versions of QSPR, 3D-QSPR, chiraphore and enantiophore modeling and other data mining approaches. The interested reader on these topics is referred to [130].

### 6.5.2. Molecular modeling

With the ever growing power of computers, software and computer graphics (for displaying structures along with their physicochemical properties) molecular modeling has become a practical tool for evaluating more complex interactions such as those of associations between chiral selectors and selectands. The field is to some extent dynamically developing and has become accepted as research tool in studying bimolecular systems, although one must not forget that computed structures always represent models with varying degree of approximation to real situations. The topic has been reviewed by Lipkowitz [226,227] and only a few comments and ideas from this review should be outlined herein. Molecular modeling of enantiodiscrimination usually involves the concept of potential energy surface, i.e. the potential energy surface of a molecule dictates its 3D structure, dynamics and reactivity. Hence energy minimizations which seek the nearest minimum rather than the global one are to be performed from different starting points for a representative sampling. Since ab initio quantum mechanical (QM) methods of typical CS, SA systems and complexes can still be computed within reasonable time on a small number of structures only, semi-empirical QM or more often molecular mechanics (MM) calculations are implemented in more comprehensive calculations. A number of approximations and assumptions have to be made in the modeling of the enantioseparation process. Instead of considering the entirety of the CSP surface the chiral selector is usually truncated (exemptions include for example recent computational studies by Cann and coworkers in which the interface of a Whelk-O1 CSP was modeled with end-caps and silanol groups [228–231]). Solvents, buffers and additives are not considered explicitly like ionization of ionizable selectors and selectands. Another simplification is related to the computations themselves: differential free energies rather than absolute free energy values are computed and due to the enantiomeric relationship of the left-hand side of Eqs. (1a) and (1b) only the right hand side complexes need to be computed. Solvation effects and entropy differences are assumed to be canceled out in the two diastereomeric complexes. Last but not least there is the sampling problem: the question is raising how many distinct CS–SA com-

plexes must be computed to make results representative for the studied system and meaningful. Various methods are applied for reducing the number of samplings on the potential energy surface. Most frequently, nowadays researchers employ nanosecond stochastic molecular dynamics (MD) simulations [24,188,232]. In molecular dynamics, successive configurations of the given CS–SA system are generated by integrating Newton's law of motion. The result is a trajectory that specifies how the positions and velocities of the particles in the system vary with time [233]. The number of sampled configurations is usually large. Instead, a Monte Carlo simulation strategy that generates configurations of a system by making random changes to the positions of the species present [233] may be adopted for which it is important that a sufficient number of relevant configurations is sampled. When the binding site or preferential binding interactions are known a motif-based docking strategy may be applied with a reduced sampling of a limited number of orientations. Intramolecular NOE derived constraints or X-ray complex structures are also good starting points for molecular docking.

Lipkowitz reviewed early computational studies about enantiomer separation by various CSPs [226] including donor–acceptor (Pirkle-type), polysaccharide, cyclodextrin, chiral ligand exchange, and protein CSPs. Some of the more recent examples of molecular modeling studies comprise the following works. Lavecchia et al. performed enantioselective docking studies of aryloxyacetic acids into the active site of penicillin G acylase [234]. Alcaro et al. proposed methodologies for a flexible automatic docking process of CS and SA employing the global molecular interaction evaluation (Glob-MollnE) computational protocol which was exemplified by the docking of (*R*)- and (*S*)-*N*-(2-naphthyl)alanine methyl ester SAs to the Pirkle-type chiral selector (*S*)-*N*-3,5-dinitrobenzoyl-leucine-*n*-propylamide [235]. In a series of papers, Lipkowitz et al. presented MD simulations of enantioselective complexation of amino acid and peptide derivatives with various cinchona alkaloid derived selectors as well as their partition into binding increments [24,188,232]. Bauvais et al. reported docking studies of amino acids and peptides on vancomycin selector and MD simulations [236]. Molecular recognition mechanisms by Whelk-O1 selector were subject of a recent computational study by Del Rio et al. [237], while Zhao and Cann performed docking studies of various analytes on Whelk-O1 accounting for the interface including silanols and end-cap groups followed by MD simulations [229,231]. Kasat et al. employed MD simulations to investigate the binding interactions of 13 structurally similar chiral solutes to an oligomer analog model of cellulose tris(3,5-dimethylphenylcarbamate) consisting of 9 glucose units with pendant 3,5-dimethylphenylcarbamate residues (“9-mer”). Supported by H-bonding information from ATR IR measurements binding into the cavities formed by the side chains could be proposed. Ye et al. combined NMR and computational methods (MD) to investigate the separation of *p*-*O*-*tert*-butyltyrosine allylester by amylose tris(3,5-dimethylphenylcarbamate) which showed exceptional enantioselectivities [238].

Besides elaborate (MD) studies simple computations employing ab initio and density functional theory computations, respectively, on diastereomeric complexes are more frequently found nowadays in the literature which, however, suffer from the fact that they may not necessarily represent the global optimum nor do they adequately account for the dynamics of CS–SA systems [33,173].

## 7. Chiral stationary phases and their properties

The key for success of enantiomer separations lies in the first place in a proper selection of a suitable chiral stationary phase having chiral distinction capability for the target solute enantiomers. Hence, knowledge about existing chiral stationary phases



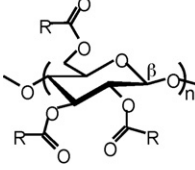
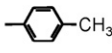
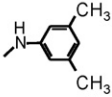
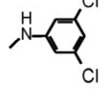
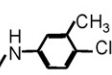
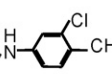
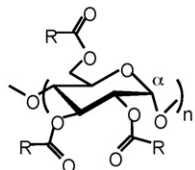
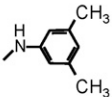
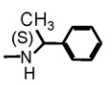
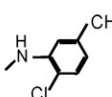
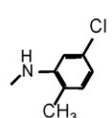
and their properties is of major importance in this field. Numerous chiral molecules from the natural chiral pool or synthesized in stereoselective form have been subject of scrutiny in terms of chromatographic enantioselectivity and suitability as chiral selectors. More than hundred CSPs are nowadays offered commercially and amongst them about 20–30 CSPs, or even less, are most frequently employed and can together cope with virtually all enantiomer separation problems of various compound classes.

### 7.1. Polysaccharide CSPs

Polysaccharide selectors have a long tradition in enantioselective liquid chromatography. Early work from Hesse und Hagel with microcrystalline cellulose triacetate (MCTA) as a polymeric selector material without supporting beads dates back to the 1970s [239,240]. Plain crosslinked beads of polysaccharide derivatives without support have also been proposed as chiral separation media and showed enhanced loading capacities, yet with some deficiencies in terms of hydrodynamic and kinetic properties [241,242]. The mechanical stability problem of MCTA could be overcome by Okamoto et al. in 1984 by coating cellulose derivatives onto the surface of macroporous silica beads (1000 Å pore size) as a thin film of about 20 wt% [243]. Such coated polysaccharide CSPs based on cellulose and amylose derivatives (i.e. carbamate and esters) with much better efficiencies have set the state-of-the-art for several decades and are since recently available from several suppliers (see Fig. 12). Most remarkable recent advancements constitute the introduction of immobilized polysaccharide CSPs with expanded solvent resistancy into the market beginning with 2005, the development of which has been an active research field since the 1990s pioneered by Francotte [4], Oliveros, Minguillon and coworkers [244] and Okamoto and coworkers [245]. Coated versions of the polysaccharide CSPs are restricted to the use with alkane-alcohol based normal-phase (NP) conditions, polar organic (PO) conditions (with polar organic solvents such as alcohols and acetonitrile) and hydro-organic reversed-phase (RP) mode (the latter with dedicated version in which the polysaccharide is coated onto a different support). By contrast, immobilized analogs become compatible with so-called “non-standard” solvents which include amongst others dichloromethane, chloroform, ethyl acetate, tetrahydrofuran, dioxane, toluene and acetone. The exposure of coated CSPs to these solvents induces swelling and/or dissolution of the physically adsorbed polymer layer ultimately destroying the column by stripping off the selector. Applications, characteristics and specific method development considerations of these immobilized polysaccharide CSPs can be found in Refs. [246] for Chiralpak IA, [247] for Chiralpak IB and [248] for Chiralpak IC.

As another trend supporting silica particles are getting smaller in diameter (from 5 μm to 3 μm for analytical applications) which is a development running somehow in parallel to UPLC directions in the RPLC field.

The exceptional chiral recognition properties of polysaccharide CSPs originate from a number of structural peculiarities. They exhibit hierarchically ordered chirality stemming from (i) molecular chirality due to the presence of several stereogenic centers of the glucopyranose units, (ii) from conformational chirality due to helical twist of the polymer backbone, and (iii) from supramolecular chirality resulting from the alignment of adjacent polymer chains forming ordered regions (with evidence of crystallinity proven by XRD [175]). A number of recent investigations by solution NMR of oligomeric surrogates [203,206,238], solid-state NMR [175], computational studies [71,175,238,249], ATR-IR [169,175], thermodynamics [37,71,250] and quantitative structure–property relationship studies [118,119,250,251] and most recently VCD greatly contributed to the knowledge of the structures of polysac-

Polymer backbone	Residue	Name	Tradename
 Cellulose		Cellulose tris(4-methylbenzoate)	a
		Cellulose tris(3,5-dimethylphenylcarbamate)	b
		Cellulose tris(3,5-dichlorophenylcarbamate)	c
		Cellulose tris(4-chloro-3-methylphenylcarbamate)	d
		Cellulose tris(3-chloro-4-methylphenylcarbamate)	e
 Amylose		Amylose tris(3,5-dimethylphenylcarbamate)	f
		Amylose tris((S)-α-methylbenzylcarbamate)	g
		Amylose tris(2-chloro-5-methylphenylcarbamate)	h
		Amylose tris(5-chloro-2-methylphenylcarbamate)	i

**Fig. 12.** Selector structures of coated and immobilized polysaccharide CSPs along with column tradenames. Note cellulose consists of 1,4-connected-β-D-glucose units and amylose of 1,4-connected-α-D-glucose units. Tradenames: Coated versions: a, Chiralcel OJ; b, Chiralcel OD, Kromasil CelluCoat, Lux Cellulose-1, RegisCell, Nucleocel delta, Eurocel 01; d, Chiralcel OZ; e, Lux Cellulose-2; f, Chiralpak AD, Kromasil AmyCoat, RegisPack, Nucleocel alpha, Europak 01; g, Chiralpak AS; h, Chiralpak AY; i, Lux Amylose-2. Immobilized versions: b, Chiralpak IB; c, Chiralpak IC; f, Chiralpak IA, Chiralcel and Chiralpak are tradenames of Daicel (Chiral Technologies), Kromasil of EKA, RegisCell and RegisPack of Regis Technologies, Lux of Phenomenex, Nucleocel of Macherey & Nagel, and Eurocel from Knauer. Structures were collected from webpages of the suppliers.

charides CSPs and the advancement of their chiral recognition mechanisms.

The linear glucopyranose polymer chains are slightly helically wound and the helical twist is minor for the cellulose derivatives than the amylose derivatives. Based on 2D NOESY and computational studies, Yamamoto et al. suggested a left-handed 4/3 helical structure for amylose tris(3,5-dimethylphenylcarbamate) as the most probable one [206]. Very recently, experimental evidence on the conformational preferences of amylose and cellulose tris(3,5-dimethylphenylcarbamate) could be provided [32]. While IR spectra of these two polymeric chiral selectors that differ only in the stereochemistry of the α-carbon of the glucopyranose unit were almost identical, their VCD spectra differed significantly (Fig. 13). ADMPC showed VCD features of two (+−) couplets in the amide I region (1754–1700 cm<sup>−1</sup>) which was interpreted as indication for a left-hand helical structure. Conversely, for CDMPC an opposite couplet (−+) feature was observed indicating a different conformation of the backbone and it was argued that it is most likely a right-handed helical structure [32]. Some of the distinct chiral

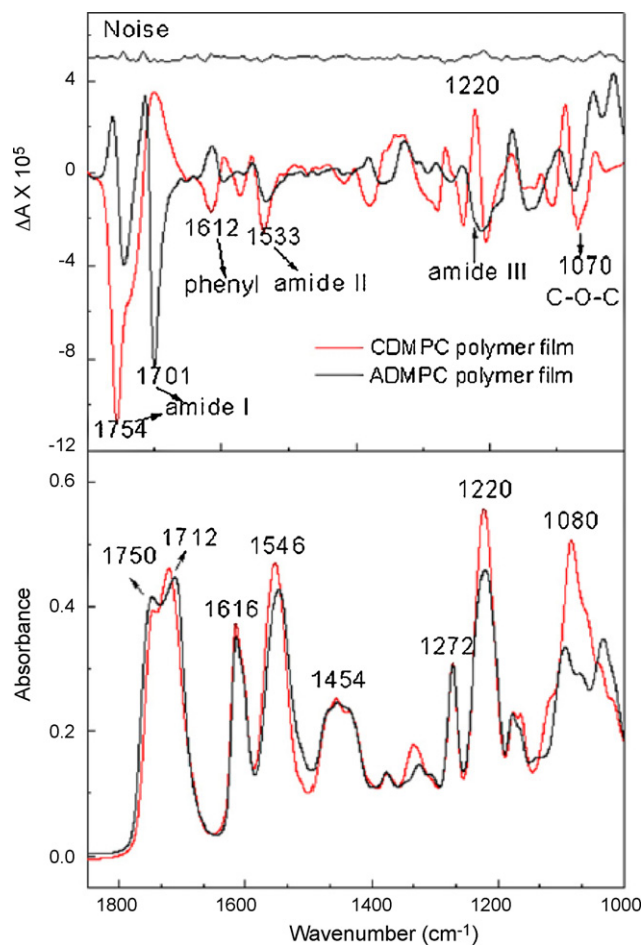


**Fig. 13.** VCD and IR spectra of the amylose tris(3,5-dimethylphenylcarbamate) (ADMPC) polymer film (black curve) and the cellulose tris(3,5-dimethylphenylcarbamate) (CDMPC) polymer film (red curve). VCD spectra are presented in the upper trace; noise level is offset for clarity. The IR spectra are presented in the lower trace. (For interpretation of the references to color in this figure legend, the reader is referred to the web version of the article.) Reprinted with permission from Ref. [32].

recognition capabilities of these two different selectors may originate from this subtle difference. Changes in the VCD spectra upon variations in the polarity of the solvent, i.e. either exchange of type or percentage of polar modifier in the mobile phase clearly suggested that the conformations are altered by such solvent effects and this is very much in agreement with former reports, e.g. solid-state and suspended state NMR ( $^1\text{H}/^{13}\text{C}$  CP/MAS) measurements on the solvent complexation capability of ADMPC CSP in dependence of the solvent composition (hexane vs. hexane-2-propanol and hexane-ethanol mixtures, respectively) [252]. Such solvent-induced conformational changes [32,253] may dramatically alter the binding and chiral recognition properties of the polymer, and even a reversal of elution order with the polarity of the mobile phase (i.e. the percentage of hexane-alcohol mixtures) has been observed and explained on basis of altered conformational states as revealed by VCD [32]. Such reversal of elution orders has also been observed upon a change between the two polar modifiers ethanol and 2-propanol with Chiralpak AD [254]. Likewise, temperature-induced alterations in the separation performance have already earlier been ascribed to conformational changes of the polymer selector by the same group [71].

Another factor that considerably governs the enantioselectivity power of polysaccharide selectors is their substitution pattern, viz. type of polar functional group (usually ester or carbamate) and

aromatic substitution (Fig. 14a). This substitution pattern creates a regular arrangement of grooves along the carbohydrate chain (Fig. 14a) which serve as enantioselective binding pockets. The driving polar hydrogen bonding interactions are buried deeply inside the cavities near the backbone and are flanked by rigid bulky aromatic substituents which are located at the surface and may control the access to the binding site via steric factors. The aromatic moieties may [169] or may not [71] be involved in supportive  $\pi$ - $\pi$ -interactions depending on other factors of the binding mode. The carbamate and ester functionalities allow for a flexible

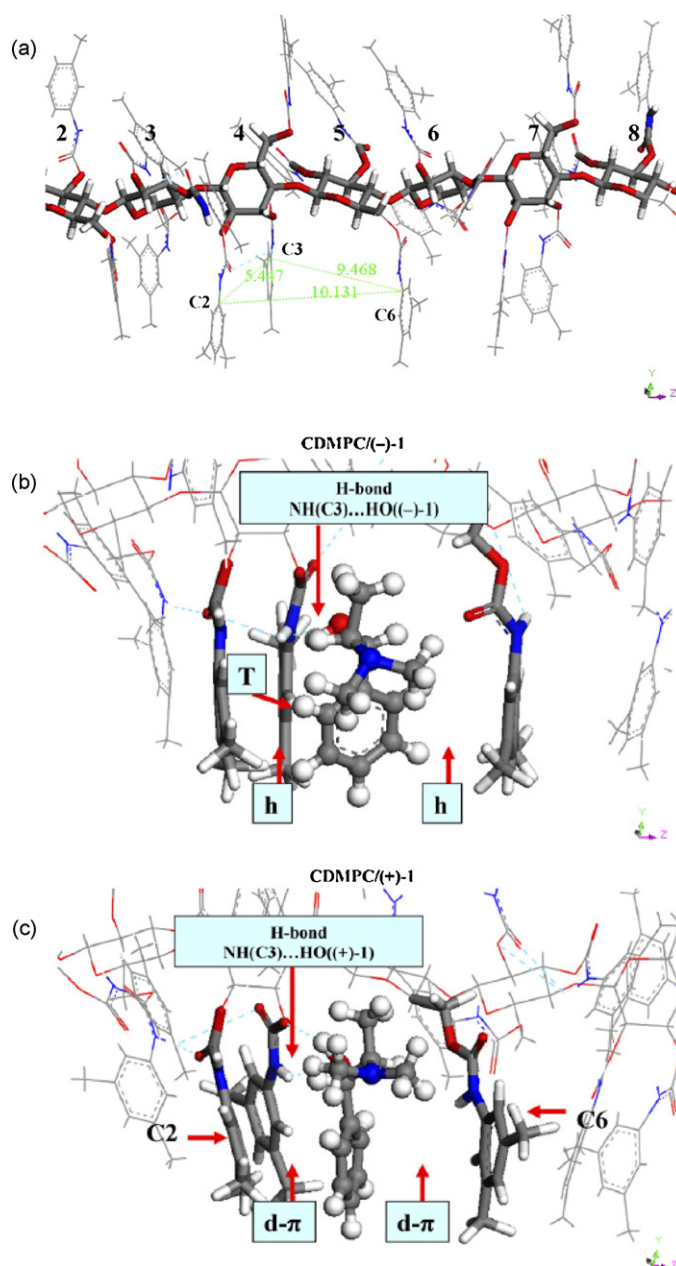


**Fig. 14.** (a) 3D structure of CDMPC (9-mer) generated using Materials Studio. The backbone atoms are shown with ball and stick representation while the side chains are shown with line representation. The monomers are numbered from 1 to 9, and monomers 2–8 are shown. The distances between C2, C3, and C6 side chains give an indication of the cavity dimensions. (b and c) Energy minimized structures of CDMPC complexes with (b) (-)-enantiomer and (c) (+)-enantiomer of N-methylephedrine. The dotted lines indicate H-bonds. The d- $\pi$ , T, and h indicate parallel displaced, T-shaped, and herringbone  $\pi$ - $\pi$ -interactions, respectively. Reprinted with permission from Ref. [169].

conformational adjustment (induced fit) of aromatic portions as to maximize their  $\pi$ - $\pi$ -interactions and to additionally stabilize the CS-SA complex. This general binding mechanism for polysaccharide CSPs has been essentially derived or supported by various NMR, IR and computational studies [71,169,203,206,238] and is in full agreement with an earlier proposed binding and chiral recognition model by Booth and Wainer [118,119]. An example of a model featuring the binding of N-methylephedrine enantiomers into the cavity of CDMPC as obtained by MD simulations is shown in Fig. 14b and c. Similarly, Kasat et al. modeled the specific binding sites for (+)- and (-)-2-amino-1-phenyl-1-propanol with three polysaccharides, amylose tris(3,5-dimethylphenylcarbamate) and amylose tris[(S)- $\alpha$ -methylbenzylcarbamate] as well as cellulose tris(3,5-dimethylphenylcarbamate) [255].

The type of side chain may also have some effect on the helical structure of the polymer. Hence, from above discussion it is understandable that, besides the backbone, the type of derivative, ester or carbamate, as well as the residue plays a major role for the enantioselectivity profiles of the polysaccharide CSPs. Detailed chromatographic investigations on the impact of aromatic substituents on the chromatographic chiral recognition characteristics of cellulose carbamate derivatives furnished the best results for 3,4- and 3,5-dimethylphenyl- and dichlorophenylcarbamate derivatives [256]. Especially the 3,5-dimethylphenylcarbamates have thus been selected as first choice for commercial CSPs, yet a larger number of other derivatives with complementary enantioselectivities is principally available and sometimes implemented in screening programs with preparative focus. Recently, also mixed methyl/chloro-substituted derivatives were introduced as commercial products providing some complementary enantioselectivity profiles (see Fig. 12).

Since the early work of Hesse and Hagel the awareness exists that microcrystallinity and supramolecular structure, respectively, as attained by the laminar arrangement of the polysaccharide chains is of relevance for enantioselectivity capability of polysaccharide selectors and may be sensitive to environmental and conditional factors, respectively. Francotte and Zhang proved the importance of such supramolecular structure for coated CSPs. Enantioselectivities were varied and even elution orders reversed when the type of solvent used for depositing the polysaccharide onto the wide pore silica was changed [257]. X-ray diffraction patterns confirmed the hypothesis that an altered supramolecular structure may be the reason for this observation.

Coated polysaccharide CSPs can be operated in normal-phase (alkane-alcohol) [205,254], polar organic mode (alcohols or acetonitrile) [258,259], reversed-phase mode (hydro-organic eluents with dedicated RP versions) [260,261] and SFC mode [165,262–264]. Additives may be required (such as DEA and TFA in NP mode or perchlorate or hexafluorophosphate for RP) and in some cases additives may induce transient or even persistent conformational changes in the polysaccharide structure, enhancing or attenuating its initial enantiomer separation characteristics (memory effects) [265] which may require prolonged equilibration times [266]. A number of studies dealt with the suggestion of method development concepts and extended systematic CSP and mobile phase automatic screening routines for these coated polysaccharide CSPs (note, the immobilized analogs may need a different screening; *vide infra*); these reports can be helpful guidelines for method development [261,267–269], and were recently extended to new chlorine-containing derivatives [270,271].

For all of these factors, multi-modal mobile phase applicability, structural diversity (due to backbone and substituents variations) and *per se* broad enantioselectivity abilities of the polysaccharide derivatives that accommodate a multitude of structurally different cavities for fitting structurally distinct SAs into them, the polysaccharide CSP family has an extremely broad applicability spectrum

[71]. Hence it is not surprising that they are nowadays the most widely used CSPs showing a high success rate in HPLC and SFC enantiomer separation with only a limited number of 3–4 distinct polysaccharide derivatives [272] due to their complementary chiral recognition profiles with respect to analyte structure and also elution orders [273,274]. In a few cases, exceptionally large  $\alpha$ -values in excess of 100 have been reported [84,274] which indicates a perfect match of the high affinity enantiomer in the binding site with multipoint attachment thus achieving remarkable receptorial recognition qualities.

The immobilized polysaccharide CSPs, Chiralpak IA, IB, and IC, have further expanded the versatility and application range [247] via their extended choice of mobile phases, resulting in an enormous flexibility for method development. They can be employed in NP, PO, RP [275] and SFC mode [276] without restriction to certain solvents. This widened applicability with an extended solvent range appears to make systematic method development and automated screening procedures more complex. However, it has been demonstrated that only five typical starting eluents are adequate for a representative initial screening with the three immobilized CSPs Chiralpak IA, IB and IC. The primary set of eluents comprises alkane-2-propanol (80:20, v/v), alkane-ethanol (80:20, v/v), methyl *tert*-butylether-ethanol (98:2, v/v), alkane-tetrahydrofuran (70:30, v/v), and alkane-dichloromethane-ethanol (50:50:2, v/v/v) and enabled baseline separation of about 90% of a series of 70 randomly selected chiral analytes [276,277]. Comparative studies of the three immobilized polysaccharide CSPs revealed that IA and IC have a greater success rate than IB in terms of producing the largest  $\alpha$  of the three (about 40:40:20) [276]. It is on the other hand also of concern how immobilized polysaccharide CSPs compare to their coated analogs. Thunberg et al. systematically compared Chiralpak IA with AD and IB with OD employing a test set of 48 chiral compounds [278]. The outcome was that the immobilization process affects enantioselectivity of the selector [247,279,280], presumably by introducing nonspecific binding contributions, usually affording lower selectivities for the immobilized phases. However, by use of non-standard solvents (such as ethers) enantioselectivities could be greatly improved (Fig. 15) so that the immobilized phases finally outperformed the coated ones [278].

Last but not least it should be emphasized that polysaccharide CSPs are also the materials of choice for preparative scale enantiomer separations. They have the highest loadabilities [4]. Solubility limitations of polar compounds in alkane-based eluents that were restricting somehow the full adsorption capacity and power in preparative applications may be overcome with the immobilized CSPs.

## 7.2. CSPs based on synthetic polymers

CSPs based on synthetic polymers as chiral selectors have been proposed as mimics of the enantiodiscrimination power of the semi-synthetic polysaccharides in that they are, like the natural polysaccharides, constructed from identical chiral subunits providing a multiplicity of identical chiral active binding sites. Such polymeric CSPs comprise Okamoto's helically chiral poly(triphenylmethacrylate), obtained by sparteine-catalyzed anionic polymerization from fully achiral monomers and coating of the tightly coiled helical polymer chains onto macroporous silica (Chiralpak OT(+)) from Daicel [281] and Blaschke's poly(*N*-acryloyl-(S)-phenylalanine ethyl ester) CSP (ChiraSpher, Merck) attached to silica by copolymerization. The former is seldom used, but a recent application reports on the HPLC enantiomer separation of 29 racemic bridged polycyclic compounds demonstrating its usefulness for specific separation tasks [282]. The latter is sometimes used for enantiomer separation of pharmaceuticals [283–285] and has shown some preparative potential [4].



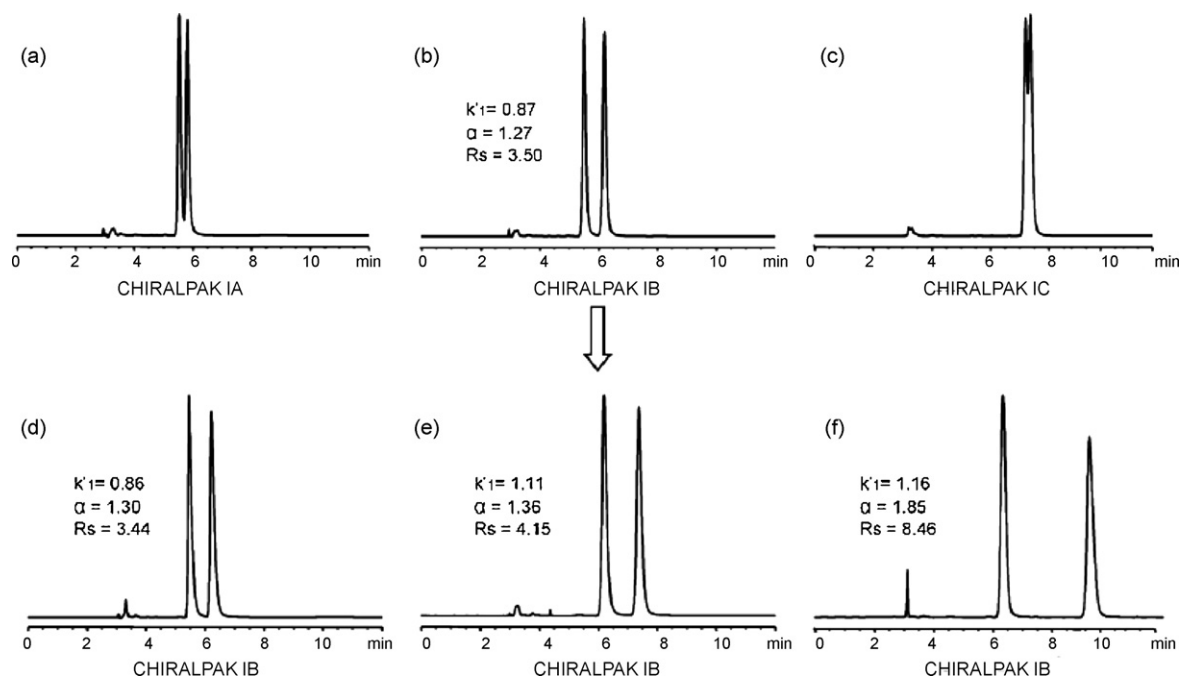


**Fig. 15.** Resolution of 1-benzocyclobutenecarbonitrile on (a) Chiralpak IA; (b, d, e, and f) Chiralpak IB; (c) Chiralpak IC. Mobile phase: (a–c) hexane–ethanol (90:10, v/v); (d) hexane–methyl *tert*-butylether (50:50, v/v); (e) hexane–2-propanol (90:10, v/v); (f) hexane–tetrahydrofuran (85:15, v/v). Reprinted with permission from Ref. [276].

Synthetic polymeric phases are commonly prepared by a *grafting-to* approach in which polymer chains grow in solution and are subsequently anchored to a vinyl-modified support by copolymerization. Blockage of pores and inhomogeneous surface coverage accompanied by kinetic limitations that translate into lower efficiencies in relation to brush-type phases are some drawbacks. Gasparrini et al. recently proposed a *grafting-from* approach in which after attachment of an initiator at the silica surface the polymer chain grows from the surface in a more regular way resulting in a well ordered surface-confined polymer layer (Fig. 16) [286]. Perturbing polymer chains grown in solution can be removed during the washing steps. The concept has been materialized with (*trans*-

1,2-diamino-1,2-diphenylethane)-*N,N*-diacrylamide as well as (*trans*-1,2-diaminocyclohexane)-*N,N*-diacrylamide as monomers and corresponding CSPs are commercially available as P-CAP-DP and P-CAP, respectively, by ASTEC. Van Deemter curves of such prepared polymer CSPs showed significantly reduced mass transfer resistance compared to reference materials obtained by the *grafting to* approach. Various chiral compounds of distinct structures can be separated primarily in normal-phase mode but also in polar organic mode [286,287]. Barnhart et al. compared a P-CAP column with various coated polysaccharide CSPs [288]. While in general the polysaccharide CSPs provided wider enantioselectivity capabilities and higher sample loadabilities, in particular cases the P-CAP

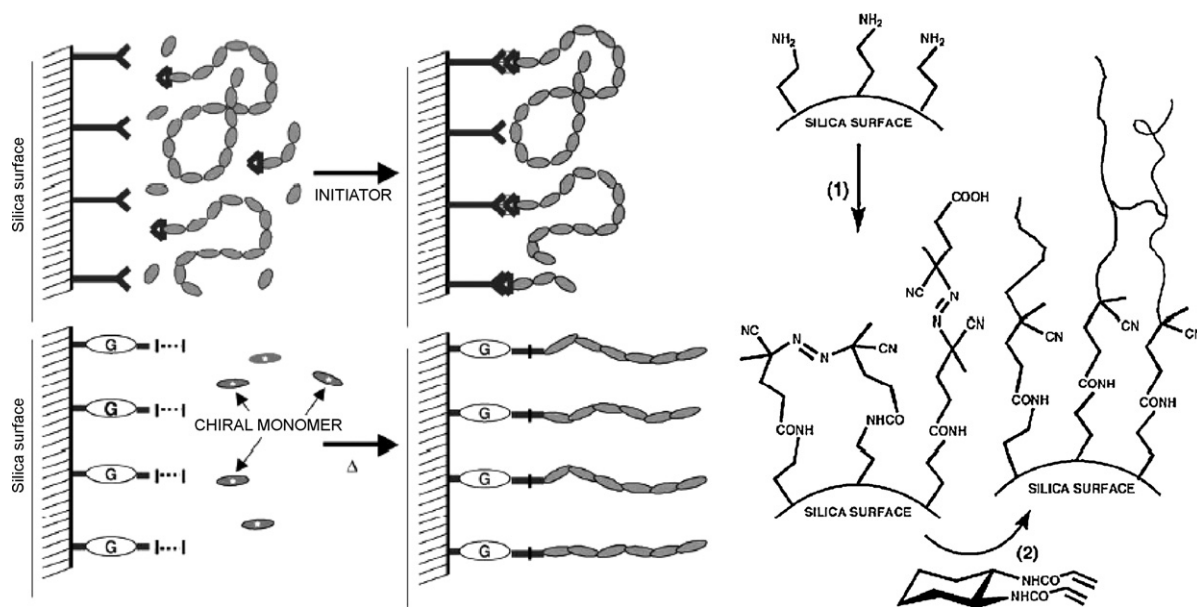


**Fig. 16.** “Grafting-to” (top left) and “grafting-from” (bottom left) approaches for the preparation of polyacrylate-type CSPs, and reaction scheme for the synthesis of poly(diaminocyclohexane-*N,N*-diacrylamide)-based CSP prepared by the “grafting-from” concept (right). Reprinted with permission from Ref. [286].



revealed better enantioselectivities. Moreover, one of the striking advantages is that the P-CAP CSP is available in both enantiomeric forms which allows for designed reversals of elution order upon request, e.g. for eluting the trace enantiomeric impurity first or enabling a better product purity for the first eluted enantiomer in preparative applications.

In yet another concept, network-type polymeric CSPs have been prepared by Allenmark et al. from *O,O'*-diaroyl-*N,N'*-diallyl-*(R,R)*-tartardiamide by crosslinking the monomers with multifunctional hydrosilanes and vinylized silica [289,290]. The thin film of chiral polymer network on the silica surface is extremely stable with low column bleed and comes as CSPs in which the tartaramides are decorated with *O,O'*-bis(3,5-dimethylbenzoyl) and *O,O'*-bis[4-(tert-butyl)benzoyl] residues (Kromasil CHI-DMB and CHI-TBB from EKA).

All of these polymer-type CSPs are typical normal-phase packings involving hydrogen bonding,  $\pi$ - $\pi$ -interactions and steric factors for retention and chiral discrimination.

### 7.3. Protein CSPs

Biochemists have long been aware of the chiral distinction capability of enzymes, plasma proteins, receptors and so forth. It is therefore no surprise that the emerging interest in drug chirality in the 1970s and 1980s attracted the attention of separation scientists towards this natural chiral pool of selectors and a variety of protein phases were developed. Allenmark, Hermansson, Miwa, Haginaka, and others have contributed to the development of a wide arsenal of protein-based CSPs which have been evaluated in research environments and are well documented in the scientific literature [291–294]. Therefrom a limited number of protein phases became also commercially available for users (Table 4). The most important ones are based on human serum albumin (HSA) [295], which is more often used for drug–protein binding studies than enantiomer separation nowadays,  $\alpha_1$ -acid glycoprotein (AGP) [296], which is also a plasma protein yet with altered binding characteristics in immobilized form due to employed crosslinking protocols, crude ovomucoid (OVM) [297] with its powerful chiral recognition ability stemming from an impurity with ovoglycoprotein (11%, w/w) in the crude OVM rather than the pure OVM [298–300], and cellobiohydrolase I (CBH I) [301]. Amongst them AGP but also OVM appear to exhibit the broadest enantiomer separation capabilities covering a wide variety of neutral, acidic and basic drug racemates and other pharmaceuticals. CBH preferably resolves basic chiral compounds (e.g.  $\beta$ -blockers) and HSA preferably acidic chiral compounds. The broad scope of applicability of some CSPs, e.g. AGP and their preferential operational mode with aqueous or aqueous-organic eluents was long time one of the greatest advantages of protein CSPs and made them first choice columns for bioanalytical studies, i.e. the stereoselective analysis of drugs and metabolites in biofluids and tissues. Their principal compatibility for straightforward hyphenation with mass spectrometric detection [302], is one of the most important advantages making them to an attractive research tool in drug discovery [303] (less in routine analysis applications like quality control). Major downsides are limited chemical and biochemical stabilities with restrictions in organic modifier content (<25% for AGP and <50% for OVM), pH (3–7.5 for AGP and OVM) and temperature (<70 °C for AGP and <40 °C for OVM) to be used, moderate to poor chromatographic efficiencies due to mass transfer limitations, and lack of sufficient sample loading capability for preparative applications. The latter is a result of the low molar concentration of binding sites per CSP (e.g. 0.79  $\mu$ mol CBH/g CSP) [40]. Due to these issues, the importance of protein CSPs has declined in the last decade not least because of attractive alternatives.

Experimental parameters such as pH, buffer type and ionic strength, type and content of organic modifiers (often 1- or 2-

propanol and acetonitrile, respectively), additives (alkylamines or quaternized ammonium salts, hydrophobic carboxylic acids, alkylsulfonates) and temperature are the key variables to regulate retention and enantioselectivities. pH and modifier variations may quite differently affect the number of available selective and non-selective adsorption sites furnishing a delicate dependence of separation factors on these variables [40,86,94]. Here, it is to be pointed out that proteins may be subject of conformational changes in dependence on the above mentioned experimental parameters. It is known for example that the ovoglycoprotein selector in the crude OVM can undergo reversible unfolding–refolding processes depending on the pH [304]. Moreover, van't Hoff plots of protein phases are sometimes non-linear which has been attributed to conformational changes of the protein [65].

Due to the structural complexity of these macromolecular protein selectors, their chiral recognition mechanisms at the molecular level remained unknown for long time. Yet, with the advent of modern techniques of structural biological chemistry comprising protein sequencing [304], modification of active sites (by chemical derivatization [305,306] or mutation [221,307]), comparative binding studies with fragments and whole proteins [207,308,309], enantioselective binding studies to investigate the role of biantennary branching glycans of AGP and its genetic variants [310], protein NMR [311], X-ray crystallography [220,221,312] and docking studies [234] the binding modes have become known for a number of protein–guest complexes.

HSA has been extremely thoroughly investigated owing to its important role as drug transporting plasma protein. Of several complexes of HSA with drugs or toxins X-ray crystal structures have been solved and are available via the Brookhaven protein data bank [312] (Fig. 17). As can be seen from Fig. 17 there exist two primary binding sites (sites 1 and 2) for drugs and a number of secondary ones where drugs can bind with varying specificity (and probably enantioselectivity at these distinct sites in case of chiral compounds). Of particular interest from a viewpoint of chiral recognition are X-ray crystal structures reported for warfarin because both of the diastereomeric complexes are available [220] (Fig. 18). Warfarin binds to the subdomain IIA and as can be seen, both *R*- and *S*-enantiomers bind in the pocket in almost identical conformations and geometric arrangement. Coumarin and benzyl moieties of the *R*- and *S*-forms are nearly perfectly superimposable in overlaid complexes. The main difference in the drug is related to conformations in the acetonyl group and to H-bond interactions that are formed between Arg222 residue and the carbonyl of the coumarin ring (in *R*-complex) and of the acetonide (in *S*-complex) [220]. The finding that the enantiomers bind in essentially the same way to HSA is consistent with the observation that they have similar binding affinities for the protein which is thus characterized for a low degree of enantioselectivity for warfarin enantiomers.

Detailed knowledge from X-ray crystal structure analysis about the molecular interaction mechanism is also available for cellobiohydrolase in complex with (*S*)-propranolol (Fig. 19) [221], a CS–SA system that was above discussed in the context of site-selective adsorption isotherm measurements. As can be seen the active site is highly acidic due to several Asp and Glu residues. (*S*)-Propranolol, which is the high affinity enantiomer, binds into this acidic active site via a multipoint interaction attachment driven by multidentate H-bond supported charge interaction of its amino group with the acidic residues of the active site. Notable is also the multiple H-bond interaction network of the secondary alcohol group with Glu212 and Gln175 residues as well as  $\pi$ - $\pi$ -interaction support by the aromatic naphthyl moiety that is stacked with the indole ring of Trp376. On the basis of this interaction network with a multiplicity of directed bonds, the high enantioselectivity can be reasonably well rationalized. The bidentate ionic interaction with Glu212 and Glu217 was apparently crucial, since no enantioselectivity

**Table 4**  
Protein-type CSPs and column tradenames along with some characteristics of the protein selectors (in modified form from Ref. [293]).

Protein	MW (kDa)	Carbohydrate (%)	Isoelectric point	Column tradename
Serum albumin				
Human (HSA)	67	0	4.7	Chiral-HSA (Chiral Technologies; Regis)
Bovine (BSA)	68	0	4.7	Resolvosil BSA (Macherey Nagel)
$\alpha_1$ -Acid glycoprotein (AGP)	44	45	2.7	Chiral-AGP (Chiral Technologies; Regis)
Ovomucoid (OVM)	28	17–34	4.5	Ultron ES-OVM (Shinwa Chemical)
Cellobiohydrolase I (CBH)	60–70	6	3.6	Chiral-CBH (Chiral Technologies; Regis)
Avidin	66	20.5	9.5–10	Bioptric AV-1 (GL Sciences)
Pepsin	70–78	–	<1	Ultron ES-Pepsin (Shinwa Chemical)

tivity was obtained with mutants deficient of these two amino acids [221].

Recent research in the field of protein-based CSPs comprises work of Massolini and coworkers about penicillin G acylase as selector [168,234] and of Hofstetter and coworkers about antibody selectors [313–315]. Both of these groups have undertaken detailed mechanistic investigations employing computational methods amongst others [234,314,315].

#### 7.4. Cyclodextrin CSPs

Cyclodextrin (CD) bonded CSPs, introduced by Armstrong and DeMond [316], are based on  $\alpha$ -,  $\beta$ - or  $\gamma$ -cyclodextrins which are macrocycles with 6, 7, and 8 glucose units connected via  $\alpha$ -1,4-

linkages that adopt the shape of a truncated cone with cavity diameters of 0.57, 0.78 and 0.95 nm, respectively [317] (Fig. 20). The internal surface of the CD-cavity is hydrophobic originating from the carbon-backbone of the sugar moieties, while the upper and lower rim surfaces are hydrophilic due to the presence of hydroxyls. Both native and a variety of derivatized CDs have been bonded to silica gel normally at the narrower ring hydroxyls either via ether linkage (*Cyclobond* columns, from ASTEC) or carbamate linkage (*ChiraDex* and *ChiraDex Gamma*, from Merck; *Ultron ES-CD* from Shinwa). Introduced functionalities may modulate the conformational flexibility of the CD, alter the cavity size and access to it and may provide additional supportive binding sites which lends them distinct enantioselectivity profiles as compared to their underivatized (native) CD counterparts [318,319].

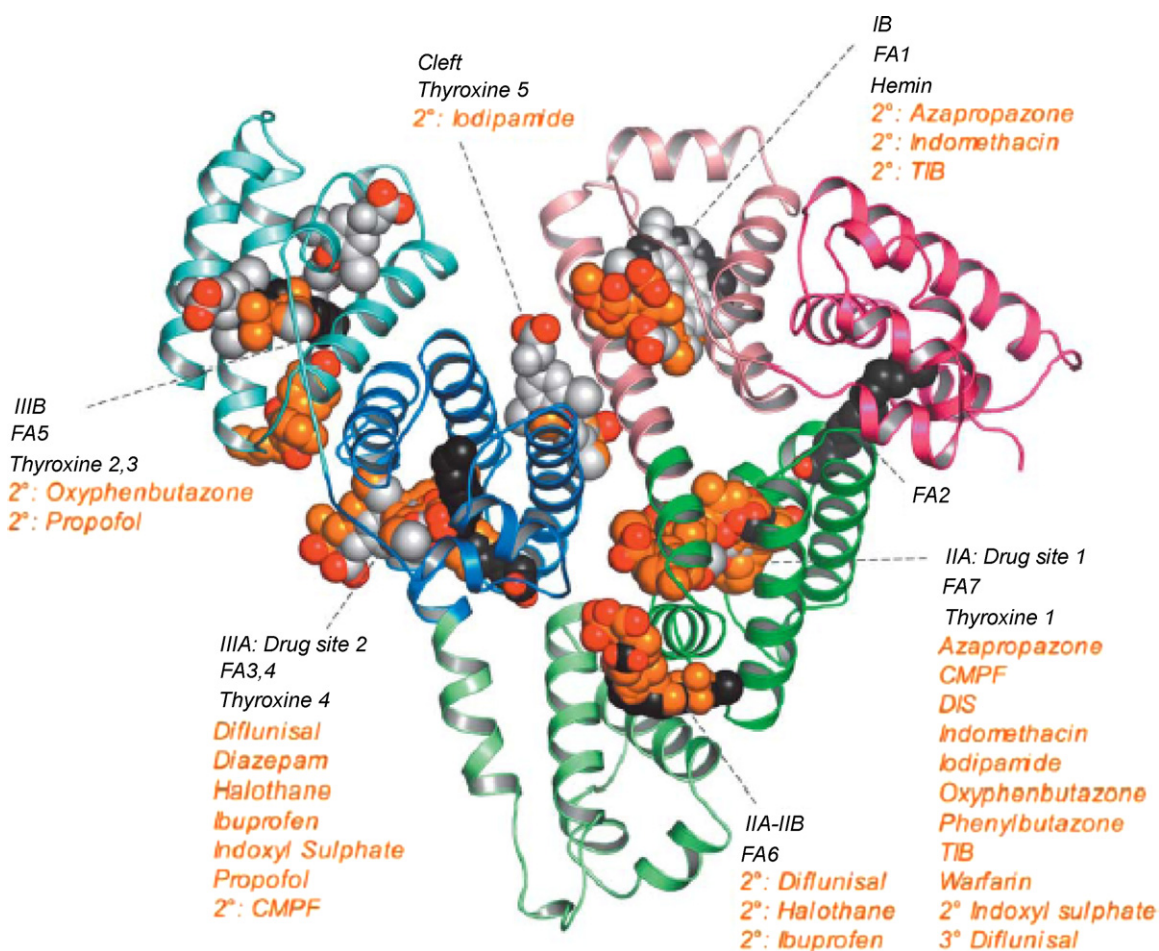


**Fig. 17.** Summary of the ligand binding capacity of HSA as defined by crystallographic studies to date. Ligands are depicted in space-filling representation; oxygen atoms are colored red; all other atoms in fatty acids (myristic acid), other endogenous ligands (hemin, thyroxine) and drugs are colored dark-grey, light grey and orange, respectively. (Abbreviations: CMPF, 3-carboxy-4-methyl-5-propyl-2-furanpropanoic acid; DIS, di-iodosalicylic acid; TIB, tri-iodobenzoic acid.) (For interpretation of the references to color in this figure legend, the reader is referred to the web version of the article.) Reprinted with permission from Ref. [312].

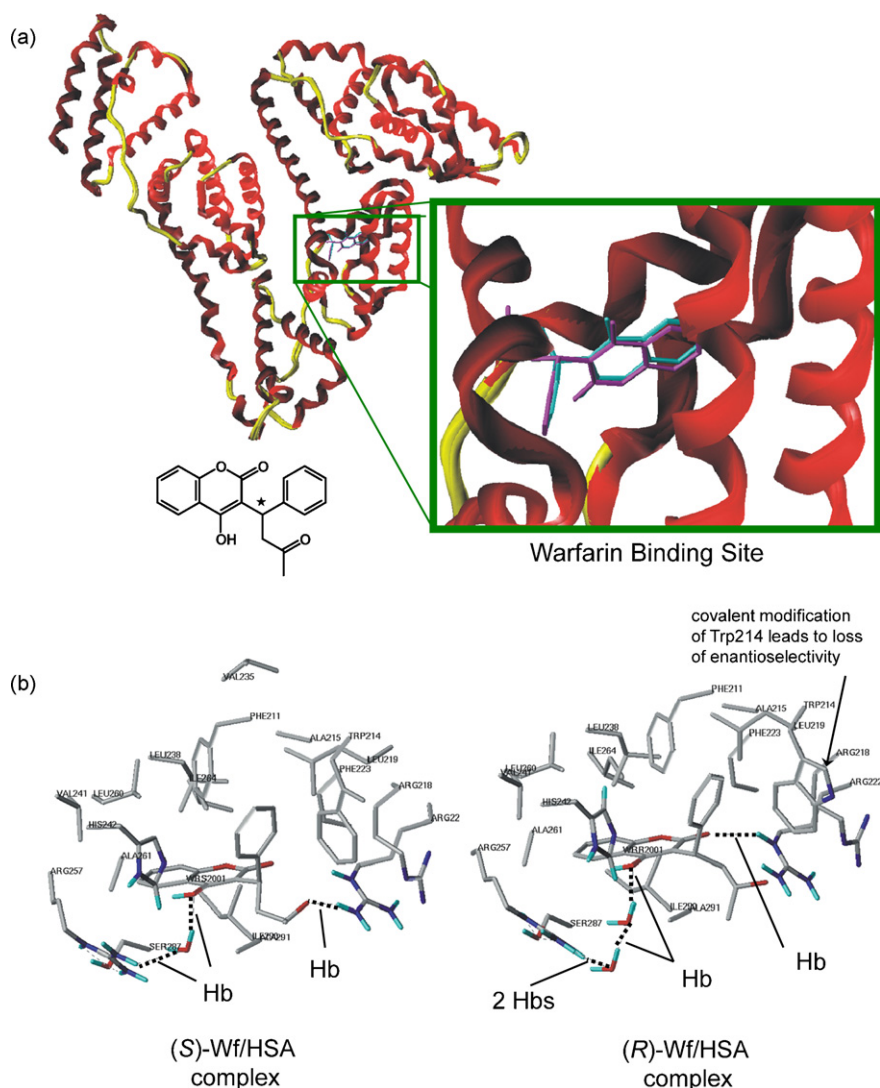


**Fig. 18.** X-ray crystal structures of HSA-warfarin (Wf) complexes. (a) Superimposed complexes, (R)-Wf (magenta), (S)-Wf (cyan). (b) Active site with binding modes. Fractional coordinates were obtained from Brookhaven protein data bank at <http://www.rcsb.org/pdb> and images were processed with SYBYL molecular modeling software from Tripos (St. Louis, MO). (For interpretation of the references to color in this figure legend, the reader is referred to the web version of the article.)

CD-based CSPs [318,319] are multi-modal in terms of elution conditions that can be used (covering NP, PO [320,321], RP and SFC conditions) as well as regarding molecular recognition mechanisms triggered under these particular conditions.

Under reversed-phase conditions using aqueous or hydro-organic eluents, lipophilic solutes interact with CD selectors via inclusion complexation driven by hydrophobic interactions (Fig. 21) [38,322]. A two-step mechanism has been proposed: the hydrophobic part of the guest molecule penetrates into the CD cavity and leads then to the release of solvent (water) molecules from guest and CD molecules (entropic effect). Further stabilization of the complex may stem from van der Waals interactions inside the cavity while additionally supporting hydrophilic interactions with hydroxyl groups at the upper and lower rim (hydrogen bonding, dipole–dipole interactions) may take place. For aromatic derivatives  $\pi$ – $\pi$ -stacking increments may exist as well. Overall, inclusion will be governed by a size match concept of the inserted lipophilic moiety into the cavity. Substituted phenyl, naphthyl and heteroaromatic rings can conveniently be accommodated in a  $\beta$ -CD cavity, while larger analytes like steroids are expected to fit preferentially into  $\gamma$ -CD, and smaller ones into  $\alpha$ -CD cavities. This structure–binding relationship may be a helpful initial guide

for column selection. This inclusion complexation mechanism has been subject of intensive research and various reviews are covering the topic in detail [38,193,194,323]. Many of the mechanistic studies are related to other fields, e.g. CE, supramolecular chemistry or pharmaceutical technology.

The effect of cavity size and substitution on inclusion properties and binding strength should be outlined by the models shown in Fig. 21 that have been derived from NMR investigations [191–193]. ROESY studies with (+)-brompheniramin complexed with  $\beta$ -CD and heptakis (2,3,6-tri-O-methyl)- $\beta$ -CD, respectively, indicated that in both cases the *p*-bromophenyl moiety was included in the CD cavity. In case of  $\beta$ -CD the solute can more deeply penetrate into the cavity (approaching from the wider rim) (Fig. 21a) than in case of the heptakis (2,3,6-tri-O-methyl)- $\beta$ -CD selector (Fig. 21b) [192]. Binding strength was by an order of magnitude larger in the former complex with deeper insertion of the aromatic ring. In another example, aminoglutethimide complexation with  $\beta$ -CD and  $\gamma$ -CD was studied by virtue of NMR [191,193]. The results of NOE measurements gave evidence that in this case the guest molecule was deeply inserted into the cavity of the CD host in both cases, yet approached the cavity from the narrower lower rim in case of  $\gamma$ -CD (cf. Fig. 21c and d).



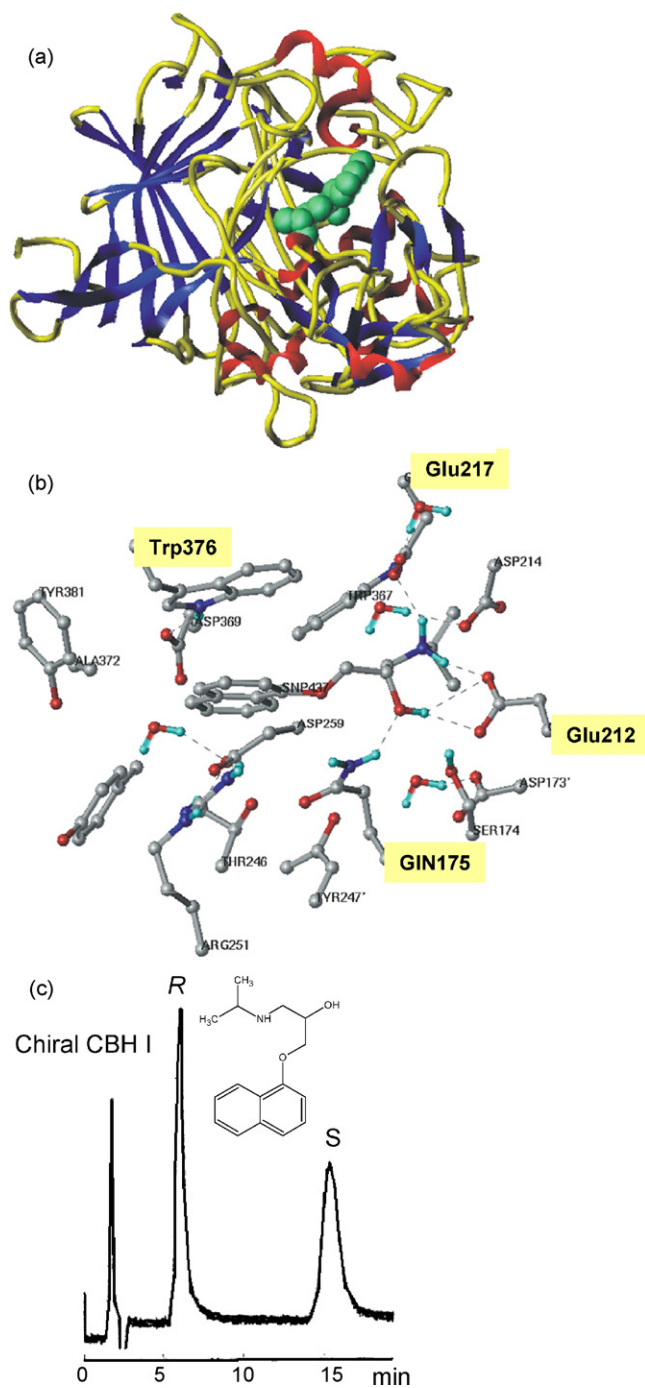


**Fig. 19.** Molecular recognition mechanism of propranolol binding to CBH. (a) Tertiary structure of the (S)-propranolol/CBH complex, (b) binding site of CBH with amino acid residues and high-affinity (S)-enantiomer displaying involved binding interactions. (c) HPLC enantiomer separation of propranolol on Chiral CBH I (from ChromTech; now available from Chiral Technologies and Regis, respectively). Eluent: 0.01 M acetate buffer, pH 5. (a and b) X-ray crystal structure image was generated with SYBYL molecular modeling software (Tripos, St. Louis, MO) from fractional coordinates extracted from the Brookhaven protein data bank (<http://www.rcsb.org/pdb/>). (c) Reprinted with permission from Ref. [293].

When CD-based and CD-derivative based CSPs are employed with polar organic mode or in normal-phase mode the inner cavity is blocked by solvent molecules preventing inclusion complexation. However, hydrophilic interactions may be reinforced in such media where solutes with hydrophilic groups bind to the polar surface of the CD (either upper or lower rim) (see Fig. 22) [322]. The

polar hydroxyls are surrounded by a chiral environment and enantioselectivity may be afforded due to differences in the strength of these polar interactions (hydrogen bonding, dipolar interactions) for the two enantiomers. Solutes with more than one polar functional group, one of which is located at or close to the stereogenic center, were found to be particularly amenable for enantiomer separation in the polar organic elution mode. Bulky groups near the stereogenic center facilitate the enantiodistinction process. Since many chiral drugs are polar this elution mode turned out to be very useful especially when reversed-phase and normal-phase modes failed to resolve the enantiomers [320]. Conversely, the normal-phase mode may be employed for less polar compounds when the elution strength of the polar organic mode is too strong.

### 7.5. Macrocyclic antibiotics CSPs

Inspired by the stereoselective inclusion capabilities of cyclodextrins, Armstrong and coworkers were elucidating other macrocyclic natural compounds with inclusion complexation properties as potential chiral selectors which has led to the discovery of a new class of powerful CSPs, the macrocyclic antibiotic CSPs. They are nowadays the second most important group of CSPs available on the market, besides the polysaccharide CSPs. Their properties, applications as well as retention and chiral recognition mechanisms were subject of several detailed reviews [324–329].

The first described CSP of this class was vancomycin-modified silica introduced by Armstrong et al. in 1994 [330]. A number of structural analogs from this glycopeptide antibiotic family were subsequently proposed as powerful chiral selectors with complementary selectivity profiles [331]. CSPs based on vancomycin [330], teicoplanin [332], ristocetin A [333] and the aglycone of teicoplanin [334] are nowadays commercially available from ASTEC and Supelco under the tradenames Chirobiotic V, T, R and TAG, respectively. Since recently, Chirobiotic V and T are available with older (V1, T1) and new bonding chemistry (V2, T2) differing also in selector coverages and to minor extent in their enantioselectivity abilities [335]. Besides these primary macrocyclic antibiotics a variety of other variants of this glycopeptide antibiotic family has been examined as chiral selector in HPLC including avoparcin [331], glycopeptide A-40,926 [336,337], Hepta-Tyr [338], norvancomycin [339], and eremomycin [340,341]. Dozens of papers demonstrated their usefulness for enantiomer separation and their broad applicability profiles [327], comprising chiral acids, bases, amphoteric and neutral compounds with the Chirobiotic T and V showing superior performance over Chirobiotic R [342]. Thereby, the enantiomer separation ability of the teicoplanin CSP for underivatized natural and synthetic amino acids [343] as well as small peptides [325] deserves particular attention. Part of the versatility of macrocyclic antibiotic CSPs is their multi-modal applicability in NP, PO, RP [330,344] and also SFC elution modes [345]. The polar organic mode (e.g. methanol plus up to 1% acetic acid and triethylamine) turned out to be the most effective one [342,346] followed by the RP mode, with some of these reported RP separations actually following a HILIC mechanism [164]. Schemes for aid in method development can be found elsewhere [344].

In spite of the importance of these CSPs, relatively little is known in detail with certainty about their chiral recognition mechanisms on the molecular level. The molecular structures of the primarily important selectors of this class are illustrated in Fig. 23. Those of less common variants mentioned above can be found in Ref. [329]. It is seen that these antibiotic selectors are of considerable structural complexity which make investigations more complicated than with other selectors. They share a common heptapeptide aglycone core with aromatic residues that are bridged to each other forming a basket-like structure with shallow pockets for inclusion complexation. The carbohydrate moieties are located at the



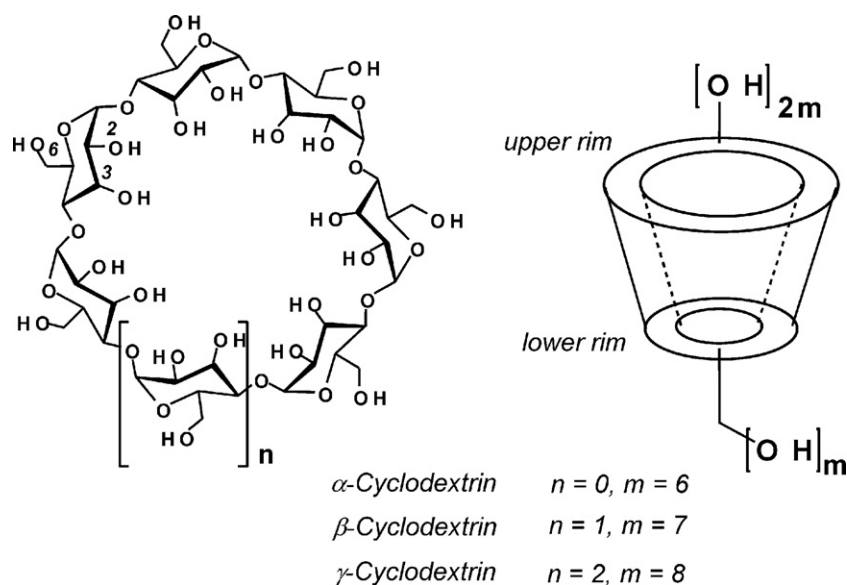


**Fig. 20.** Structure of cyclodextrins and corresponding CSPs. Commercial columns: *Cyclobond I* (native  $\beta$ -CD), *II* (native  $\gamma$ -CD), *III* (native  $\alpha$ -CD) (from ASTEC) *Cyclobond I SP* or *RSP* ((*S*)- or (*RS*)-2-hydroxypropylether- $\beta$ -CD) (from ASTEC) *Cyclobond I RN* or *SN* ((*R*)- or (*S*)-1-(1-naphthyl)ethylcarbamate- $\beta$ -CD) (from ASTEC) *ChiraDex* (native  $\beta$ -CD) and *ChiraDex Gamma* (native  $\gamma$ -CD) (from Merck) *Ultron ES-CD* (native  $\beta$ -CD) and *Ultron ESPhCD* (phenylcarbamoylated  $\beta$ -CD) (from Shinwa).

surface. All these selectors have plenty of potential interaction sites closely attached to stereogenic centers, including various H-donor/acceptor functionalities, aromatic rings for  $\pi$ - $\pi$ -interaction, acidic and basic groups that may be involved in electrostatic interactions. It is obvious that despite of some conformational flexibility there are also sufficient steric constraints entailing stereoselective binding to some of these sites. Chiral recognition mechanisms with exact structural details of the involved complexes have not been reported on a wider basis yet, except for valuable systematic

chromatographic [83], thermodynamic [48,347] and extrathermodynamic investigations [136,138–140]. Some of thus inferred mechanistic discussions are somehow controversial though. For example, Berthod claimed that for amino acids a charge–charge (i.e. ionic) interaction between the anionic carboxylate group of the amino acid and an ammonium group of the macrocyclic peptide selector is the key docking interaction [328]. Gasparrini and coworkers, in contrast, showed that amino acids can be separated into enantiomers on TAG-based CSP in which the single *N*-terminal

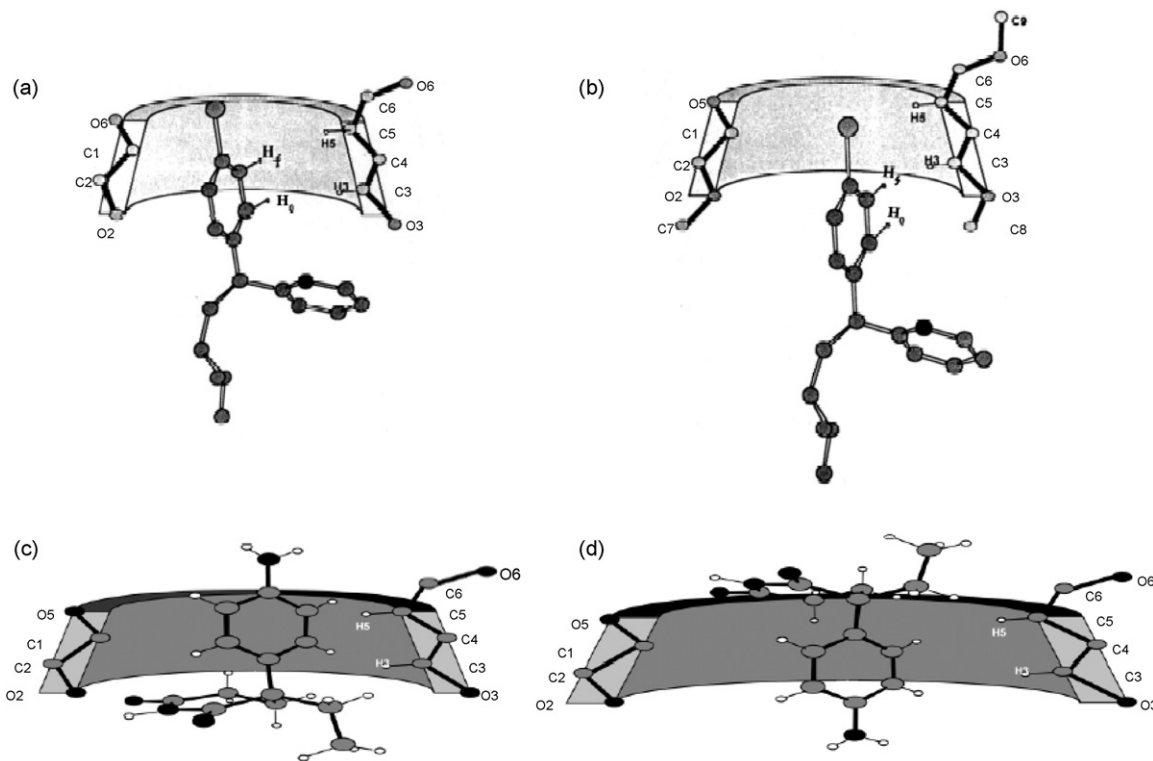


**Fig. 21.** Preferred binding modes of complexes between (a) (+)-brompheniramin with  $\beta$ -CD, and (b) (+)-brompheniramin with heptakis(2,3,6-tri-O-methyl)- $\beta$ -CD, (c) aminoglutethimide with  $\beta$ -CD, and (d) aminoglutethimide with  $\gamma$ -CD as derived from ROESY measurements. Reprinted with permission from Refs. [192] (a and b) and [193] (c and d).

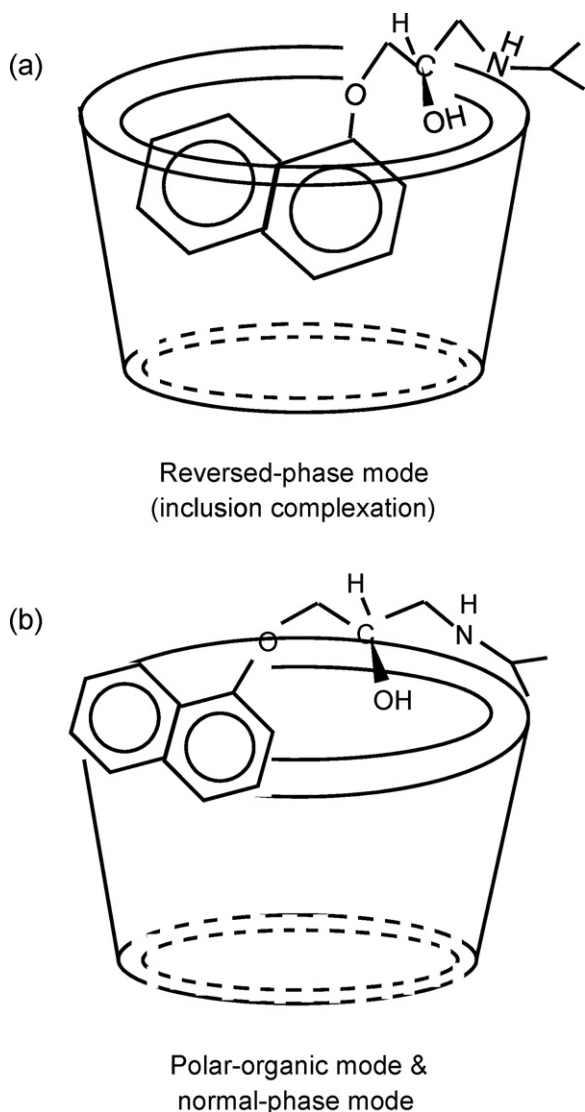


**Fig. 22.** Preferred molecular recognition mechanisms of CDs in reversed-phase mode (top) as well as polar organic and normal-phase mode (bottom), respectively. In the aqueous RP mode lipophilic portions of the guest molecule bind in the cavity by inclusion complexation (driven by hydrophobic interactions) (top) while in organic media complexation is driven by hydrophilic interactions at the rim surfaces (bottom).

Redrawn in modified form from Ref. [322].

amino acid of the selector is utilized for binding via urea linkage and no ammonium group is therefore available [334]. Such ionic interaction is therefore no longer possible anymore. Support for this hypothesis comes from a paper by Cavazzini et al. [348]. They found linear dependencies between  $\ln k$  and  $\ln C_i$  (i.e. the ion concentration in the eluent) on the employed teicoplanin-based CSP according to Eq. (26). For basic solutes such as amino acid methyl esters the slope  $Z$  of Eq. (26) adopted a negative sign indicating a cation exchange process and for acidic solutes such as *N*-acetyl amino acids the slope  $Z$  had positive sign giving rise to the assumption that repulsive electrostatic interactions were dominating. These dependencies point towards a net negative charge of the teicoplanin CSP under employed conditions ( $pI$  of the selector  $\sim 4.2$ ) and an anion-exchange interaction as postulated above is unlikely. Thus, other interactions seem to play a major role.

Some light about the involvement of the carboxylic acid group of the solute in docking interactions on Chirobiotic CSPs could be shed on this issue by the X-ray crystal structure images of

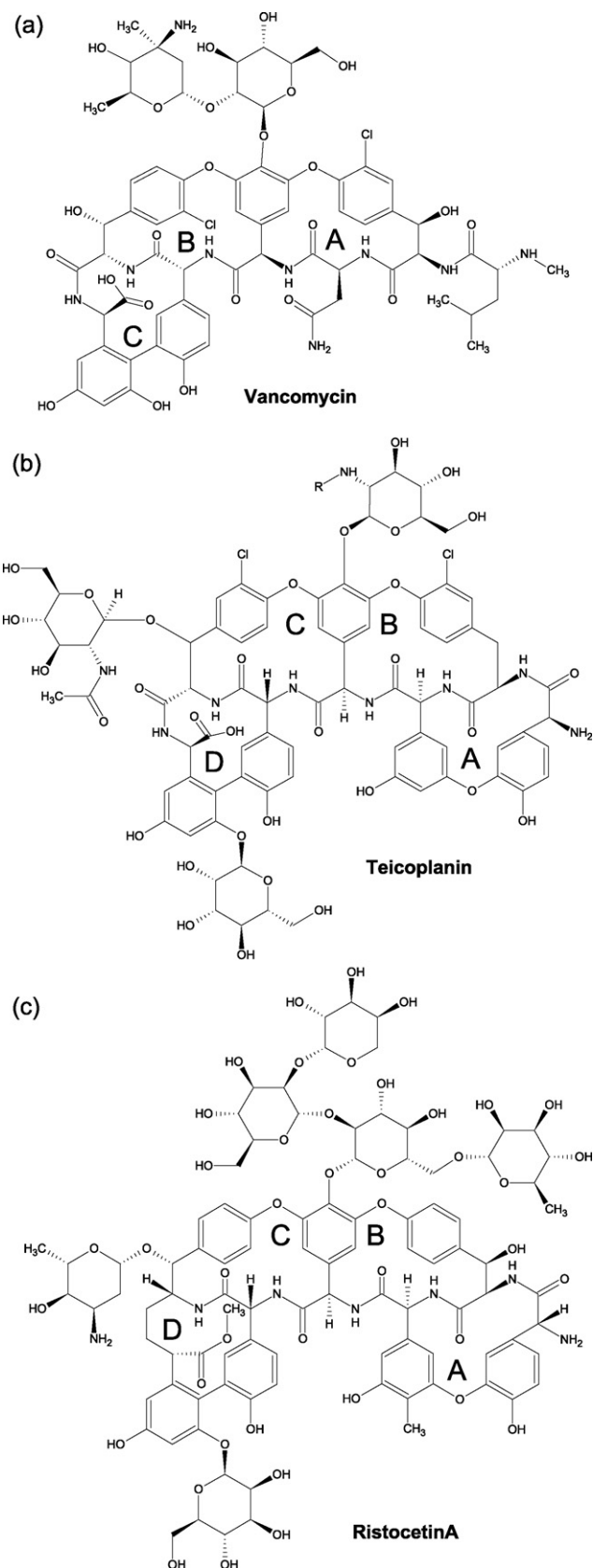


**Fig. 23.** Structures of glycopeptide antibiotics: (a) vancomycin (molecular mass,  $\sim 1449$ ; 1 sugar moiety; 3 cavities A, B, C;  $pK_a$ , 2.9, 7.2, 8.6, 9.6, 10.4, and 11.7;  $pI$ , 7.2) (b) teicoplanin (molecular mass,  $\sim 1885$ ; 3 sugar moieties; R, decanoic acid residue; 4 inclusion cavities, A, B, C, D;  $pI$ , 4.2); (c) ristocetin A (molecular mass,  $\sim 2066$ ; 6 sugar moieties; 4 inclusion cavities A, B, C, D;  $pI$ , 7.5).

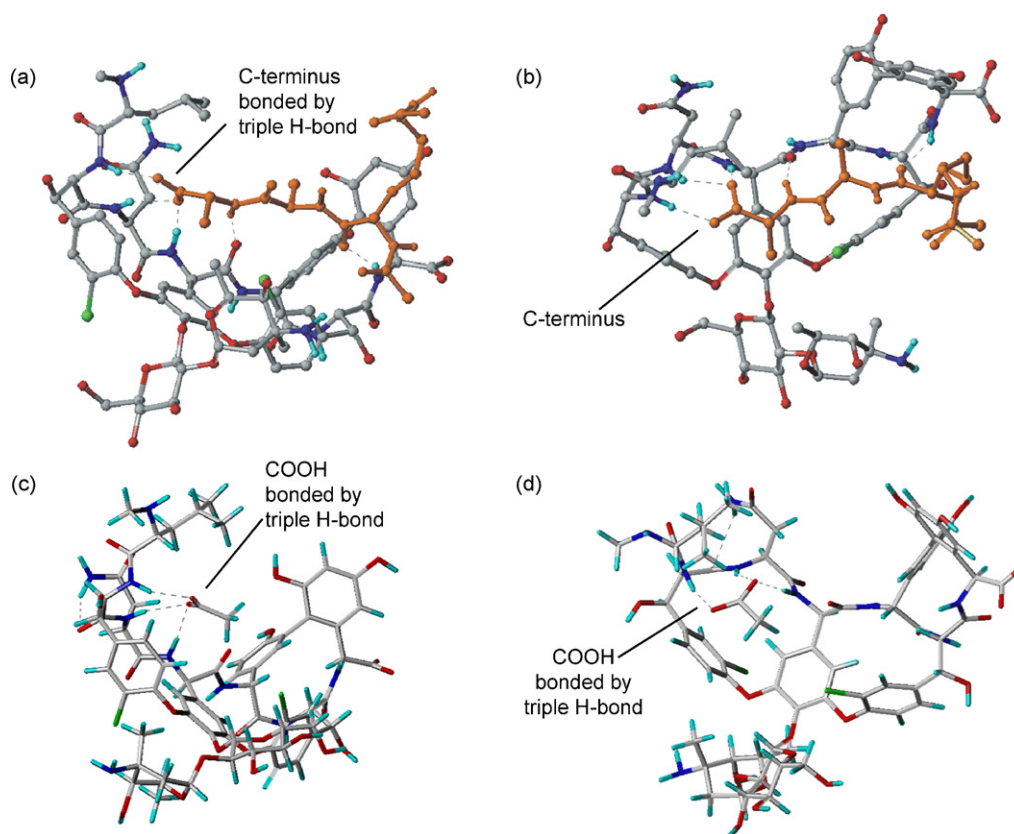


**Fig. 24.** Basket-like shape and molecular recognition mechanism of vancomycin for its natural ligand with C-terminal d-Ala-D-Ala sequence (a and b) as well as of acetate (c and d) as revealed by X-ray crystal structures of complexes of vancomycin with  $N_{\alpha},N_{\omega}$ -diacetyl-L-Lys-D-Ala-D-Ala (a and b) and acetate [349] (c and d). (a and c) side view; (b and d) top view. X-ray crystal structure images were generated with SYBYL molecular modeling software (Tripos, St. Louis, MO) from fractional coordinates extracted from the Brookhaven protein databank (<http://www.rcsb.org/pdb/>). Note the favorable triple hydrogen bonding of the carboxyl-terminus in both structures.

vancomycin in complex with  $N_{\alpha},N_{\omega}$ -diacetyl-L-Lys-D-Ala-D-Ala complex (Fig. 24a and b) and with acetate (Fig. 24c and d) [349]. The former guest molecule is a biomimetic model ligand for peptidoglycan precursors with  $N$ -acyl-D-Ala-D-Ala C-terminal sequence that are produced during bacteria cell wall biosynthesis and the binding of which stops bacterial growth. In this particular case, the inclusion complexation seems to be driven by polar interactions, most notably by triple hydrogen bonding of the carboxylic terminus of the tripeptide guest solute supported by additional hydrogen bonding interactions. The methyl residues, at least the one at the C-terminus are placed in close proximity to the aromatic planes of the selector so that in an aqueous or hydro-organic environment hydrophobic interactions might be activated. It may be surprising that triple H-bonding with the carboxylate appears to be energetically more favorable over ionic interaction at amino groups of vancomycin. Similar binding modes could exist for other carboxylic acid-containing guests, also for teicoplanin and teicoplanin aglycone selectors. Acetate for example binds this way to vancomycin too (Fig. 24c and d) [349,350]. Moreover, it is safe to assume that the binding mechanism is similar in teicoplanin and teicoplanin aglycone selectors as outlined above for vancomycin. Together with the rich chiral information originating from multiple stereogenic centers the heterogeneous multifunctionality with the structural specificity of the glycopeptides provides a variety of potentially stereoselective binding modes which appears to be the origin of the broad enantioselectivity profiles of these CSPs, for a variety of drugs and pharmaceuticals.

The mentioned complementary enantioselectivity profiles of the distinct macrocyclic antibiotics emerge from subtle differences in the glycopeptide structures and their binding properties [326]

as well as different glycosylation patterns (Fig. 23). The role of the latter, i.e. of the carbohydrate moieties, on the chiral recognition capability of a teicoplanin-based CSP has been addressed in a study by Berthod et al. [334]. Chromatographic comparison of the native teicoplanin-based CSP with a corresponding teicoplanin aglycone (TAG) CSP, in which all the sugar moieties were removed, revealed that the sugar units considerably reduce enantioselectivity for amino acids (Fig. 25). This clearly indicates that the active chiral distinction site is located in the aglycone part. Typical differences in differential free energies of binding between  $R$ - and  $S$ -enantiomers  $\Delta\Delta G_{R/S}$  between teicoplanin and teicoplanin-aglycone in the range of 0.3–1 kcal/mol (up to fourfold increase in  $\alpha$ -value) in favor of the latter were observed [334]. However, for other solutes the sugar units may be beneficial supporting the enantioselectivity process.

#### 7.6. Chiral crown-ether CSPs

Pioneering work by Cram and coworkers with chiral 18-crown-6 derivatives in which two opposite ethylene elements were replaced by 1,1'-binaphth-2,2'-diyl units illustrated already in the 1970s the potential for enantioselective host-guest complexation of chiral ammonium compounds by HPLC on corresponding silica- and polystyrene-supported materials [351]. A CSP with a structural analog of this chiral crown-ether (CE) type selector developed by Shinbo's group using (3,3'-diphenyl-1,1'-binaphth-2,2'-diyl)-20-crown-6 dynamically coated onto octadecyl-silica [352] was later introduced into the market by Daicel as Crownpak CR which is still available. Since such crown ethers are of synthetic origin both enantiomeric forms are readily accessible denoted as Crownpak CR(+) and CR(-) which furnish opposite elu-

tion orders. Various other structurally distinct chiral crown ethers were later synthesized and examined for their chiral recognition capabilities. These included covalently bonded CSPs with tartaric acid derived CE [353–356], pyridino-CE [357], (3,3'-diphenyl-1,1'-binaphth-2,2'-diyl)-containing CE [358], pseudo-18-crown-6 ether having 1-phenyl-1,2-cyclohexanediol as a chiral unit [359], pseudo-CE with phenolic hydroxyl group incorporated into the ring [360], acridino-18-crown-6 CE [361], hybrids of CEs incorporating (3,3'-diphenyl-1,1'-binaphth-2,2'-diyl) and tartaric elements [362]. One of them, viz. (18-crown-6)-2,3,11,12-tetracarboxylic acid (i.e. two tartaric acid units incorporated into the crown ether), bivalently immobilized via two carboxylic acid functionalities onto 3-aminopropylated-silica turned out to be most powerful and is now on market as ChiroSil RCA(+) and SCA(–) (from Regis, Morton Grove, IL) (Fig. 26a).

In general, crown-ether based CSPs cover application spectra that are essentially restricted to primary amines, comprising mainly amino acids [363–366], amino acid esters and amides, di- and tripeptides [367], amino alcohols [368] and chiral drugs with free primary amino functionality [369,370]. It can be explained fundamentally by the specific molecular recognition mechanism of such CSPs. They are run with strongly acidic aqueous eluents (pH between 1 and 3.5) which ensures full protonation of the solutes' amino functionality. Thus generated chiral ammonium ions can bind enantioselectively to the macrocyclic crown ether through inclusion complexation driven by triple hydrogen bond formation between the ammonium ion and three oxygens of the

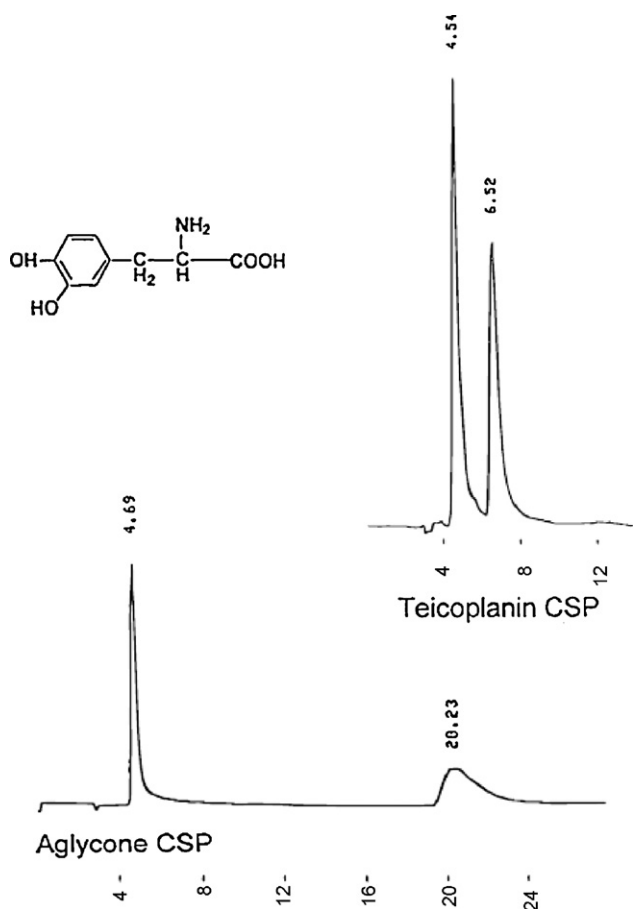


**Fig. 25.** Enantiomer separation of D,L-DOPA on the native teicoplanin CSP (top) and the teicoplanin aglycone CSP (bottom). Conditions: eluent, methanol–triethylammonium acetate pH 4.1 (60:40, v/v); UV detection, 254 nm; temperature, 22 °C; flow rate, 1 mL/min. Reprinted with permission from Ref. [334].

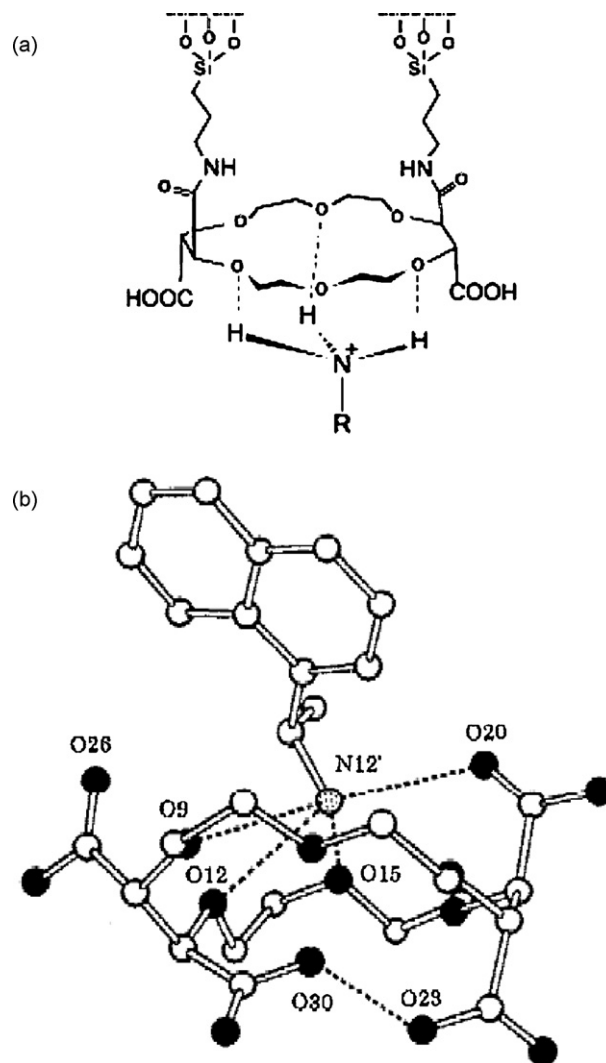


**Fig. 26.** Molecular recognition mechanism of chiral crown-ethers exemplified by a (18-crown-6)-2,3,11,12-tetracarboxylic acid based CSP (ChiroSil RCA): (a) schematic representation of solute-selector interaction driven by triple hydrogen bonding (reprinted from the Regis webpage), and (b) X-ray crystal structure of (18-crown-6)-2,3,11,12-tetracarboxylic acid host and 1-(1-naphthyl)ammonium guest. Reprinted with permission from Ref. [39] (a) and Ref. [195] (b).

crown-ether (Fig. 26b). As the X-ray crystal structure in Fig. 26b shows, the carboxylic function may provide a further complex stabilizing contact by an additional ionic interaction in case of the (18-crown-6)-2,3,11,12-tetracarboxylic acid derived selector. Enantioselectivity may be governed by steric factors of the substituents of the chiral ammonium ions and the residues attached to the chiral moieties that are incorporated into the 18-crown-6. Such a binding and chiral recognition mechanism was fully supported by NMR [196] and X-ray crystal structures [195,219] (see Fig. 26b and Table 3). Rare exemptions to this fundamental structure–enantioselectivity relationship exist, however, for the (18-crown-6)-2,3,11,12-tetracarboxylic acid based CSP. Upon use with nonaqueous polar organic eluents, this stationary phase may act as chiral cation exchanger for the separation of secondary amines such as  $\beta$ -blockers which bind in this case at the exterior of the macrocycle by ion-pair formation [371]. More details on crown-ether based CSPs, method development with such CSPs and their applications for HPLC enantiomer separation can be found in recent reviews by Hyun [372,373].



**Table 5**  
Selection of important commercially available donor–acceptor (Pirkle-type) CSPs.

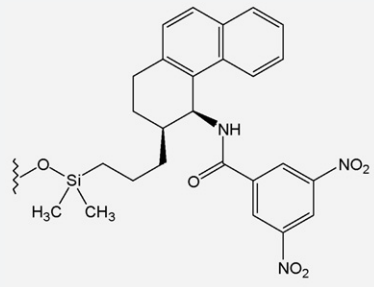
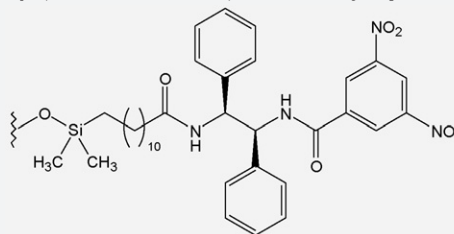
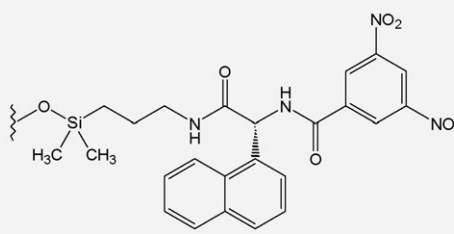
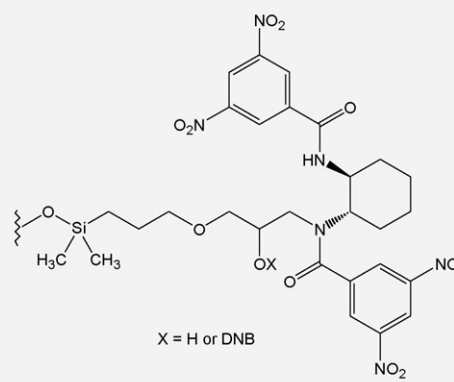
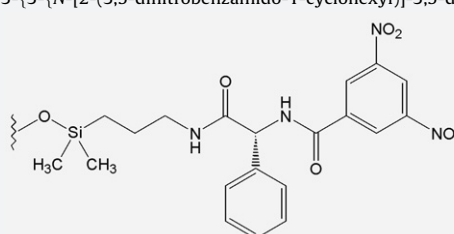
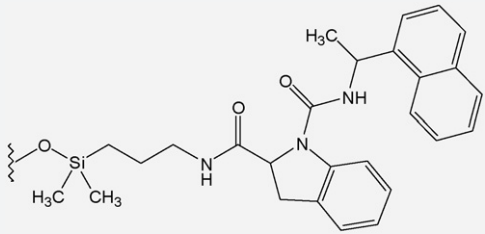
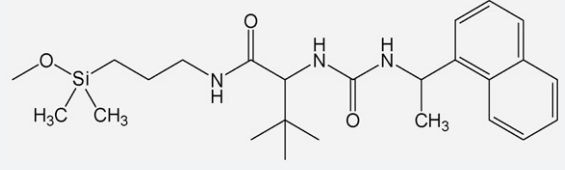
Chiral selector	Column tradename	Supplier
<i>π</i> -Electron acceptor/ <i>π</i> -electron donor phases		
	Whelk-O1	Regis
3-[1-(3,5-dinitrobenzamido)-1,2,3,4-tetrahydrophenanthrene-2-yl]-propyl-silica [382]		
	ULMO	Regis
11-[2-(3,5-dinitrobenzamido)-1,2-diphenylethylamino]-11-oxoundecyl-silica [383]		
	Chirex 3005 (Sumichiral 2500)	Phenomenex (Sumitomo)
( <i>R</i> )-3-[ <i>N</i> -(3,5-dinitrobenzoyl)-1-naphthylglycine-amido]propyl-silica [384]		
<i>π</i> -Electron acceptor phases		
 <p>X = H or DNB</p>	DACH-DNB	Regis
3-{3-[ <i>N</i> -(2-(3,5-dinitrobenzamido-1-cyclohexyl))-3,5-dinitrobenzamido]-2-hydroxy-propoxy}-propyl-silica [385,386]		
	Phenylglycine DNBPG Chirex 3001 Phenomenex	Regis Merck
3-[ <i>N</i> -(3,5-dinitrobenzoyl) phenylglycine-amido]propyl-silica [387]		

Table 5 (Continued)

Chiral selector	Column tradename	Supplier
<i><math>\pi</math>-Electron donor phases</i>		
 <p>(S)-indoline-2-carboxylic acid and (R)-1-(<math>\alpha</math>-naphthyl)ethylamine urea linkage [388]</p>	Chirex 3022 (Sumichiral OA 4900)	Phenomenex (Sumitomo)
 <p>(S)-tert-leucine and (R)-1-(<math>\alpha</math>-naphthyl)ethylamine urea linkage [388]</p>	Chirex 3020 (Sumichiral OA 4700)	Phenomenex (Sumitomo)

### 7.7. Donor–acceptor phases (brush-type or Pirkle-type CSPs)

In the end of the 1970s, the first silica bound CSPs with entirely synthetic selectors have been proposed [374,375]. This work paved the way for a class of CSPs that are known as brush type or Pirkle-type CSPs (in recognition of his pioneering role Pirkle played in this field over decades). This class of CSPs makes use of neutral synthetic chiral low-molecular mass selectors. They can be classified as classical normal-phase packings under which conditions they are capable of most effectively activating donor–acceptor interactions such as hydrogen bonding, face-to-face or face-to-edge  $\pi$ – $\pi$  interaction (between electron-rich and electron-poor aromatic groups), and dipole–dipole-stacking. Bulky and rigid structural elements are often incorporated which may represent effective steric barriers triggering or amplifying their enantioselectivity potential. Several powerful CSPs evolved from Pirkle's laboratory through systematic selector development based on chromatographic [376] and spectroscopic [148,179,213] studies of chiral recognition phenomena as well as the consistent exploitation of the reciprocity principle of chiral recognition [377,378]. Such concepts and tools have been instrumentalized for the rational design of new advanced CSPs [376] and were comprehensively reviewed by Welch [379]. Newer developments in this field were described in a more recent review by Gasparrini et al. [380] and research on organic polymer-based brush-type phases as well as combinatorial approaches for Pirkle selector optimization was summarized by Vec et al. [381]. A list with selected commercially available Pirkle-type CSPs is given in Table 5.

Since these donor–acceptor phases are almost always run in the normal-phase mode, method development is straightforward, usually starting with a mixture of alkane/2-propanol as polar modifier (1–10%; with 0.1% diethylamine and trifluoroacetic acid as additive for basic and acidic solutes, respectively) followed by optimization of the modifier percentage and, if necessary type. Other benefits arising from the synthetic and low-molecular mass nature of Pirkle-type selectors include the availability of such CSPs in both enantiomeric forms with opposite configurations displaying reversed elution orders, a valuable tool in practical routine work such as impurity detection [389]. Elevated sample loading capacities, especially compared to protein phases, macrocyclic antibiotics CSPs and cyclodextrin-based CSPs, is another advantage [4]. This property promotes their preparative application in preclinical drug discovery research. In this field SFC becomes increasingly the method of choice and Pirkle-type CSPs have

proved to be fully compatible and remarkably successful in this field [390–392].

Amongst the above listed Pirkle-type CSPs, Whelk-O1 appears to have nowadays the broadest distribution in industrial and academic laboratories. It is also the one of which the chiral recognition mechanism has been investigated in detail. On the one hand, it has been rationally designed based on mechanistic considerations and, on the other hand, it was subject of intensive scrutiny of its chiral recognition mechanism by various researchers employing chromatographic [180], thermodynamic [53], NMR [179,180,185], X-ray diffraction [185,215] and computational methods [229–231,237], amongst others.

The Whelk-O1 phase (Table 5) was originally designed by Pirkle and Welch as a naproxen-specific CSP employing an immobilized guest approach (principle of reciprocity) [379]. It combines both  $\pi$ -electron donor (tetrahydrophenanthrene moiety) and  $\pi$ -electron acceptor (3,5-dinitrobenzoyl group) with amide hydrogen donor–acceptor site in a semi-rigid scaffold (Fig. 27a). Presence of donor and acceptor functionalities in the CSP should extend the application range to selectands with electron-deficient and electron-rich aromatic moieties. Donor and acceptor planes adopt perpendicular orientations yielding a cleft like arrangement for guest insertion (see Fig. 27b) [237] with the polar H-bonding site right in the center of this cleft. Upon guest insertion in this cleft (possibly driven by strong hydrogen bonding interaction) a simultaneous face-to-face and face-to-edge  $\pi$ – $\pi$  interaction may be possible. This is essentially what is shown in Fig. 27c and d that display diastereomeric X-ray crystal structures of the Whelk-O1 selector and a selectand. Both complexes display face-to-face  $\pi$ – $\pi$  interaction between the DNB group of Whelk-O1 selector **1** and the bromophenyl ring of the selectand **2** as well as hydrogen bond formation between the benzamide NH of **1** and the carbonyl of **2** [215]. While in the more stable homochiral complex (Fig. 27c) the SA-enantiomer sits in the cleft in such a way that allows additional stabilization via a face-to-edge  $\pi$ – $\pi$  interaction of **2** with the phenanthroline ring of the Whelk-O1 selector **1**, these two interaction sites are spatially offset in the weaker heterochiral complex precluding this additional complex stabilization force (Fig. 27d). NMR data confirmed the complex geometry of the more stable diastereomeric complex in solution [179,215]. In later comprehensive <sup>1</sup>H-NMR studies performed with 22 analytes in presence of the soluble Whelk-O1 selector most of the analytes were found to produce chemical shift inequivalencies in complex with the Whelk-O1 selector [186]. It was concluded that the enantiomer of the

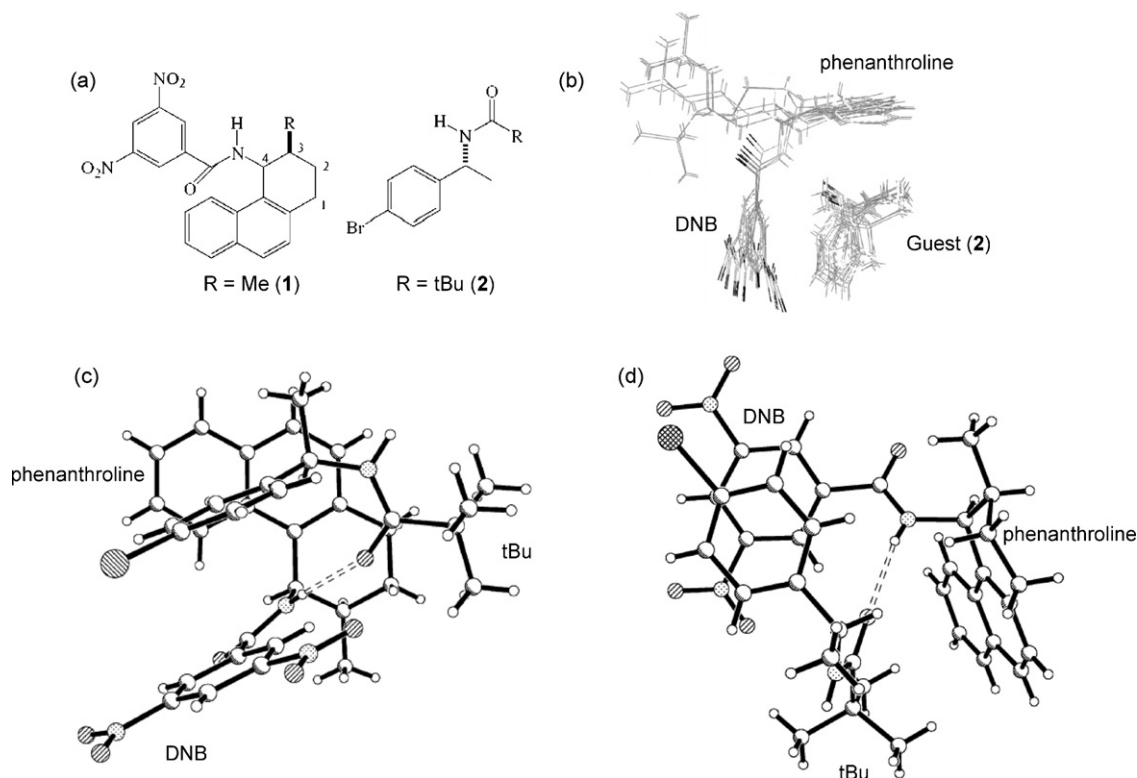


**Fig. 27.** X-ray crystal structures of diastereomeric selector–selectand complexes unveiling the molecular recognition process of the Whelk-O1 phase (note, reciprocal system used for investigation): (a) chemical structures of Whelk-O1 selector (1) and *p*-bromo- $\alpha$ -phenylethylamine solute (2), (b) computer simulation showing lowest energy conformations for host and guest, (c) crystal structure of homo-chiral complex (“stronger complex”), i.e. (3*R*,4*R*)-1 co-crystallized with (*R*)-2 (stabilized by face-to-face  $\pi$ - $\pi$ -interaction between DNB of 1 and aromatic plane of 2 as well as by H-bond between amide NH of 1 and carbonyl oxygen of 2; the close approach of the aryl group of 2 to the naphthyl portion of 1 is suggestive for additional complex stabilization by a face-to-edge  $\pi$ - $\pi$ -interaction), (d) crystal structure of hetero-chiral complex (“weaker complex”), i.e. (3*S*,4*S*)-1 co-crystallized with (*R*)-2 (face-to-face  $\pi$ - $\pi$ -interaction and H-bond seem to be amenable like for the stronger complex; however, the additional face-to-edge- $\pi$ - $\pi$ -interaction appears to be absent). Reprinted with permission from Ref. [215] (a, c, and d) and Ref. [237] (b).

stronger complex binds inside the cleft while the weaker binding enantiomer docks outside of the cleft.

Recently, in a series of papers Cann and coworkers performed MD simulations with a Whelk-O1 chromatographic interface considering besides the selector also end-capping groups and silanols as well as solvent (*n*-hexane) in the simulation cell (Fig. 28) [228–231]. This model was then used to carry out docking experiments with various ligands including naproxen [229–231]. The most probable docking arrangement could be identified in the simulations which included hydrogen bonding, ring–ring interactions and steric hindrance which contributed to enantioselectivity in the simulations. It was also concluded that both hydrogen bonding and ring–ring interactions are necessary to localize the analytes within the Whelk-O1 cleft [230]. The approach was then used to optimize the Whelk-O1 selector *in silico* by rational design [231]. With this methodology computer simulations of chiral chromatographic separations entered into a new stage in which the entire interface is simulated in fluid environment. It also accounts for the dynamics of the system and is supposed to provide a more realistic picture of the separation process.

### 7.8. Chiral ion-exchangers

Chiral ion-exchangers may be regarded as a subset of Pirkle-type phases from which they differ in that they utilize ionizable selectors and exploit long-range ionic interaction between oppositely charged selectors and selectands for ion-pairing at the sorbent as primary driving force for solute adsorption and retention, respectively. Following this concept, chiral anion-exchangers based on

cinchona alkaloid derivatives (Fig. 29a) [29,158,393] and tergruride [216,394,395] have been developed for enantiomer separation of chiral cation exchangers (Fig. 29b) based on chiral amino sulfonic and carboxylic acids for separation of chiral bases [396], and more recently zwitterionic ion-exchangers (Fig. 29c) combining structural elements of both with scope of applicability for acids, bases as well as zwitterionic solutes such as underivatized biogenic and synthetic amino acids and peptides have been proposed [397–399]. So far, only chiral anion-exchangers with cinchona carbamate selectors have become commercial products (Chiralpak QN-AX and Chiralpak QD-AX from Chiral Technologies). The abbreviation AX in the tradename refers to their weak anion-exchanger characteristics, while QN and QD denote the type of cinchona alkaloid employed as backbone of the selectors, viz. quinine (QN) and quinidine (QD). The experimental behavior of these two diastereomeric alkaloids and corresponding derivatives is under  $C_3$  stereocontrol where they exhibit opposite configurations. Hence, they frequently reveal pseudo-enantiomeric characteristic which is chromatographically materialized in reversed elution orders (Fig. 30).

These cinchona-alkaloid based anion-exchanger columns exhibit broad applicability for enantiomer separation of chiral acids, preferentially in polar organic and reversed-phase modes, comprising carboxylic, sulfonic, phosphonic, phosphinic and phosphoric acids [158]. With (weakly) acidic mobile phases, the quinuclidine nitrogen becomes protonated and acts as the fixed-charge of the chiral anion-exchanger. Acidic analytes are then primarily retained by an ion-exchange process. Accordingly, the retention on such CSPs can be readily described by a stoichiomet-

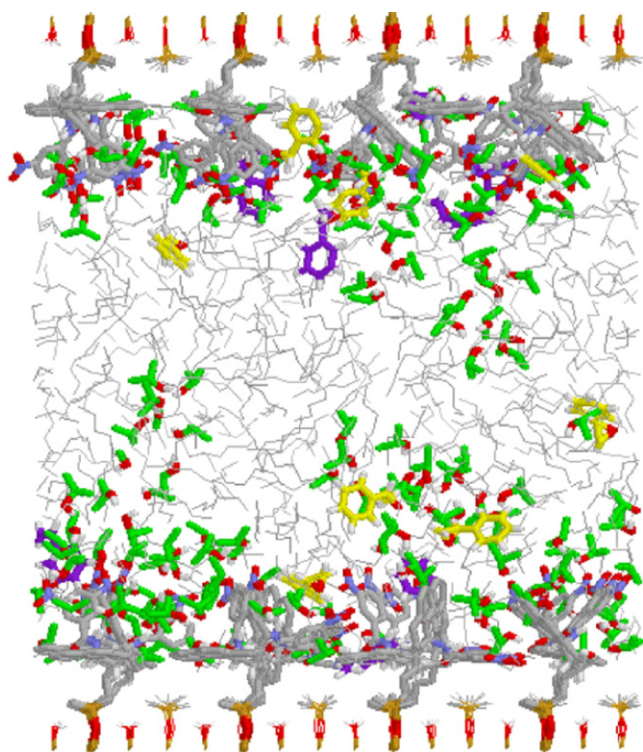


**Fig. 28.** (a) A side view of the simulation cell showing two interfaces with Whelk-O1 selectors, end-caps, and silanol groups. The solvent consists of *n*-hexane (thin grey lines), 2-propanol (green), *R*-styrene oxide (yellow), and *S*-styrene oxide (purple). (For interpretation of the references to color in this figure legend, the reader is referred to the web version of the article.) Reprinted with permission from Ref. [229].

ric ion-exchange model [158]. The buffer anions act as competitors for the solute at the charge center of the ion-exchanger. Thus, in accordance with a stoichiometric displacement model as outlined above (Eq. (26)),  $\log k$  decreases linearly with  $\log[C_i]$  (wherein  $C_i$  represents the counterion concentration) and the slope thus adopts negative values. The derived coefficient  $Z$  (i.e. the slope) provides some insight into the involved charges [158]. For example, the absolute value of the slope  $Z$  for a given solute will be lower, the higher the effective charge number  $n$  of the employed counterion [158,401]. It will increase with the effective charge of the solutes [158]. In other words, multiply charged solute species respond stronger to a change in the counterion concentration. Favorably, such alterations in the counterion concentration may be exploited to adjust retention, while it has almost no effect on enantioselectivities. In sharp contrast, also the type of counterion exerts a significant impact on the retention due to distinct affinities for the fixed-charge center of the ion-exchanger (i.e. it largely determines the eluotropic strength which for example increases in the order acetate  $\leq$  formate  $<$  phosphate  $<$  citrate) but affects considerably enantioselectivities as well [401]. Hence, type and concentration of the counterions (i.e. of the buffer anions) in the eluent play a pivotal role as mobile phase variable for adjusting solute retention. To account appropriately for counterion effects on solute adsorption in the course of process optimization of preparative chromatographic enantiomer separations, Arnell et al. simulated recently adsorption isotherms for Fmoc- $\alpha$ -allylglycine using an equilibrium-dispersive model and competitive Langmuir isotherms employing the inverse method [96]. The studies showed reasonable agreement between simulated and experimental runs confirming the suitability of the employed models and revealed a close to homogeneous adsorption mechanism with high mass loading capacities up to 20 mg/g CSP depending on the concentration of counterions.

Other variables with influence on retention and enantioselectivity include pH (in RP mode) or acid–base ratio (in PO mode), which affect the ionization degree of selector, solutes and buffer ions, as well as type and content of organic solvents. They allow for dedicated optimizations of enantiomer separations in the course of method development.

Cinchona alkaloid selectors and corresponding CSPs have been subject of numerous studies about their molecular recognition mechanisms. Such investigations primarily focused on chromatographic [103,218,393], FTIR [170,173] and NMR spectroscopic [24,25,33,166], thermodynamic [33,55], molecular modeling (MD simulations) [24,188] and X-ray diffraction studies [24,25,33,166,218]. For instance, NMR investigations showed that upon protonation of the quinuclidine nitrogen and in the course of complexation with acidic solutes, respectively, the chiral selector undergoes a conformational transition from a closed-conformation (access of anion-exchange site precluded by quinoline ring; quinuclidine nitrogen points towards the quinoline ring nitrogen) to an open-conformation (anti-open) (Fig. 31) giving the acidic solutes free access to the primary ion-exchange site for binding via a H-bond supported ionic interaction (ionic H-bond). This prefer-

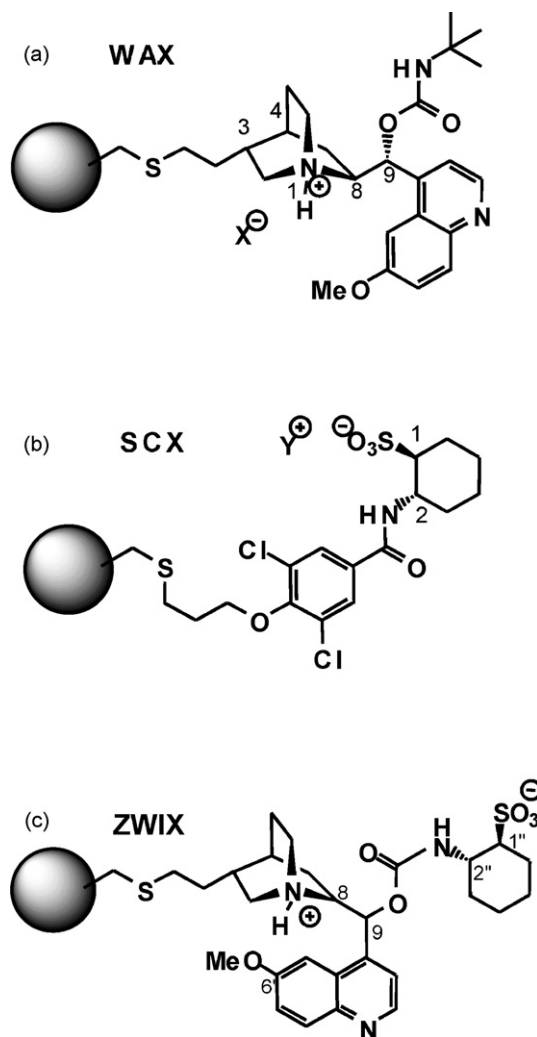


**Fig. 29.** Chiral anion-exchangers. (a) Commercially available cinchona alkaloid-derived weak chiral anion-exchangers (WAX) [158]: quinine-derived, Chiralpak QN-AX (8*S*,9*R*); quinidine-derived, Chiralpak QD-AX (8*R*,9*S*); configurations in position N<sub>1</sub>, C<sub>3</sub>, C<sub>4</sub> are always (1*S*,3*R*,4*S*). (b) Strong chiral cation exchanger (SCX) derived from *trans*-2-aminohexanesulfonic acid [396]. (c) Zwitterionic ion-exchangers (ZWIX) obtained by merging structural elements of above anion and cation exchangers [397].



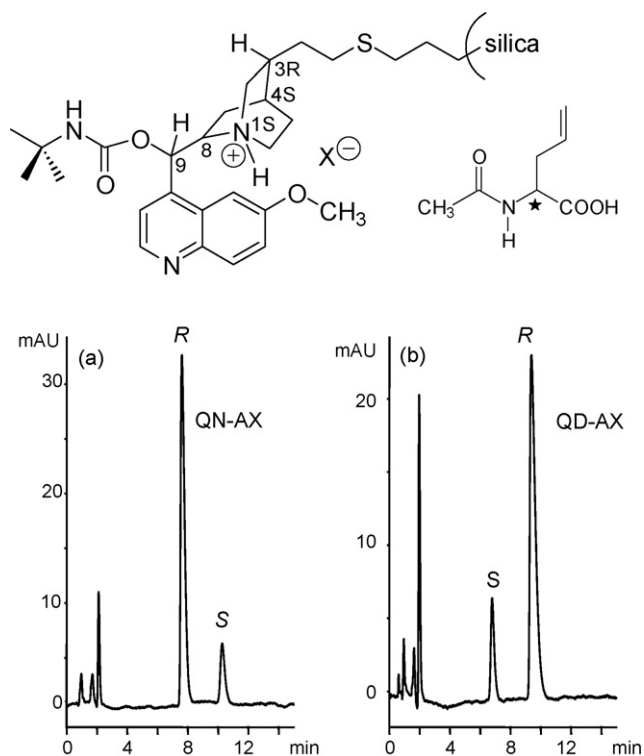


**Fig. 30.** Reversal of elution orders on quinine (8*S*,9*R*) (Chiralpak QN-AX) and quinidine (8*R*,9*S*) (Chiralpak QD-AX) derived anion-exchanger CSPs. Experimental conditions: column dimension, 150 mm × 4 mm ID; eluent, 1% acetic acid in methanol; temperature, 25 °C; flow rate, 1 mL/min; UV detection at 230 nm. Reprinted in modified form from Ref. [400].

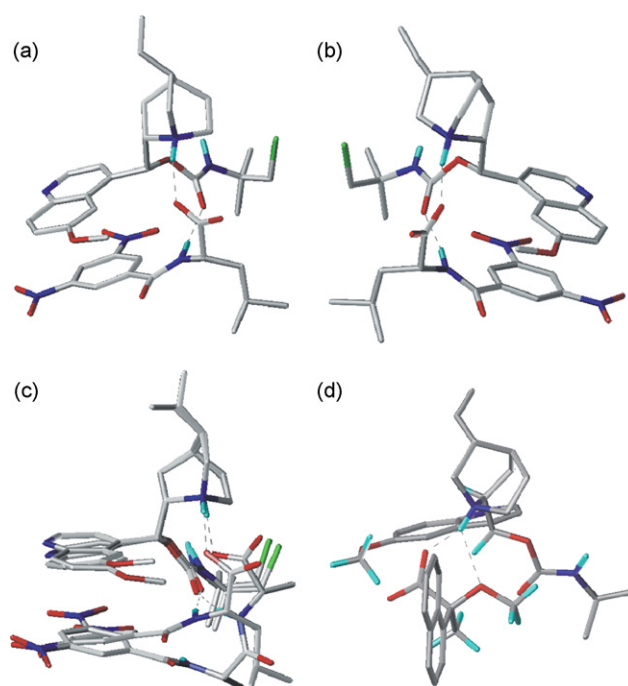


**Fig. 32.** X-ray crystal structures of more stable selector–selectand complexes (ion-pairs): (a) *O*-9-(β-chloro-*tert*-butylcarbamoyl)quinine with *N*-(3,5-dinitrobenzoyl)-(*S*)-leucine, (b) the pseudo-enantiomeric complex of *O*-9-(β-chloro-*tert*-butylcarbamoyl)quinidine with *N*-(3,5-dinitrobenzoyl)-(*R*)-leucine, (c) superposition of complexes between *O*-9-(β-chloro-*tert*-butylcarbamoyl)quinine with *N*-(3,5-dinitrobenzoyl)-(*S*)-leucine and *N*-(3,5-dinitrobenzoyl)-(*S*)-alanyl-(*S*)-alanine, and (d) *O*-9-(*tert*-butylcarbamoyl)quinine with (*S*)-2-methoxy-2-(1-naphthyl)propionic acid. Most hydrogens have been omitted for the purpose of clarity. Reprinted with permission from Ref. [166] (a–c) and Ref. [25] (d).

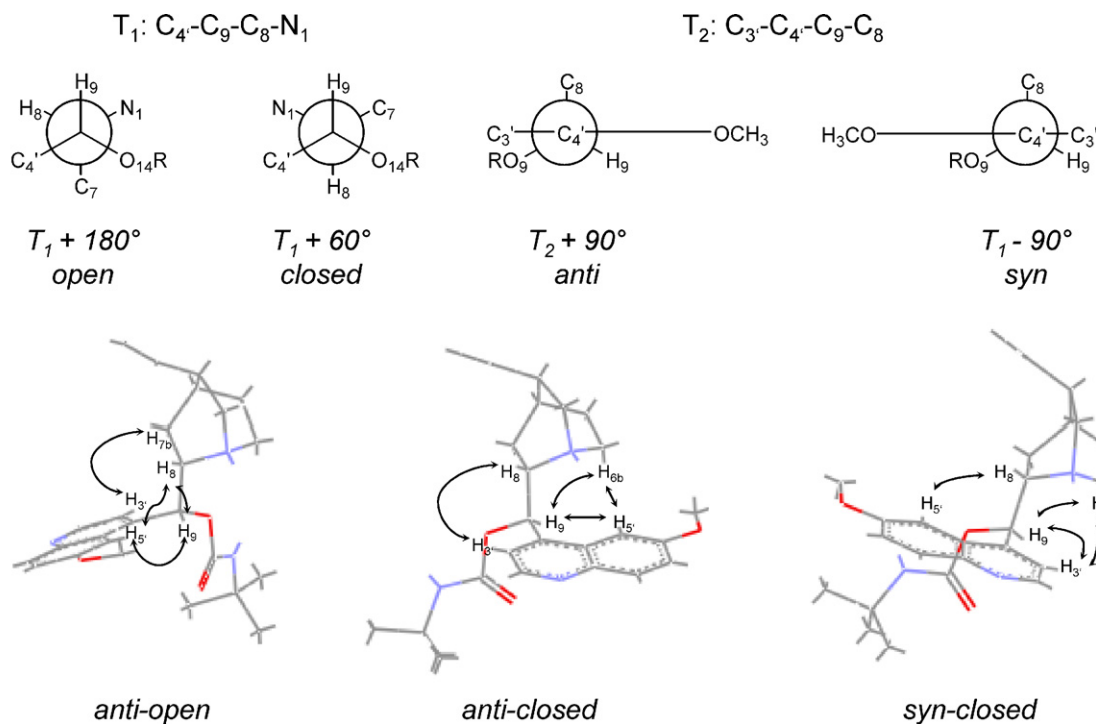


**Fig. 31.** Preferential conformational states of cinchona carbamate selectors shown in Newman projection (top) and line models of 3D images (bottom) as exemplified by *O*-9-(*tert*-butylcarbamoyl)quinine (arrows indicate intramolecular NOEs). Reproduced with permission from Ref. [25].

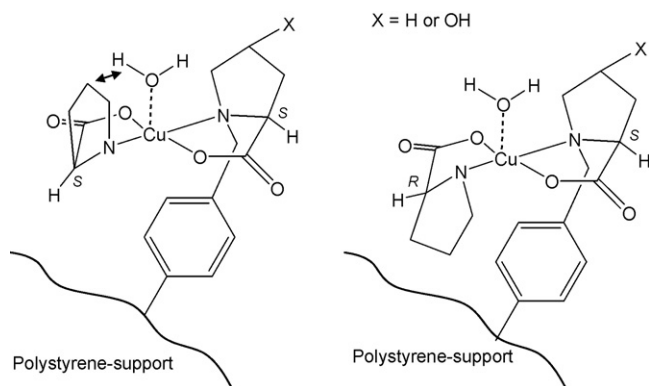


**Fig. 33.** Basic principle of CLEC and typical model for sorption complexes: ternary diastereomeric Cu(II)-complexes of immobilized (*S*)-proline (Pro) ligand (or hydroxyproline  $X=OH$ ) with (*R*)- (right) and (*S*)-proline (left) analyte, respectively. Retention of (*S*)-Pro is diminished by the steric interaction with the water molecule coordinated in the axial position of the Cu(II) ion. Retention of (*R*)-Pro is enhanced by the hydrophobic interaction with the non-polar polystyrene chain (favorable in the aqueous mobile phase). Redrawn in modified form from Ref. [408].

ence for the open-conformation in the complexed state has been confirmed also by solid-state X-ray crystal structures and typical docking modes, which are prevailing also for other host–guest pairs [33], are shown in Fig. 32. Besides the H-bond mediated ionic contact hydrogen bonding interactions of the carbamate group may substantially stabilize the complex, e.g. of *N*-acylated amino acids (Fig. 32a–c). Aromatic residues may be involved in face-to-face  $\pi$ – $\pi$ -interaction with the quinoline ring of the selector. Both quinoline and carbamate are flexible enough as to slightly adopt their conformations to fit the binding prerequisite of the guest molecule (Fig. 32c). Comparison of the structures in Fig. 32a and b nicely illustrates the pseudo-enantiomeric character of quinine and quinidine carbamates making their reversed elution orders understandable. In Fig. 32d a complex with a guest having completely distinct lead structure being docked to the quinine carbamate selector is depicted. It shows that it has fewer contacts and a lower degree of mutual surface saturation. Nonetheless, this solute still yields a chromatographic  $\alpha$ -value of about 1.8. While X-ray crystal structures and NMR spectra established the above mentioned anti-open conformation as preferential conformational arrangement of the cinchona alkaloid selectors in complexed state, NMR revealed that a minor population of the closed conformers can be found in solution as well, which was derived from specific intramolecular NOEs indicated in Fig. 31 [24,25,33,166].

### 7.9. Chiral ligand-exchange CSPs

In the late 1960s the first complete separation of a racemate (amino acid) by chromatography could be accomplished by Davankov with enantioselective ligand exchange technology employing proline as selector immobilized onto a polystyrene support in combination with Cu(II)-ions in the eluent [402]. Although being a long-established method with some restrictions it is still being used, in particular for enantiomer separation of  $\alpha$ -amino acids and  $\alpha$ -hydroxyl carboxylic acids [403–407]. The topic has been reviewed recently [404,408,409].

The basic principle of chiral ligand exchange chromatography (CLEC) is the reversible coordination of chelating analyte species from the mobile phase into the coordination sphere of a metal ion that is immobilized by complexation with a chelating chiral selector forming mixed ternary metal-ion/selector/solute complexes (Fig. 33) [404,408]. Depending on the steric and functional properties of the analytes these diastereomeric ternary chelate complexes

show different rates of formation and/or thermodynamic stabilities, giving rise to different retention times of corresponding solute enantiomers. During the chromatographic process, the coordinated ligands are reversibly replaced by other ligands from the mobile phase such as ammonia, water and other components of the eluent [410]. It is also of importance that the exchange kinetics of the ligands at the metal center is fast enough, since peak performance would be compromised otherwise.

Applicability of ligand-exchange chromatography relies on the presence of metal-chelating functionalities in both selector and analyte [404]. Suitable structural features are bidentate or tridentate ligands with two or three electron-donating functional groups, such as hydroxyl, amino and carboxylic functionalities, binding prerequisites that are typically found in  $\alpha$ -amino acids, amino alcohols and  $\alpha$ -hydroxy acids. The chelating metal ion of first choice is Cu(II). However, Zn(II) as well as Ni(II) may be proper alternatives. Frequently employed CLEC-type selectors include cyclic amino acids such as proline [404] and hydroxyproline [407] as well as sulfur-containing amino acids derived from cysteine [406,411] and penicillamine [405,412–415], but also amino alcohols have been tested [416–419]. These chelating selectors are either (i) covalently attached to silica and organic polymer particles, respectively, or (ii) dynamically coated onto reversed-phase materials via lipophilic moieties of the chiral selectors [404]. Owing to adsorptive immobilization via hydrophobic interactions in the latter case, only low organic modifier percentages are tolerated in the eluents with such CLEC-type CSPs. Usually, eluents are doped with small quantities of metal ions to compensate for metal removal from the column during chromatography. This precaution improves the reproducibility of the separations. As a favorable side effect of the metal ions in the eluent non-chromophoric amino acids and hydroxy acids become detectable by UV due to the formation of colored complexes, yet their presence in the effluent may be sometimes detrimental with other detection schemes such as ELSD and mass spectrometric detection. In general, the repertoire of experimental parameters exploitable for method optimization includes besides mobile phase pH, type and concentration of buffer salts, nature and content of organic modifier and column temperature also the concentration of metal ion in the mobile phase.

CLEC type CSPs are commercially available as Chiralpak MA+ (based on *N,N*-dioctyl-*L*-alanine coated onto RP18) from Chiral Technologies, as Nucleosil Chiral-1 (based on *L*-hydroxyproline chemically bonded to silica) from Macherey-Nagel, or as Chirex 3126 (based on *N,S*-dioctyl-penicillamine coated onto RP18) from Phenomenex. For a long time, this separation principle was the only one that enabled the direct enantiomer separation of amino acids without derivatization which is less important today due to attractive alternatives.

## 8. Concluding remarks

Liquid chromatographic enantiomer separations are routinely performed in various research and routine laboratories. The technology is of particular importance for pharmaceutical industries in drug discovery and quality control of enantiomeric drug substances and corresponding products. A rich toolbox is available for analytical chemists nowadays to solve virtually any problem with modern chiral stationary phases being the workhorses of enantioselective liquid chromatography. Proper choice of a selective chiral stationary phase is the most critical step at first place in the development of enantiomer separations. Reliable predictions of suitable columns and appropriate operation conditions for new selectands remained hitherto an unrealized scientific goal. Databases such as ChirBase may provide some aid on column and starting mobile phase selection by substructure analogies [223,224]. However,

the sensitivity of enantioselectivity to minor substituent effects reduces its usefulness and it must fail for completely new structures due to lack of entries. In practice, extended automatic screening methodologies are therefore put in place in larger pharmaceutical companies to solve this dilemma most efficiently [420,421] and multiparallel microfluidic high-performance liquid chromatography provides thereby a real high-throughput option with great promise [422]. With such screening routines the most promising CSP can be quickly identified following optimization of other experimental variables. The advantage of enantioselective HPLC and its popularity in drug discovery derives also from their straightforward scalability from analytical to preparative scale separations to produce rapidly quantities of each enantiomer sufficient for biological testings. Further, continuous chromatography modes such as simulated moving bed (SMB) technology opened up the avenue for production scale liquid chromatographic enantiomer separations yielding production rates of single enantiomers in the order of hundreds of tons enantiomeric product per year. Overall, enantioselective HPLC has become an extraordinarily powerful technology that greatly contributed to set new standards in terms of quality and safety of chiral drugs.

## Nomenclature

$a_0, a_1, \dots, a_n$	coefficients of predictor variables in QSPR equations
$a$	initial slope of the adsorption isotherm
$\alpha$ or $A$	hydrogen bond acidity (in LSER eq.)
$b$	equilibrium binding constant at individual adsorption site $i$
$\beta$ or $B$	hydrogen bond basicity (in LSER eq.)
$C$	equilibrium concentration of solute in the mobile phase (non-adsorbed)
$D$ (log $D$ )	octanol–water distribution coefficient of ionizable compounds considering the degree of ionization
$D$	diffusion coefficient
$E$	solute's excess polarizability (in LSER eq.)
$E_S$	Taft's steric parameter
$f$	hydrophobic fragmental constant (from Rekker)
$F$	Fisher's $F$ value (in ANOVA)
$k_r$	rate constant of adsorption–desorption process
$K_m$	the equilibrium constant for the corresponding competitive adsorption reaction of the modifier molecules on the stationary phase surface (in NPLC retention model)
$K_S$	equilibrium constant for the stoichiometric exchange of solvent molecule (diluent) on the active site of the sorbent by solute (sorbate) (in NPLC retention model)
$K_Z$ (log $K_Z$ )	log $K_Z$ is intercept in stoichiometric displacement model for ion-exchange process ( $K_Z$ is a system-specific constant that is related to the ion-exchange equilibrium constant $K$ )
$P$ (log $P$ )	octanol–water partition coefficient (logarithm of $P$ )
$P_{(i)}$	population of conformer $i$
$P_{obs}$	observed (NMR) spectral parameter
$q$	equilibrium concentration of solute in the stationary phase (adsorbed)
$q_s$	saturation capacities (number of accessible binding sites)
$q_x$	charge density on the ion-exchanger surface, i.e. number of ion-exchange sites $q_x$ available for adsorption (in mol m <sup>-2</sup> ) (in context of stoichiometric displacement model for ion-exchange process)
$R^s$	selective relaxation rates (in NMR)
$s$	standard deviation of residuals (in QSPR eq.)
$S$	dipolarity (in LSER eq.)
$S$	solute-dependent parameter related to its solvent-accessible surface (in LSS eq.)

$S$	surface area (in m <sup>2</sup> g <sup>-1</sup> ) (in context of stoichiometric displacement model for ion-exchange process)
SP	solute property
$T_1$	relaxation times (in NMR)
$T_{iso}$	isoelectronic temperature
$V$	analytes' molar volume (in LSER eq.)
$V_0$ or $V_M$	volume of the mobile phase in a column
$V_S$	volume of the stationary phase in a column
$X_B$ or $X_m$	molar fraction of the polar modifier (in NPLC retention models)
$X_{CS}$	mol fraction of chiral sector (in Job's plot)
$x_{SA}$	mol fraction of selectand (in Job's plot)
$Z$	slope in stoichiometric displacement model for ion-exchange process ( $Z = m/n$ ; wherein $m$ is the effective charge number of the solute ion and $n$ the effective charge number of the counterion in the mobile phase)

## Greek symbols

$\alpha_{true}$	true enantioselectivity ( $a_{I,S}/a_{I,R}$ )
$\beta$	phase ratio according to IUPAC ( $\beta = V_0/V_S$ , i.e. reciprocal of $\phi$ ( $\beta = 1/\phi$ ))
$\beta_{EEC}$	compensation temperature
$\delta$	Hildebrand solubility parameter (in LSER eq.)
$\delta$	chemical shift (in NMR)
$\Delta\delta$	complexation-induced chemical shift (CIS)
$\Delta\Delta\delta$	non-equivalence of CIS between diastereomeric CS–SA associates
$\pi$	substituent constant for lipophilicity (Hansch's lipophilicity parameter)
$\pi^*$	polarizability/polarity
$\sigma$	Hammett's substituent constant
$\tau_c$	correlation time (in NMR)
$\phi$	phase ratio ( $V_S/V_M$ )
$\chi$	molecular connectivity index (in QSPR)
$\omega$	Larmor frequency

## Acknowledgements

The financial support of the Austrian Christian-Doppler Research Society and the industry partners AstraZeneca (Mölnal, Sweden), Merck KGaA (Darmstadt, Germany), Fresenius Kabi Austria (Graz, Austria), Sandoz (Kundl, Austria) and piCHEM (Graz, Austria) is gratefully acknowledged. The author is also grateful to Dr. Beatrix Föllrich for the help in the course of the preparation of this manuscript.

## References

- [1] H.Y. Aboul-Enein, I.W. Wainer (Eds.), *The Impact of Stereochemistry on Drug Development and Use*, Wiley, New York, 1997.
- [2] I. Ali, H.Y. Aboul-Enein, *Chiral Pollutants: Distribution, Toxicity and Analysis by Chromatography and Capillary Electrophoresis*, Wiley, Chichester, West Sussex, England, 2004.
- [3] O. McConnell, A.B. II, C. Balibar, N. Byrne, Y. Cai, G. Carter, M. Chlenov, L. Di, K. Fan, I. Goljer, Y. He, D. Herold, M. Kagan, E. Kerns, F. Koehn, C. Kraml, V. Marathias, B. Marquez, L. McDonald, L. Nogle, C. Petucci, G. Schlingmann, G. Tawa, M. Tischler, R.T. Williamson, A. Sutherland, W. Watts, M. Young, M.-Y. Zhang, Y. Zhang, D. Zhou, D. Ho, *Chirality* 19 (2007) 658.
- [4] E.R. Francotte, *J. Chromatogr. A* 906 (2001) 379.
- [5] S. Andersson, in: G. Subramanian (Ed.), *Chiral Separation Techniques*, 3rd ed., Wiley-VCH, Weinheim, 2007, p. 585.
- [6] W. Lindner, in: G. Helmchen, R.W. Hoffmann, J. Mulzer, E. Schaumann (Eds.), *Stereoselective Synthesis, Series: Methods of Organic Chemistry (Houben-Weyl)*, vol. 21a, Thieme, Stuttgart, 1995, p. 225.
- [7] W.H. Pirkle, T.C. Pochapsky, *Chem. Rev.* 89 (1989) 347.
- [8] N.M. Maier, W. Lindner, in: E. Francotte, W. Lindner (Eds.), *Chirality in Drug Research*, Wiley-VCH, Weinheim, 2006, p. 189.
- [9] A. Berthod, *Anal. Chem.* 78 (2006) 2093.
- [10] R. Bentley, *Arch. Biochem. Biophys.* 414 (2003) 1.
- [11] L.H. Easson, E. Stedman, *Biochem. J.* 27 (1933) 1257.
- [12] A.G. Ogston, *Nature* 162 (1948) 963.



- [13] P.E. Wilcox, C. Heidelberger, R.V. Potter, *J. Am. Chem. Soc.* 72 (1950) 5019.
- [14] L. Salem, X. Chapuisat, G. Segal, P.C. Hiberty, C. Minot, C. Leforestier, P. Sautet, *J. Am. Chem. Soc.* 109 (1987) 2887.
- [15] S. Topiol, M. Sabio, *J. Am. Chem. Soc.* 111 (1989) 4109.
- [16] R. Bentley, *Perspect. Biol. Med.* 38 (1995) 188.
- [17] S. Topiol, *Chirality* 1 (1989) 69.
- [18] A.D. Mesecar, D.E. Koshland Jr., *Nature* 403 (2000) 614.
- [19] K. Jozwiak, R. Moaddel, S. Ravichandran, A. Plazinska, J. Kozak, S. Patel, R. Yamaguchi, I.W. Wainer, *J. Chromatogr. B* 875 (2008) 200.
- [20] C.E. Dalgliesh, *J. Chem. Soc.* 132 (1952) 3940.
- [21] V.A. Davankov, *Chirality* 9 (1997) 99.
- [22] T.D. Booth, D. Wahnon, I.W. Wainer, *Chirality* 9 (1997) 96.
- [23] G. Uccello-Barretta, C. Bertucci, E. Domenici, P. Salvadori, *J. Am. Chem. Soc.* 113 (1991) 7017.
- [24] N.M. Maier, S. Scheffick, G.M. Lombardo, M. Feliz, K. Rissanen, W. Lindner, K.B. Lipkowitz, *J. Am. Chem. Soc.* 124 (2002) 8611.
- [25] K. Akasaka, K. Gyimesi-Forrás, M. Lämmerhofer, T. Fujita, M. Watanabe, N. Harada, W. Lindner, *Chirality* 17 (2005) 544.
- [26] H.-J. Böhm, G. Klebe, H. Kubinyi, *Wirkstoffdesign, Spektrum, Heidelberg*, 1996.
- [27] H. Kubinyi, *QSAR: Hansch Analysis and Related Approaches*, VCH, Weinheim, Germany, 1993.
- [28] H. Gohlke, G. Klebe, *Angew. Chem. Int. Ed.* 41 (2002) 2644.
- [29] M. Lämmerhofer, W. Lindner, *J. Chromatogr. A* 741 (1996) 33.
- [30] C.C. Pfeiffer, *Science* 124 (1956) 29.
- [31] B. Feibush, *Chirality* 10 (1998) 382.
- [32] S. Ma, S. Shen, H. Lee, M. Eriksson, X. Zeng, J. Xu, K. Fandrick, N. Yee, C. Senanayake, N. Grinberg, *J. Chromatogr. A* 1216 (2009) 3784.
- [33] W. Bicker, I. Chiorescu, V.B. Arion, M. Lämmerhofer, W. Lindner, *Tetrahedron: Asymmetry* 19 (2008) 97.
- [34] W. Ajay, M.A. Murcko, *J. Med. Chem.* 38 (1995) 4953.
- [35] D.H. Williams, E. Stephens, D.P. O'Brien, M. Zhou, *Angew. Chem. Int. Ed.* 43 (2004) 6596.
- [36] K.B. Lipkowitz, D.A. Demeter, R. Zegarra, R. Larter, T. Darden, *J. Am. Chem. Soc.* 110 (1988) 3446.
- [37] R.W. Stringham, J.A. Blackwell, *Anal. Chem.* 68 (1996) 2179.
- [38] M.V. Rekharsky, Y. Inoue, *Chem. Rev.* 98 (1998) 1875.
- [39] H.J. Choi, Y.J. Park, M.H. Hyun, *J. Chromatogr. A* 1164 (2007) 235.
- [40] T. Fornstedt, P. Sajonz, G. Guiochon, *J. Am. Chem. Soc.* 119 (1997) 1254.
- [41] R. Cirilli, M.R. Del Giudice, R. Ferretti, F. La Torre, *J. Chromatogr. A* 923 (2001) 27.
- [42] A. Sztajkov-Ivanov, I. Sztamari, A. Peter, F. Fulop, *J. Sep. Sci.* 28 (2005) 2505.
- [43] X. Wang, C.B. Ching, *J. Sep. Sci.* 30 (2007) 333.
- [44] W. Lao, J. Gan, *J. Sep. Sci.* 30 (2007) 2590.
- [45] B. Loun, D.S. Hage, *Anal. Chem.* 66 (1994) 3814.
- [46] S. Fanali, G. D'Orazio, A. Rocco, *J. Sep. Sci.* 29 (2006) 1423.
- [47] A. Péter, E. Vékés, D.W. Armstrong, *J. Chromatogr. A* 958 (2002) 89.
- [48] A. Berthod, B.L. Heb, T.E. Beesley, *J. Chromatogr. A* 1060 (2004) 205.
- [49] G.-S. Ding, Y. Liu, R.-Z. Cong, J.-D. Wang, *Talanta* 62 (2004) 997.
- [50] N. Morin, Y.C. Guillaume, E. Peyrin, J.-C. Rouland, *Anal. Chem.* 70 (1998) 2819.
- [51] X. Li, V.L. McGuffin, *J. Liq. Chromatogr. Related Technol.* 30 (2007) 937.
- [52] X. Li, V.L. McGuffin, *J. Liq. Chromatogr. Related Technol.* 30 (2007) 965.
- [53] J. Dungalova, J. Lehotay, J. Krupcik, J. Cizmarik, D.W. Armstrong, *J. Sep. Sci.* 27 (2004) 983.
- [54] H. Yan, K.H. Row, *Anal. Chim. Acta* 584 (2007) 160.
- [55] W.R. Oberleitner, N.M. Maier, W. Lindner, *J. Chromatogr. A* 960 (2002) 97.
- [56] L. Asnin, G. Guiochon, *J. Chromatogr. A* 1091 (2005) 11.
- [57] L. Asnin, G. Goetmar, G. Guiochon, *J. Chromatogr. A* 1091 (2005) 183.
- [58] S. Jonsson, A. Schoen, R. Isaksson, C. Pettersson, G. Pettersson, *Chirality* 4 (1992) 505.
- [59] K. Cabrera, D. Lubda, *J. Chromatogr. A* 666 (1994) 433.
- [60] E. Kuesters, C. Spoendlin, *J. Chromatogr. A* 737 (1996) 333.
- [61] K. Yaku, K. Aoe, N. Nishimura, F. Morishita, *J. Chromatogr. A* 848 (1999) 337.
- [62] C.B. Castells, P.W. Carr, *Chromatographia* 52 (2000) 535.
- [63] B. Yao, F. Zhan, G. Yu, Z. Chen, W. Fan, X. Zeng, Q. Zeng, W. Weng, *J. Chromatogr. A* 1216 (2009) 5429.
- [64] W.H. Pirkle, P.G. Murray, *J. High Resolut. Chromatogr.* 16 (1993) 285.
- [65] M.S. Waters, D.R. Sidler, A.J. Simon, C.R. Middaugh, R. Thompson, L.J. August, G. Bicker, H.J. Perpall, N. Grinberg, *Chirality* 11 (1999) 224.
- [66] E. Peyrin, Y.C. Guillaume, C. Guinchar, *Anal. Chem.* 69 (1997) 4979.
- [67] Y. Berezinski, R. Lobrutto, N. Variankaval, R. Thompson, K. Thompson, P. Sajonz, L.S. Crocker, J. Kowal, D. Cai, M. Journet, T. Wang, J. Wyvratt, N. Grinberg, *Enantiomer* 7 (2002) 305.
- [68] O. Gyllenhaal, M. Stefansson, *Chirality* 17 (2005).
- [69] W.H. Pirkle, *J. Chromatogr.* 558 (1991) 1.
- [70] F. Wang, D. Yeung, J. Han, D. Semin, J.S. McElvain, J. Cheetham, *J. Sep. Sci.* 31 (2008) 604.
- [71] T. O'Brien, L. Crocker, R. Thompson, K. Thompson, P.H. Toma, D.A. Conlon, B. Feibush, C. Moeder, G. Bicker, N. Grinberg, *Anal. Chem.* 69 (1997) 1999.
- [72] R.R. Krug, W.G. Hunter, R.A. Grieger, *J. Phys. Chem.* 80 (1976) 2341.
- [73] R.R. Krug, W.G. Hunter, R.A. Grieger, *J. Phys. Chem.* 80 (1976) 2335.
- [74] A. Cornish-Bowden, *J. Biosci.* 27 (2002) 121.
- [75] K. Sharp, *Protein Sci.* 10 (2001) 661.
- [76] R. Ranatunga, M.F. Vitha, P.W. Carr, *J. Chromatogr. A* 946 (2002) 47.
- [77] A. Vailaya, C. Horvath, *J. Phys. Chem.* 100 (1996) 2447.
- [78] M. Kazusaki, T. Shoda, H. Kawabata, *Chromatography* 24 (2003) 121.
- [79] D. Mericko, J. Lehotay, I. Skacani, *J. Liq. Chromatogr. Related Technol.* 32 (2009) 182.
- [80] E. Peyrin, Y.C. Guillaume, *Talanta* 49 (1999) 415.
- [81] T. Rojkovicova, J. Lehotay, D. Mericko, J. Cizmarik, D.W. Armstrong, *J. Liq. Chromatogr. Related Technol.* 27 (2004) 2477.
- [82] W. Weng, Q.L. Zeng, B.X. Yao, W.S. Lin, Q.H. Wang, X.L. You, *Chromatographia* 64 (2006) 463.
- [83] E. Peyrin, A. Ravel, C. Grosset, A. Villet, C. Ravelet, E. Nicolle, J. Alary, *Chromatographia* 53 (11/12) (2001) 645.
- [84] R. Cirilli, S. Alcaro, R. Fioravanti, D. Secci, S. Fiore, F. La Torre, F. Ortuso, *J. Chromatogr. A* 1216 (2009) 4673.
- [85] S. Jacobson, S. Golshan-Shirazi, G. Guiochon, *J. Chromatogr. A* 522 (1990) 23.
- [86] T. Fornstedt, G. Götmar, M. Andersson, G. Guiochon, *J. Am. Chem. Soc.* 121 (1999) 1164.
- [87] G. Götmar, T. Fornstedt, G. Guiochon, *Anal. Chem.* 72 (2000) 3908.
- [88] G. Götmar, T. Fornstedt, G. Guiochon, *Chirality* 12 (2000) 558.
- [89] G. Götmar, T. Fornstedt, M. Andersson, G. Guiochon, *J. Chromatogr. A* 905 (2001) 3.
- [90] G. Götmar, N.R. Albareda, T. Fornstedt, *Anal. Chem.* 74 (2002) 2950.
- [91] G. Götmar, L. Asnin, G. Guiochon, *J. Chromatogr. A* 1059 (2004) 43.
- [92] J. Lindholm, T. Fornstedt, *J. Chromatogr. A* 1095 (2005) 50.
- [93] L. Asnin, K. Kaczmarek, A. Felinger, F. Gritti, G. Guiochon, *J. Chromatogr. A* 1101 (2006) 158.
- [94] G. Goetmar, J. Samuelsson, A. Karlsson, T. Fornstedt, *J. Chromatogr. A* 1156 (2007) 3.
- [95] A. Cavazzini, G. Nadalini, V. Costa, F. Dondi, *J. Chromatogr. A* 1143 (2007) 134.
- [96] R. Arnell, P. Forssén, T. Fornstedt, R. Sardella, M. Lämmerhofer, W. Lindner, *J. Chromatogr. A* 1216 (2009) 3480.
- [97] L. Asnin, K. Kaczmarek, G. Guiochon, *J. Chromatogr. A* 1192 (2008) 62.
- [98] J. Samuelsson, R. Arnell, T. Fornstedt, *J. Sep. Sci.* 32 (2009) 1491.
- [99] P. Jandera, V. Bačkovská, A. Felinger, *J. Chromatogr. A* 919 (2001) 67.
- [100] P. Forssén, R. Arnell, M. Kaspereit, A. Seidel-Morgenstern, T. Fornstedt, *J. Chromatogr. A* 1212 (2008) 89.
- [101] K. Mihlbachler, K. Kaczmarek, A. Seidel-Morgenstern, G. Guiochon, *J. Chromatogr. A* 955 (2002) 35.
- [102] K. Mihlbachler, M.A.D. Jesús, K. Kaczmarek, M.J. Sepaniak, A. Seidel-Morgenstern, G. Guiochon, *J. Chromatogr. A* 1113 (2006) 148.
- [103] M. Lämmerhofer, P. Franco, W. Lindner, *J. Sep. Sci.* 29 (2006) 1486.
- [104] R. Kaliszan, *Chem. Rev.* 107 (2007) 3212.
- [105] K. Héberger, *J. Chromatogr. A* 1158 (2007) 273.
- [106] A.J.P. Martin, *Biochem. Soc. Symp.* 3 (1949) 4.
- [107] A. Berthod, S.C. Chang, D.W. Armstrong, *Anal. Chem.* 64 (1992) 395.
- [108] G. Nadalini, F. Dondi, A. Massi, A. Dondoni, T. Zhang, A. Cavazzini, *J. Chromatogr. A* 1126 (2006) 357.
- [109] C. Hansch, A. Leo, *Exploring QSAR: Fundamentals and Applications in Chemistry and Biology*, American Chemical Society, Washington, 1995.
- [110] C. Hansch, A. Leo, D. Hoekman, *Exploring QSAR: Hydrophobic, Electronic and Steric Constants*, American Chemical Society, Washington, 1995.
- [111] R. Todeschini, V. Consonni, *Handbook of Molecular Descriptors*, Wiley-VCH, Weinheim, Germany, 2000.
- [112] Dragon, Software for Calculation of Molecular Descriptors, <http://www.disat.unimib.it/chm/Dragon.htm>; e-Dragon, <http://www.vclab.org/lab/edragon/>; more information also at: <http://michem.disat.unimib.it/chm/>.
- [113] I.V. Tetko, J. Gasteiger, R. Todeschini, A. Mauri, D. Livingstone, P. Ertl, V.A. Palyulin, E.V. Radchenko, N.S. Zefirov, A.S. Makarenko, V.Y. Tanchuk, V.V. Prokopenko, *J. Comput. Aided Mol. Des.* 19 (2005) 453.
- [114] R.M. Wolf, E. Francotte, D. Lohmann, *J. Chem. Soc., Perkin Trans. 2: Phys. Org. Chem.* (1988) 893.
- [115] R. Kaliszan, T.A.G. Noctor, I.W. Wainer, *Chromatographia* 33 (1992) 546.
- [116] V. Andrisano, C. Bertucci, V. Cavrini, M. Recanatini, A. Cavalli, L. Varoli, G. Felix, I.W. Wainer, *J. Chromatogr. A* 876 (2000) 75.
- [117] V. Andrisano, T.D. Booth, V. Cavrini, I.W. Wainer, *Chirality* 9 (1997) 178.
- [118] T.D. Booth, I.W. Wainer, *J. Chromatogr. A* 741 (1996) 205.
- [119] T.D. Booth, I.W. Wainer, *J. Chromatogr. A* 737 (1996) 157.
- [120] C. Altomare, A. Carotti, S. Cellamare, F. Fanelli, F. Gasparrini, C. Villani, P.A. Carrupt, B. Testa, *Chirality* 5 (1993) 527.
- [121] C. Altomare, S. Cellamare, A. Carotti, M.L. Barreca, A. Chimirri, A.-M. Monforte, F. Gasparrini, C. Villani, M. Cirilli, F. Mazza, *Chirality* 8 (1996) 556.
- [122] A. Carotti, C. Altomare, S. Cellamare, A. Monforte, G. Bettoni, F. Loidice, N. Tangari, V. Tortorella, *J. Comput. Aided Mol. Des.* 9 (1995) 131.
- [123] P. Camilleri, D.J. Livingstone, J.A. Murphy, D.T. Manallack, *J. Comput. Aided Mol. Des.* 7 (1993) 61.
- [124] C.A. Montanari, Q.B. Cass, M.E. Tiritan, A.L.S.d. Souza, *Anal. Chim. Acta* 419 (2000) 93.
- [125] C. Roussel, B. Bonnet, A. Piederriere, C. Suteu, *Chirality* 13 (2001) 56.
- [126] T. Suzuki, S. Timofei, B.E. Iuoras, G. Uray, P. Verdino, W.M.F. Fabian, *J. Chromatogr. A* 922 (2001) 13.
- [127] S. Caetano, Y. Vander Heyden, *Chemom. Intell. Lab. Syst.* 84 (2006) 46.
- [128] M. Szalenienc, A. Dudzik, M. Pawul, B. Kozik, *J. Chromatogr. A* 1216 (2009) 6224.
- [129] C. Prakashvudhisarn, P. Wolschann, L. Lawtrakul, *Int. J. Mol. Sci.* 10 (2009) 2107.
- [130] A. Del Rio, *J. Sep. Sci.* 32 (2009) 1566.
- [131] S. Scheffick, M. Lämmerhofer, W. Lindner, K.B. Lipkowitz, M. Jalaie, *Chirality* 12 (2000) 742.
- [132] W.M.F. Fabian, W. Stampfer, M. Mazur, G. Uray, *Chirality* 15 (2003) 271.
- [133] B. Natalini, A. Macchiarulo, R. Sardella, A. Massarotti, R. Pellicciari, *J. Sep. Sci.* 31 (2008) 2395.



- [134] M. Vitha, P.W. Carr, *J. Chromatogr. A* 1126 (2006) 143.
- [135] R. Kaliszán, in: K. Valkó (Ed.), *Separation Methods in Drug Synthesis and Purification*, Elsevier, Amsterdam, 2000, p. 503.
- [136] J. Lokajova, E. Tesarova, D.W. Armstrong, *J. Chromatogr. A* 1088 (2005) 57.
- [137] P.N. Nesterenko, V.V. Krotov, S.M. Staroverov, *J. Chromatogr. A* 667 (1994) 19.
- [138] K. Kalikova, J. Lokajova, E. Tesarova, *J. Sep. Sci.* 29 (2006) 1476.
- [139] A. Berthod, C.R. Mitchell, D.W. Armstrong, *J. Chromatogr. A* 1166 (2007) 61.
- [140] C.R. Mitchell, D.W. Armstrong, A. Berthod, *J. Chromatogr. A* 1166 (2007) 70.
- [141] C.R. Mitchell, N.J. Benz, S. Zhang, *J. Chromatogr. B* 875 (2008) 65.
- [142] C. West, Y. Zhang, L. Morin-Allory, Poster at the HPLC 2009 Symposium in Dresden, 2009.
- [143] D. Hage, *J. Sep. Sci.* 32 (2009) 1507.
- [144] T. Fornstedt, G. Zhong, G. Guiochon, *J. Chromatogr. A* 741 (1996) 1.
- [145] T. Fornstedt, G. Zhong, G. Guiochon, *J. Chromatogr. A* 742 (1996) 55.
- [146] B. Loun, D.S. Hage, *Anal. Chem.* 68 (1996) 1218.
- [147] J. Chen, J.E. Schiel, D.S. Hage, *J. Sep. Sci.* 32 (2009) 1632.
- [148] W.H. Pirkle, T.C. Pochapsky, *J. Am. Chem. Soc.* 109 (1987) 5975.
- [149] P. Bartak, P. Bednar, L. Kubacek, M. Lämmerhofer, W. Lindner, *Z. Stransky, Anal. Chim. Acta* 506 (2004) 105.
- [150] P.D. Ferguson, D.M. Goodall, J.S. Loran, *J. Chromatogr. A* 745 (1996) 25.
- [151] C. Andre, Y.-C. Guillaume, *Electrophoresis* 24 (2003) 1620.
- [152] J. Oravcova, B. Boehs, W. Lindner, *J. Chromatogr. B* 677 (1996) 1.
- [153] U. Skogsberg, S. Allenmark, *J. Chromatogr. A* 921 (2001) 161.
- [154] L. Fielding, *Tetrahedron* 56 (2000) 6151.
- [155] J. Lah, N.M. Maier, W. Lindner, G. Vesnaver, *J. Phys. Chem. B* 105 (2001) 1670.
- [156] K. Schug, P. Frycak, N.M. Maier, W. Lindner, *Anal. Chem.* 77 (2005) 3660.
- [157] A. Peter, E. Vekes, A. Arki, D. Tourwe, W. Lindner, *J. Sep. Sci.* 26 (2003) 1125.
- [158] M. Lämmerhofer, W. Lindner, in: E. Grushka, N. Grinberg (Eds.), *Advances in Chromatography*, CRC Press, Boca Raton, FL, USA, 2008, p. 1.
- [159] K. Gyimesi-Forrás, N.M. Maier, J. Kökösi, A. Gergely, W. Lindner, *Chirality* 21 (2009) 199.
- [160] L.R. Snyder, *Anal. Chem.* 46 (1977) 1384.
- [161] E. Soczewiński, *J. Chromatogr.* 130 (1977) 23.
- [162] S.N. Lanin, Y.S. Nikitin, *Z. Anal. Khim.* 46 (1991) 1493.
- [163] J. Stahlberg, *J. Chromatogr. A* 855 (1999) 3.
- [164] C. Wang, C. Jiang, D.W. Armstrong, *J. Sep. Sci.* 31 (2008) 1980.
- [165] K.W. Phinney, *Anal. Bioanal. Chem.* 382 (2005) 639.
- [166] C. Czerwenka, M. Lämmerhofer, N.M. Maier, K. Rissanen, W. Lindner, *Anal. Chem.* 74 (2002) 5658.
- [167] C. Czerwenka, M. Lämmerhofer, W. Lindner, *J. Sep. Sci.* 26 (2003) 1499.
- [168] G. Massolini, G. Fracchiolla, E. Calleri, G. Carbonara, C. Temporini, A. Lavecchia, S. Cosconati, E. Novellino, F. Loiodice, *Chirality* 18 (2006) 633.
- [169] R.B. Kasat, S.Y. Wee, J.X. Loh, N.-H.L. Wang, E.I. Franses, *J. Chromatogr. B* 875 (2008) 81.
- [170] J. Lesnik, M. Lämmerhofer, W. Lindner, *Anal. Chim. Acta* 401 (1999) 3.
- [171] P. Hinsmann, L. Arce, P. Svasek, M. Lämmerhofer, B. Lendl, *Appl. Spectrosc.* 58 (2004) 662.
- [172] R. Wirz, T. Buergi, A. Baiker, *Langmuir* 19 (2003) 785.
- [173] R. Wirz, T. Buergi, W. Lindner, A. Baiker, *Anal. Chem.* 76 (2004) 5319.
- [174] M. Bieri, C. Gautier, T. Buergi, *Phys. Chem. Chem. Phys.* 9 (2007) 671.
- [175] R.B. Kasat, N.-H.L. Wang, E.I. Franses, *Biomacromolecules* 8 (2007) 1676.
- [176] R. Wirz, D. Ferri, T. Buergi, A. Baiker, *Spectrosc. Eur.* 19 (2007) 8.
- [177] O. Julinek, M. Urbanova, W. Lindner, *Anal. Bioanal. Chem.* 393 (2009) 303.
- [178] J. Reeder, P.P. Castro, C.B. Knobler, E. Martinborough, L. Owens, F. Diederich, *J. Org. Chem.* 59 (1994) 3151.
- [179] W.H. Pirkle, S.R. Selness, *J. Org. Chem.* 60 (1995) 3252.
- [180] W.H. Pirkle, C.J. Welch, *J. Chromatogr. A* 683 (1994) 347.
- [181] W.H. Pirkle, P.G. Murray, D.J. Rausch, S.T. McKenna, *J. Org. Chem.* 61 (1996) 4769.
- [182] G. Uccello-Barretta, F. Balzano, C. Quintavalli, P. Salvadori, *J. Org. Chem.* 65 (2000) 3596.
- [183] M. Kato, T. Fukushima, N. Shimba, I. Shimada, Y. Kawakami, K. Imai, *Biomed. Chromatogr.* 15 (2001) 227.
- [184] L. Vaton-Chanvrier, H. Oulyadi, Y. Combret, G. Coquerel, J.C. Combret, *Chirality* 13 (2001) 668.
- [185] G.E. Job, A. Shvets, W.H. Pirkle, S. Kuwahara, M. Kosaka, Y. Kasai, H. Taji, K. Fujita, M. Watanabe, N. Harada, *J. Chromatogr. A* 1055 (2004) 41.
- [186] M.E. Koscho, W.H. Pirkle, *Tetrahedron: Asymmetry* 16 (2005) 3345.
- [187] D.M. Forjan, M. Vinkovic, D. Kontrec, A. Lesac, V. Vinkovic, *Struct. Chem.* 18 (2007) 585.
- [188] C. Czerwenka, M.M. Zhang, H. Kaehlig, N.M. Maier, K.B. Lipkowitz, W. Lindner, *J. Org. Chem.* 68 (2003) 8315.
- [189] C. Hellriegel, U. Skogsberg, K. Albert, M. Lämmerhofer, N.M. Maier, W. Lindner, *J. Am. Chem. Soc.* 126 (2004) 3809.
- [190] L. Castellani, M. Flieger, L. Mannina, P. Sedmera, A.L. Segre, M. Sinibaldi, *Chirality* 6 (1994) 543.
- [191] B. Chankvetadze, M. Fillet, N. Burjanadze, D. Bergenthal, C. Bergander, H. Luftmann, J. Crommen, G. Blaschke, *Enantiomer* 5 (2000) 313.
- [192] B. Chankvetadze, N. Burjanadze, G. Pintore, D. Bergenthal, C. Bergander, C. Mühlenbrock, J. Breitkreuz, G. Blaschke, *J. Chromatogr. A* 875 (2000) 471.
- [193] B. Chankvetadze, *Chem. Soc. Rev.* 33 (2004) 337.
- [194] H. Dodziuk, W. Kozminski, A. Ejchart, *Chirality* 16 (2004) 90.
- [195] Y. Machida, H. Nishi, K. Nakamura, *Chirality* 11 (1999) 173.
- [196] Y. Machida, H. Nishi, K. Nakamura, *J. Chromatogr. A* 810 (1998) 33.
- [197] E. Bang, J.-W. Jung, W. Lee, D.W. Lee, W. Lee, *J. Chem. Soc., Perkin Trans. 2* (2001) 1685.
- [198] Y. Machida, M. Kagawa, H. Nishi, *J. Pharm. Biomed. Anal.* 30 (2003) 1929.
- [199] W. Lee, E. Bang, C.-S. Baek, W. Lee, *Magn. Reson. Chem.* 42 (2004) 389.
- [200] A.E. Lovely, T.J. Wenzel, *Org. Lett.* 8 (2006) 2823.
- [201] A.E. Lovely, T.J. Wenzel, *Chirality* 20 (2008) 370.
- [202] E. Yashima, M. Yamada, Y. Okamoto, *Chem. Lett.* (1994) 579.
- [203] E. Yashima, C. Yamamoto, Y. Okamoto, *J. Am. Chem. Soc.* 118 (1996) 4036.
- [204] Y. Okamoto, E. Yashima, C. Yamamoto, *Macromol. Symp.* 120 (1997) 127.
- [205] E. Yashima, *J. Chromatogr. A* 906 (2001) 105.
- [206] C. Yamamoto, E. Yashima, Y. Okamoto, *J. Am. Chem. Soc.* 124 (2002) 12583.
- [207] T.C. Pinkerton, W.J. Howe, E.L. Ulrich, J.P. Comiskey, J. Haginaka, T. Murashima, W.F. Walkenhorst, W.M. Westler, J.L. Markley, *Anal. Chem.* 67 (1995) 2354.
- [208] G. Uccello-Barretta, L. Di Bari, P. Salvadori, *Magn. Res. Chem.* 30 (1992) 1054.
- [209] T. Buergi, A. Baiker, *J. Am. Chem. Soc.* 120 (1998) 12920.
- [210] L.F.B. Malta, Y. Cordeiro, L.W. Tinoco, C.C. Campos, M.E. Medeiros, O.A.C. Antunes, *Tetrahedron: Asymmetry* 19 (2008) 1182.
- [211] E. Bednarek, W. Bocian, K. Michalska, *J. Chromatogr. A* 1193 (2008) 164.
- [212] W.H. Pirkle, J.A. Burke III, S.R. Wilson, *J. Am. Chem. Soc.* 111 (1989) 9222.
- [213] W.H. Pirkle, P.G. Murray, S.R. Wilson, *J. Org. Chem.* 61 (1996) 4775.
- [214] K. Okamura, K.-I. Aoe, N. Nishimura, Y. Fujiwara, Y. Sumida, K. Hashimoto, *Enantiomer* 2 (1997) 99.
- [215] M.E. Koscho, P.L. Spence, W.H. Pirkle, *Tetrahedron: Asymmetry* 16 (2005) 3147.
- [216] J. Olšovska, M. Flieger, F. Bachechi, A. Messina, M. Sinibaldi, *Chirality* 11 (1999) 291.
- [217] F. Bachechi, M. Flieger, M. Sinibaldi, *Struct. Chem.* 17 (2006) 509.
- [218] N.M. Maier, L. Nicoletti, M. Lämmerhofer, W. Lindner, *Chirality* 11 (1999) 522.
- [219] H. Nagata, H. Nishi, M. Kamiguchi, T. Ishida, *Chem. Pharm. Bull.* 54 (2006) 452.
- [220] I. Petitpas, A.B. Bhattacharya, S. Twine, M. East, S. Curry, *J. Biol. Chem.* 276 (2001) 22804.
- [221] J. Stahlberg, E. Henriksson, C. Divne, R. Isaksson, G. Pettersson, G. Johansson, T.A. Jones, *J. Mol. Biol.* 305 (2001) 79.
- [222] F. Bachechi, M. Flieger, M. Sinibaldi, *Struct. Chem.* 13 (2002) 41.
- [223] C. Roussel, J. Pierrrot-Sanders, I. Heitmann, P. Piras, in: G. Subramanian (Ed.), *Chiral Separation Techniques*, 2nd ed., Wiley-VCH, Weinheim, Germany, 2001, p. 95.
- [224] P. Piras, C. Roussel, *J. Pharm. Biomed. Anal.* 46 (2008) 839.
- [225] A. Del Rio, P. Piras, C. Roussel, *Chirality* 17 (Suppl.) (2005) S74.
- [226] K.B. Lipkowitz, *J. Chromatogr. A* 906 (2001) 417.
- [227] K.B. Lipkowitz, in: K. Busch, M. Busch (Eds.), *Chiral Analysis*, Elsevier, Amsterdam, Netherlands, 2006, p. 97.
- [228] C. Zhao, N.M. Cann, *J. Chromatogr. A* 1131 (2006) 110.
- [229] C. Zhao, N.M. Cann, *J. Chromatogr. A* 1149 (2007) 197.
- [230] C.F. Zhao, N.M. Cann, *Anal. Chem.* 80 (2008) 2426.
- [231] C.F. Zhao, S. Diemert, N.M. Cann, *J. Chromatogr. A* 1216 (2009) 5968.
- [232] S. Schefzick, W. Lindner, K.B. Lipkowitz, *Chirality* 12 (2000) 7.
- [233] A.R. Leach, *Molecular Modelling: Principles and Applications*, Longman, Essex, England, 1996.
- [234] A. Lavecchia, S. Cosconati, E. Novellino, E. Calleri, C. Temporini, G. Massolini, G. Carbonara, G. Fracchiolla, F. Loiodice, *J. Mol. Graphics Modell.* 25 (2007) 773.
- [235] S. Alcaro, F. Gasparrini, O. Incani, L. Caglioti, M. Pierini, C. Villani, *J. Comput. Chem.* 28 (2007) 1119.
- [236] C. Bauvais, F. Barbault, Y. Zhu, M. Petitjean, B.T. Fan, *SAR QSAR Environ. Res.* 17 (2006) 253.
- [237] A. Del Rio, J.M. Hayes, M. Stein, P. Piras, C. Roussel, *Chirality* 16 (Suppl.) (2004) S1.
- [238] Y.K. Ye, S. Bai, S. Vyas, M.J. Wirth, *J. Phys. Chem. B* 111 (2007) 1189.
- [239] G. Hesse, R. Hagel, *Chromatographia* 6 (1973) 277.
- [240] G. Hesse, R. Hagel, *Justus Liebig's Annalen der Chemie* (1976) 996.
- [241] E. Francotte, R.M. Wolf, *Chirality* 3 (1991) 43.
- [242] T. Ikai, C. Yamamoto, M. Kamigaito, Y. Okamoto, *J. Sep. Sci.* 30 (2007) 971.
- [243] Y. Okamoto, M. Kawashima, K. Hatada, *J. Am. Chem. Soc.* 106 (1984) 5357.
- [244] P. Franco, A. Senso, L. Oliveros, C. Minguión, *J. Chromatogr. A* 906 (2001) 155.
- [245] T. Ikai, C. Yamamoto, M. Kamigaito, Y. Okamoto, *J. Chromatogr. B* 875 (2008) 2.
- [246] T. Zhang, C. Kientzy, P. Franco, A. Ohnishi, Y. Kagamihara, H. Kurosawa, *J. Chromatogr. A* 1075 (2005) 65.
- [247] T. Zhang, D. Nguyen, P. Franco, T. Murakami, A. Ohnishi, H. Kurosawa, *Anal. Chim. Acta* 557 (2006) 221.
- [248] T. Zhang, D. Nguyen, P. Franco, Y. Isobe, T. Michishita, T. Murakami, *J. Pharm. Biomed. Anal.* 46 (2008) 882.
- [249] E. Yashima, M. Yamada, Y. Kaida, Y. Okamoto, *J. Chromatogr. A* 694 (1995) 347.
- [250] T.D. Booth, W.J. Lough, M. Saeed, T.A.G. Noctor, I.W. Wainer, *Chirality* 9 (1997) 173.
- [251] T.D. Booth, K. Azzaoui, I.W. Wainer, *Anal. Chem.* 69 (1997) 3879.
- [252] J. Wenslow, R.M.T. Wang, *Anal. Chem.* 73 (2001) 4190.
- [253] S. Ma, S. Shen, H. Lee, N. Yee, C. Senanayake, L.A. Nafie, N. Grinberg, *Tetrahedron: Asymmetry* 19 (2008) 2111.
- [254] T. Wang, Y.W. Chen, A. Vailaya, *J. Chromatogr. A* 902 (2000) 345.
- [255] R.B. Kasat, N.-H.L. Wang, E.I. Franses, *J. Chromatogr. A* 1190 (2008) 110.
- [256] Y. Okamoto, M. Kawashima, K. Hatada, *J. Chromatogr.* 363 (1986) 173.
- [257] E. Francotte, T. Zhang, *J. Chromatogr. A* 718 (1995) 257.
- [258] B. Chankvetadze, C. Yamamoto, Y. Okamoto, *J. Chromatogr. A* 922 (2001) 127.
- [259] K.G. Lynam, R.W. Stringham, *Chirality* 18 (2005) 1.

- [260] K. Tachibana, A. Ohnishi, *J. Chromatogr. A* 906 (2001) 127.
- [261] N. Matthijs, C. Perrin, M. Maftouh, D.L. Massart, Y.V. Heyden, *J. Chromatogr. A* 1041 (2004) 119.
- [262] J.L. Bernal, L. Toribio, M.J.d. Nozal, E.M. Nieto, M.I. Montequi, *J. Biochem. Biophys. Methods* 54 (2002) 245.
- [263] M. Maftouh, C. Granier-Loyaux, E. Chavana, J. Marini, A. Pradines, Y. Vander Heyden, C. Picard, *J. Chromatogr. A* 1088 (2005) 67.
- [264] R.W. Stringham, *J. Chromatogr. A* 1070 (2005) 163.
- [265] R.W. Stringham, K.G. Lynam, B.S. Lord, *Chirality* 16 (2004) 493.
- [266] S. Caccamese, S. Bianca, G.T. Carter, *Chirality* 19 (2007) 647.
- [267] C. Perrin, V.A. Vu, N. Matthijs, M. Maftouh, D.L. Massart, Y. Vander Heyden, *J. Chromatogr. A* 947 (2002) 69.
- [268] C. Perrin, N. Matthijs, D. Mangelings, C. Granier-Loyaux, M. Maftouh, D.L. Massart, Y. Vander Heyden, *J. Chromatogr. A* 966 (2002) 119.
- [269] N. Matthijs, M. Maftouh, Y. Vander Heyden, *J. Chromatogr. A* 1111 (2006) 48.
- [270] H. Ates, D. Mangelings, Y. Vander Heyden, *J. Chromatogr. B* 875 (2008) 57.
- [271] L. Zhou, C. Welch, C. Lee, X. Gong, V. Antonucci, Z. Ge, *J. Pharm. Biomed. Anal.* 49 (2009) 964.
- [272] P. Borman, B. Boughtelower, K. Cattana, K. Crane, K. Freebairn, G. Jonas, I. Mutton, A. Patel, M. Sanders, D. Thompson, *Chirality* 15 (2003) S1.
- [273] Y. Okamoto, S. Yoshida, *Angew. Chem. Int. Ed.* 37 (1998) 1021.
- [274] B. Chankvetadze, C. Yamamoto, Y. Okamoto, *Chem. Lett.* (2009) 1176.
- [275] R. Cirilli, R. Ferretti, B. Gallinella, A.R. Bilia, F.F. Vincieri, F. La Torre, *J. Sep. Sci.* 31 (2008) 2206.
- [276] T. Zhang, D. Nguyen, P. Franco, *J. Chromatogr. A* 1191 (2008) 214.
- [277] P. Franco, T. Zhang, *J. Chromatogr. B* 875 (2008) 48.
- [278] L. Thunberg, J. Hashemi, S. Andersson, *J. Chromatogr. B* 875 (2008) 72.
- [279] A. Ghanem, H. Aboul-Enein, *J. Liq. Chromatogr.* 28 (2005) 2863.
- [280] A. Ghanem, H. Hoenen, H.Y. Aboul-Enein, *Talanta* 68 (2006) 602.
- [281] Y. Okamoto, S. Honda, I. Okamoto, H. Yuki, *J. Am. Chem. Soc.* 103 (1981) 6971.
- [282] P. Peluso, S. Cossu, F. Moretto, M. Marchetti, *Chirality* 21 (2009) 507.
- [283] M. Schulte, R. Devant, R. Grosser, *J. Pharm. Biomed. Anal.* 27 (2002) 627.
- [284] R. Cirilli, R. Costi, R.D. Santo, M. Artico, A. Roux, B. Gallinella, L. Zanitti, F.L. Torre, *J. Chromatogr. A* 993 (2003) 17.
- [285] G. Cannazza, D. Braghiroli, P. Iuliani, C. Parenti, *Tetrahedron: Asymmetry* 17 (2006) 3158.
- [286] F. Gasparrini, D. Misiti, R. Rompietti, C. Villani, *J. Chromatogr. A* 1064 (2005) 25.
- [287] Q. Zhong, X. Han, L. He, T.E. Beesley, W.S. Trahanovsky, D.W. Armstrong, *J. Chromatogr. A* 1066 (2005) 55.
- [288] W.W. Barnhart, K.H. Gahm, Z. Hua, W. Goetzinger, *J. Chromatogr. B* 875 (2008) 217.
- [289] S.G. Allenmark, S. Andersson, P. Möller, D. Sanchez, *Chirality* 7 (1995) 248.
- [290] S. Andersson, S. Allenmark, P. Moeller, B. Persson, D. Sanchez, *J. Chromatogr. A* 741 (1996) 23.
- [291] S.G. Allenmark, S. Andersson, *J. Chromatogr. A* 666 (1994) 167.
- [292] J. Haginaka, *J. Chromatogr. A* 906 (2001) 253.
- [293] M.C. Millot, *J. Chromatogr. B* 797 (2003) 131.
- [294] J. Haginaka, *J. Chromatogr. B* 875 (2008) 12.
- [295] E. Domenici, C. Brett, P. Salvadori, G. Felix, I. Cahagne, S. Motellier, I.W. Wainer, *Chromatographia* 29 (1990) 170.
- [296] J. Hermansson, *J. Chromatogr.* 269 (1983) 71.
- [297] T. Miwa, M. Ichikawa, M. Tsuno, T. Hattori, T. Miyakawa, M. Kayano, Y. Miyake, *Chem. Pharm. Bull.* 35 (1987) 682.
- [298] J. Haginaka, C. Seyama, T. Murashima, *J. Chromatogr. A* 704 (1995) 279.
- [299] J. Haginaka, C. Seyama, N. Kanasugi, *Anal. Chem.* 67 (1995) 2539.
- [300] J. Haginaka, H. Takehira, *J. Chromatogr. A* 777 (1997) 241.
- [301] P. Erlandsson, I. Marle, L. Hansson, R. Isaksson, C. Pettersson, G. Pettersson, *J. Am. Chem. Soc.* 112 (1990) 4573.
- [302] J. Chen, W.A. Korfmacher, Y. Hsieh, *J. Chromatogr. B* 820 (2005) 1.
- [303] L. Zhou, B. Mao, Z. Ge, *J. Pharm. Biomed. Anal.* 46 (2008) 898.
- [304] I. Kato, J. Schrode, W.J. Kohr, M. Laskowski, *Biochemistry* 26 (1987) 193.
- [305] T.A.G. Noctor, I.W. Wainer, *Pharmaceut. Res.* 9 (1992) 480.
- [306] H. Matsunaga, J. Haginaka, *J. Chromatogr. A* 1106 (2006) 124.
- [307] F. Zsila, Y. Iwao, *Biochem. Biophys. Acta* 1770 (2007) 797.
- [308] S. Andersson, S. Allenmark, O. Erlandsson, S. Nilsson, *J. Chromatogr.* 498 (1990) 81.
- [309] J. Haginaka, N. Kanasugi, *J. Chromatogr. A* 694 (1995) 71.
- [310] T. Kimura, A. Shibukawa, K. Matsuzaki, *Pharm. Res.* 23 (2006) 1038.
- [311] A.M. Krezel, P. Darba, A.D. Robertson, J. Fejzo, S. Macura, J.L. Markley, *J. Mol. Biol.* 242 (1994) 203.
- [312] J. Ghuman, P.A. Zunsain, I. Petitpas, A.A. Bhattacharya, M. Ottagiri, S. Curry, *J. Mol. Biol.* 353 (2005) 38.
- [313] E.J. Franco, H. Hofstetter, O. Hofstetter, *J. Sep. Sci.* 29 (2006) 1458.
- [314] D.I. Ranieri, D.M. Corgliano, E.J. Franco, H. Hofstetter, O. Hofstetter, *Chirality* 20 (2008) 559.
- [315] D.I. Ranieri, H. Hofstetter, O. Hofstetter, *J. Sep. Sci.* 32 (2009) 1686.
- [316] D.W. Armstrong, W. DeMond, *J. Chromatogr. Sci.* 22 (1984) 411.
- [317] J. Szejtli, *Chem. Rev.* 98 (1998) 1743.
- [318] F. Bressolle, M. Audran, T.-N. Pham, J.-J. Vallon, *J. Chromatogr. B* 687 (1996) 303.
- [319] C.R. Mitchell, D.W. Armstrong, in: G. Gübitz, M.G. Schmid (Eds.), *Chiral Separations*, Humana Press, Totowa, NJ, United States, 2004, p. 61.
- [320] S.C. Chang, G.L. Reid III, S. Chen, C.D. Chang, D.W. Armstrong, *Trends Anal. Chem.* 12 (1993) 144.
- [321] D.W. Armstrong, S. Chen, C. Chang, S. Chang, *J. Liq. Chromatogr.* 15 (1992) 545.
- [322] D.W. Armstrong, L.W. Chang, S.C. Chang, X. Wang, H. Ibrahim, G.R. Reid, T. Beesley, *J. Liq. Chromatogr.* 20 (1997) 3279.
- [323] H.-J. Schneider, F. Hackett, V. Rüdiger, *Chem. Rev.* 98 (1998) 1755.
- [324] T.J. Ward, A.B. Farris III, *J. Chromatogr. A* 906 (2001) 73.
- [325] I. Ilisz, R. Berkecz, A. Peter, *J. Sep. Sci.* 29 (2006) 1305.
- [326] T.L. Xiao, D.W. Armstrong, in: G. Gübitz, M.G. Schmid (Eds.), *Chiral Separations*, Humana Press, Totowa, NJ, United States, 2004, p. 113.
- [327] I. D'Acquarica, F. Gasparrini, D. Misiti, M. Pierini, C. Villani, in: E. Grushka, N. Grinberg (Eds.), *Advances in Chromatography*, CRC Press, Boca Raton, FL, United States, 2008, p. 108.
- [328] A. Berthod, *Chirality* 21 (2009) 167.
- [329] I. Ilisz, R. Berkecz, A. Peter, *J. Chromatogr. A* 1216 (2009) 1845.
- [330] D.W. Armstrong, Y. Tang, S. Chen, Y. Zhou, C. Bagwill, J.-R. Chen, *Anal. Chem.* 66 (1994) 1473.
- [331] K.H. Ekborg-Ott, J.P. Kullman, X. Wang, K. Gahm, L. He, D.W. Armstrong, *Chirality* 10 (1998) 627.
- [332] D.W. Armstrong, Y. Liu, K.H. Ekborg-Ott, *Chirality* 7 (1995) 474.
- [333] K. Ekborg-Ott, Y. Liu, D.W. Armstrong, *Chirality* 10 (1998) 434.
- [334] A. Berthod, X. Chen, J.P. Kullman, D.W. Armstrong, F. Gasparrini, I. D'Acquarica, C. Villani, A. Carotti, *Anal. Chem.* 72 (2000) 1767.
- [335] M. Honetschlagerova-Vadinska, S. Srkalova, Z. Bosakova, P. Coufal, E. Tesarova, *J. Sep. Sci.* 32 (2009) 1704.
- [336] A. Berthod, T. Yu, J.P. Kullman, D.W. Armstrong, F. Gasparrini, I. D'Acquarica, D. Misiti, A. Carotti, *J. Chromatogr. A* 897 (2000) 113.
- [337] I. D'Acquarica, F. Gasparrini, D. Misiti, G. Zappia, C. Cimarelli, G. Palmieri, A. Carotti, S. Cellamare, C. Villani, *Tetrahedron: Asymmetry* 11 (2000) 2375.
- [338] S. Fanali, G. D'Orazio, M.G. Quaglia, A. Rocco, *J. Chromatogr. A* 1051 (2004) 247.
- [339] G.S. Ding, X.J. Huang, Y. Liu, J.D. Wang, *Chromatographia* 59 (2004) 443.
- [340] K. Petrussevska, M.A. Kuznetsov, K. Gedicke, V. Meshko, S.M. Staroverov, A. Seidel-Morgenstern, *J. Sep. Sci.* 29 (2006) 1447.
- [341] S.M. Staroverov, M.A. Kuznetsov, P.N. Nesterenko, G.G. Vasiarov, G.S. Katrukha, G.B. Fedorova, *J. Chromatogr. A* 1108 (2006) 263.
- [342] M.E. Andersson, D. Aslan, A. Clarke, J. Roeraade, G. Hagman, *J. Chromatogr. A* 1005 (2003) 83.
- [343] A. Berthod, Y. Liu, C. Bagwill, D.W. Armstrong, *J. Chromatogr. A* 731 (1996) 123.
- [344] T.E. Beesley, J.-T. Lee, *J. Liq. Chromatogr. Related Technol.* 32 (2009) 1733.
- [345] Y. Liu, A. Berthod, C.R. Mitchell, T.L. Xiao, B. Zhang, D.W. Armstrong, *J. Chromatogr. A* 978 (2002) 185.
- [346] T.E. Beesley, J.T. Lee, A.X. Wang, in: G. Subramanian (Ed.), *Chiral Separation Techniques*, 2nd ed., Wiley-VCH, Weinheim, 2001, p. 25.
- [347] A. Peter, G. Torok, D.W. Armstrong, G. Toth, D. Tourwe, *J. Chromatogr. A* 828 (1998) 177.
- [348] A. Cavazzini, G. Nadalini, F. Dondi, F. Gasparrini, A. Ciogli, C. Villani, *J. Chromatogr. A* 1031 (2004) 143.
- [349] M. Schäfer, T.R. Schneider, G.M. Sheldrick, *Structure* 4 (1996) 1509.
- [350] M. Lämmerhofer, W. Lindner, in: K. Valkó (Ed.), *Separation Methods in Drug Synthesis and Purification*, Elsevier, Amsterdam, 2000, p. 337.
- [351] L.R. Sousa, G.D.Y. Sogah, D.H. Hoffman, D.J. Cram, *J. Am. Chem. Soc.* 100 (1978) 4569.
- [352] T. Shinbo, T. Yamaguchi, K. Nishimura, M. Sugiura, *J. Chromatogr.* 405 (1987) 145.
- [353] Y. Machida, H. Nishi, K. Nakamura, H. Nakai, T. Sato, *J. Chromatogr. A* 805 (1998) 85.
- [354] M.H. Hyun, J.S. Jin, W. Lee, *J. Chromatogr. A* 822 (1998) 155.
- [355] M.H. Hyun, Y.J. Cho, *J. Sep. Sci.* 28 (2005) 31.
- [356] M.H. Hyun, D.H. Kim, Y.J. Cho, J.S. Jin, *J. Sep. Sci.* 28 (2005) 421.
- [357] G. Horvath, P. Huszthy, S. Szarvas, G. Szokan, J.T. Redd, J.S. Bradshaw, R.M. Izatt, *Ind. Eng. Chem. Res.* 39 (2000) 3576.
- [358] M.H. Hyun, S.C. Han, B.H. Lipshutz, Y.-J. Shin, C.J. Welch, *J. Chromatogr. A* 910 (2001) 359.
- [359] K. Hirose, J. Yongzhu, T. Nakamura, R. Nishioka, T. Ueshige, Y. Tobe, *J. Chromatogr. A* 1078 (2005) 35.
- [360] Y. Jin, K. Hirose, T. Nakamura, R. Nishioka, T. Ueshige, Y. Tobe, *J. Chromatogr. A* 1129 (2006) 201.
- [361] S. Lakatos, J. Fetter, F. Bertha, P. Huszthy, T. Toth, V. Farkas, G. Orosz, M. Hollosi, *Tetrahedron* 64 (2007) 1012.
- [362] Y.J. Cho, H.J. Choi, M.H. Hyun, *J. Chromatogr. A* 1191 (2008) 193.
- [363] R. Berkecz, I. Ilisz, A. Misicka, D. Tymecka, F. Fulop, H.J. Choi, M.H. Hyun, A. Peter, *J. Sep. Sci.* 32 (2009) 981.
- [364] R. Berkecz, I. Ilisz, Z. Pataj, F. Fulop, H.J. Choi, M.H. Hyun, A. Peter, *Chromatographia* 68 (2008) S13.
- [365] A. Peter, G. Torok, F. Fulop, *J. Chromatogr. Sci.* 36 (1998) 311.
- [366] G. Torok, A. Peter, F. Fulop, *Chromatographia* 48 (1998) 20.
- [367] U. Conrad, B. Chankvetadze, G.K.E. Scriba, *J. Sep. Sci.* 28 (2005) 2275.
- [368] M.H. Hyun, Y. Song, Y.J. Cho, D.H. Kim, *J. Chromatogr. A* 1108 (2006) 208.
- [369] M.H. Hyun, S.C. Han, J.S. Jin, W. Lee, *Chromatographia* 52 (2000) 473.
- [370] W. Lee, C. Yong Hong, *J. Chromatogr. A* 879 (2000) 113.
- [371] R.J. Steffek, Y. Zelechnonok, K.H. Gahm, *J. Chromatogr. A* 947 (2002) 301.
- [372] M.H. Hyun, *J. Sep. Sci.* 26 (2003) 242.
- [373] M.H. Hyun, *Bull. Korean Chem. Soc.* 26 (2005) 1153.
- [374] W. Pirkle, D. House, *J. Org. Chem.* 44 (1979) 1957.
- [375] F. Mikes, G. Boshart, *J. Chromatogr.* 149 (1978) 455.

- [376] W.H. Pirkle, M.H. Hyun, A. Tsiouras, B.C. Hamper, B. Banks, J. Pharm. Biomed. Anal. 2 (1984) 173.
- [377] W.H. Pirkle, D.W. House, J.M. Finn, J. Chromatogr. 192 (1980) 143.
- [378] W.H. Pirkle, R. Dappen, J. Chromatogr. 404 (1987) 107.
- [379] C.J. Welch, J. Chromatogr. A 666 (1994) 3.
- [380] F. Gasparrini, D. Misiti, C. Villani, J. Chromatogr. A 906 (2001) 35.
- [381] F. Svec, D. Wulff, J.M.J. Fréchet, in: G. Subramanian (Ed.), Chiral Separation Techniques: A Practical Approach, Wiley-VCH, Weinheim, Germany, 2001, p. 55.
- [382] W.H. Pirkle, C.J. Welch, Tetrahedron: Asymmetry 5 (1994) 777.
- [383] N.M. Maier, G. Uray, J. Chromatogr. A 732 (1996) 215.
- [384] N. Oi, H. Kitahara, Y. Matsumoto, H. Nakajima, Y. Horikawa, J. Chromatogr. 462 (1989) 382.
- [385] F. Gasparrini, D. Misiti, C. Villani, Chirality 4 (1992) 447.
- [386] F. Gasparrini, D. Misiti, C. Villani, F. La Torre, J. Chromatogr. 539 (1991) 25.
- [387] W.H. Pirkle, J.M. Finn, J. Org. Chem. 47 (1982) 4037.
- [388] N. Oi, M. Nagase, T. Doi, J. Chromatogr. 257 (1983) 111.
- [389] E. Badaloni, W. Cabri, A. Ciogli, R. Deias, F. Gasparrini, F. Giorgi, A. Vigevani, C. Villani, Anal. Chem. 79 (2007) 6013.
- [390] P. Maccaudiere, A. Tambute, M. Caude, R. Rosset, M.A. Alembik, I.W. Wainer, J. Chromatogr. 371 (1986) 177.
- [391] A.M. Blum, K.G. Lynam, E.C. Nicolas, Chirality 6 (1994) 302.
- [392] C.M. Kraml, D. Zhou, N. Byrne, O. McConnell, J. Chromatogr. A 1100 (2005) 108.
- [393] A. Mandl, L. Nicoletti, M. Lämmerhofer, W. Lindner, J. Chromatogr. A 858 (1999) 1.
- [394] M. Flieger, M. Sinibaldi, L. Cvak, L. Castellani, Chirality 6 (1994) 549.
- [395] P. Padiglioni, C.M. Polcaro, S. Marchese, M. Sinibaldi, M. Flieger, J. Chromatogr. A 756 (1996) 119.
- [396] C.V. Hoffmann, M. Laemmerhofer, W. Lindner, J. Chromatogr. A 1161 (2007) 242.
- [397] C.V. Hoffmann, R. Pell, M. Lämmerhofer, W. Lindner, Anal. Chem. 80 (2008) 8780.
- [398] C.V. Hoffmann, R. Reischl, N.M. Maier, M. Lämmerhofer, W. Lindner, J. Chromatogr. A 1216 (2009) 1147.
- [399] C.V. Hoffmann, R. Reischl, N.M. Maier, M. Lämmerhofer, W. Lindner, J. Chromatogr. A 1216 (2009) 1157.
- [400] M. Lämmerhofer, N.M. Maier, W. Lindner, Nachrichten aus der Chemie 50 (2002) 1037.
- [401] K. Gyimesi-Forras, K. Akasaka, M. Laemmerhofer, N.M. Maier, T. Fujita, M. Watanabe, N. Harada, W. Lindner, Chirality 17 (2005) S134.
- [402] V.A. Davankov, Enantiomer 5 (2000) 209.
- [403] N. Grobuschek, M.G. Schmid, C. Tuscher, M. Ivanova, G. Gübitz, J. Pharm. Biomed. Anal. 27 (2001) 599.
- [404] V.A. Davankov, in: G. Gübitz, M.G. Schmid (Eds.), Chiral Separations, Humana Press, Totowa, NJ, United States, 2004, p. 207.
- [405] I. Ilisz, D. Tourwe, D.W. Armstrong, A. Peter, Chirality 18 (2006) 539.
- [406] B. Natalini, R. Sardella, A. Macchiarulo, R. Pellicciari, J. Chromatogr. B 875 (2008) 108.
- [407] J. Koidl, H. Hoedl, M.G. Schmid, B. Neubauer, M. Konrad, S. Petschauer, G. Guebitz, J. Biochem. Biophys. Methods 70 (2008) 1254.
- [408] V.A. Davankov, J. Chromatogr. A 666 (1994) 55.
- [409] G. Guebitz, M.G. Schmid, in: G. Subramanian (Ed.), Chiral Separation Techniques, 3rd ed., Wiley-VCH, Weinheim, 2007, p. 155.
- [410] B. Natalini, R. Sardella, G. Carbone, A. Macchiarulo, R. Pellicciari, Anal. Chim. Acta 638 (2009) 225.
- [411] B. Natalini, R. Sardella, A. Macchiarulo, R. Pellicciari, Chirality 18 (2006) 509.
- [412] T. Miyazawa, H. Minowa, K. Imagawa, T. Yamada, Anal. Lett. 30 (1997) 867.
- [413] T. Miyazawa, H. Minowa, K. Imagawa, T. Yamada, Chromatographia 60 (2004) 45.
- [414] T. Miyazawa, H. Minowa, Y. Shindo, T. Yamada, J. Liq. Chromatogr. Related Technol. 23 (2000) 1061.
- [415] M. Schlauch, A.W. Frahm, Anal. Chem. 73 (2001) 262.
- [416] M.H. Hyun, S.C. Han, S.H. Whangbo, J. Chromatogr. A 992 (2003) 47.
- [417] M.H. Hyun, J.I. Kim, Y.J. Cho, S.C. Han, Chromatographia 60 (2004) 275.
- [418] M.H. Hyun, J.I. Kim, Y.J. Cho, J.-J. Ryoo, Bull. Korean Chem. Soc. 25 (2004) 1707.
- [419] B. Natalini, R. Sardella, A. Macchiarulo, S. Natalini, R. Pellicciari, J. Sep. Sci. 30 (2007) 21.
- [420] T. Huybrechts, G. Török, T. Vennekens, R. Sneyers, S. Vrielynck, I. Somers, LC–GC Eur. 20 (2007) 320.
- [421] H.A. Wetli, E. Francotte, J. Sep. Sci. 30 (2007) 1255.
- [422] P. Sajonz, W. Schafer, X. Gong, S. Shultz, T. Rosner, C.J. Welch, J. Chromatogr. A 1145 (2007) 149.